CIRCE a new software to predict the steady state equilibrium of chemical reactions

Qi Liu

Par **Qi LIU**

CIRCE a new software to predict the steady state equilibrium of chemical reactions

Thèse présentée pour l'obtention du grade de Docteur de l'UTC

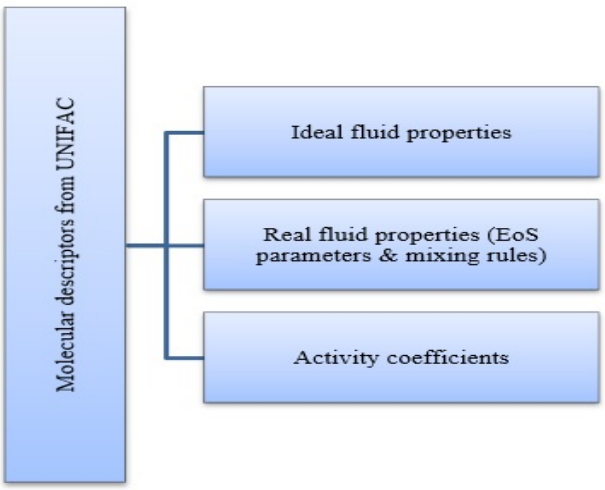

Figure. Organization of the thermodynamical properties generator of CIRCE software.

The final organization of the thermodynamical properties generator of CIRCE.

Soutenue le 11 décembre 2018
Spécialité : Génie des Procédés : Transformations intégrées de la matière renouvelable (EA-4297)

D2455

SORBONNES UNIVERSITES-UNIVERSITY OF TECHNOLOGY OF COMPIEGNE - UTC

DOCTORAL SCHOOL

Process Engineering

Qi LIU

Spécialité : Génie des Procédés

CIRCE a new software to predict the steady state equilibrium of chemical reactions

Thesis Defended the 11th of December 2018

Examiners:

Christophe PROUST (Supervisor)	Professor, TIMR, UTC, France
Christophe LEN (Supervisor)	Professor, UTC, France
Jérôme DAUBECH (Examiner)	Research Engineer, INERIS, PHDS, France
Denis DOCHAIN (Reviewer)	Professor, Ecole Polytechnique de Louvain, Belgique
Frédérique BATTIN-LECLERC (Reviewer)	Professor, LRGP, INPL, University of Nancy, France
Denis LUART (Examiner)	Assistant Professor, TIMR, ESCOM, France

Dedicated to my family, friends and mentors without whom this milestone would never have been reached !!

ACKNOWLEDGEMENT

I would like to thank the Director and Co-director of my thesis, Pr. Christophe PROUST, and Pr. Christophe LEN respectively, for their invaluable supervision, guidance, and inspiring me to finish my thesis during these years. I would always be grateful to Christophe PROUST for providing me with this opportunity. He motivated me a lot to work in the field simulation of thermodynamics to the chemical equilibrium. His expertise, patience and guidance, which I experienced during the complete course of this PhD, combined with his continuous and stimulating participation, always kept me motivated and enthusiastic.

I thank the honorary jury members who have taken time from their busy schedule and accepted to bring their expertise for assessing the present PhD work.

The EPRIFE group in Lab -T.I.M.R- Génie des procédés has been instrumental in providing me with the necessary scientific, technical and logistical tools and services to finish my thesis. I would like to thank the lab-staff at UTC including Mr. Bruno Dauzat, Mr. Michaël Lefebvre, and Dr. Hervé Leclerc. Dr. Denis LUART and Dr. François GOMEZ who gave me help and support.

Thanks very much to sylvan Martin, one of my idols, who brought me into the field numerical and also thanks to Mikel Leturia for his enthusiastic help. Thanks to Mr. SALEH's care and consideration.

Also, thanks to Xing Shitao who gives a lot of support and suggestion in work and amusement, and Dr. Wu Jing who asked me constantly to pursue further studies.

Compiegne is a peaceful city and it has provided me much fun with my friends. These relationships which I made during my time there would always be special to me. I would like to thank my dear friend and flatmate Somik who taught me English and supported me whenever I needed. Thank you to Theophile GAUDIN, Kate CORSYN, Maia A. RAMIREZ, Sarra

Tadrent, Franco Ttaola, Lorine LE PRIOL, Chunmei LIU for helping me realize there is fun outside work.

ABSTRACT

The objective of this work is to develop a new code to predict the final equilibrium of a complex chemical process with many species/reactions and several phases.

Numerical methods were developed in the last decades to predict final chemical equilibria using the principle of minimizing the Gibbs free energy of the system. Most of them use the "Lagrange Multipliers" method and solve the resulting system of equations under the form of an approximate step by step convergence technique. Notwithstanding the potential complexity of the thermodynamic formulation of the "Gibbs problem," the resulting mathematical formulation is always strongly non-linear so that solving multiphase systems may be very tricky and having the difficult to reach the absolute minimum.

An alternative resolution method (MCGE) is developed in this work based on a Monte Carlo technique associated to a Gaussian elimination method to map the composition domain while satisfying the atom balance. The Gibbs energy is calculated at each point of the composition domain and the absolute minimum can be deduced very simply. In theory, the technique is not limited, the Gibbs function needs not be discretised and multiphase problem can be handled easily.

It is further shown that the accuracy of the predictions depends to a significant extent on the "coherence" of the input thermodynamic data such the formation Gibbs energy of the species and molecular interaction parameters. The absolute value of such parameters does not matter as much as their evolution as function of the process parameters (pressure, temperature, …). So, a self-consistent estimation method is required.

To achieve this, the group contribution theory is used (UNIFAC descriptors) and extended somewhat outside the traditional molecular interaction domain, for instance to predict the Gibbs energy of formation of the species, the specific heat capacity…

Lastly the influence of the choice of the final list of products is discussed. It is shown that the relevancy of the prediction depends to a large extent on this initial choice. A first technique is proposed, based on Brignole and Gani's work, to avoid omitting species and another one to select, in this list, the products likely to appear given the process conditions.

These techniques were programmed in a new code name CIRCE. Brignole and Gani-'s method is implemented on the basis of the atomic composition of the reactants to predict all "realisable" molecules. The extended group contribution theory is implemented to calculate the thermodynamic parameters. The MCGE method is used to find the absolute minimum of

the Gibbs energy function.

The code seems to be more versatile than the traditional ones (CEA, ASPEN,…) but more expensive in calculation costs. It can also be more predictive. Examples are shown illustrating the breadth of potential applications in chemical engineering.

Keywords: Thermodynamic equilibrium, Numerical chemistry, Multiphase equilibrium

RESUME (en français)

L'objectif de cette thèse est de développer un nouveau code pour prédire l'équilibre final d'un processus chimique complexe impliquant beaucoup de produits, plusieurs phases et plusieurs processus chimiques.

Des méthodes numériques ont été développées au cours des dernières décennies pour prédire les équilibres chimiques finaux en utilisant le principe de minimisation de l'enthalpie libre du système. La plupart des méthodes utilisent la méthode des «multiplicateurs de Lagrange» et résolvent les équations en employant une approximation du problème de Lagrange et en utilisant un algorithme de convergence pas à pas de type Newton-Raphson. Les équations mathématiques correspondant restent cependant fortement non linéaires, de sorte que la résolution, notamment de systèmes multiphasiques, peut être très aléatoire.

Une méthode alternative de recherche du minimum de l'énergie de Gibbs (MCGE) est développée dans ce travail, basée sur une technique de Monte Carlo associée à une technique de Pivot de Gauss pour sélectionner des vecteurs composition satisfaisant la conservation des atomes. L'enthalpie libre est calculée pour chaque vecteur et le minimum est recherché de manière très simple. Cette méthode ne présente a priori pas de limite d'application (y compris pour las mélanges multiphasiques) et l'équation permettant de calculer l'énergie de Gibbs n'a pas à être discrétisée.

Il est en outre montré que la précision des prédictions dépend assez significativement des valeurs thermodynamiques d'entrée telles l'énergie de formation des produits et les paramètres d'interaction moléculaire. La valeur absolue de ces paramètres n'a pas autant d'importance que la précision de leur évolution en fonction des paramètres du process (pression, température, ...). Ainsi, une méthode d'estimation cohérente est requise.

Pour cela, la théorie de la « contribution de groupe » est utilisée (ceux de UNIFAC) et a été étendue en dehors du domaine d'interaction moléculaire traditionnel, par exemple pour prédire l'énergie de formation d'enthalpie libre, la chaleur spécifique...

Enfin, l'influence du choix de la liste finale des produits est discutée. On montre que la prédictibilité dépend du choix initial de la liste de produits et notamment de son exhaustivité. Une technique basée sur le travail de Brignole et Gani est proposée pour engendrer automatiquement la liste des produits stable possibles.

Ces techniques ont été programmées dans un nouveau code : CIRCE. Les travaux de Brignole et de Gani sont mis en œuvre sur la base de la composition atomique des réactifs pour prédire toutes les molécules «réalisables». La théorie de la 'contribution du groupe' est mise en œuvre pour le calcul des propriétés de paramètres thermodynamiques. La méthode MCGE est enfin utilisée pour trouver le minimum absolu de la fonction d'enthalpie libre.

Le code semble plus polyvalent que les codes traditionnels (CEA, ASPEN, ...) mais il est plus coûteux en termes de temps de calcul. Il peut aussi être plus prédictif. Des exemples de génie des procédés illustrent l'étendue des applications potentielles en génie chimique.

Mots-clés: équilibre thermodynamique, chimie numérique, équilibre multiphasique

Nomenclature:

Basic parameters

A, B, C	constant coefficients matrices (linear programming).
a_{ij}	number of atom j in molecule (species) i.
b_j	total number of atom j in the mixture.
v, d*v*	volume and infinitesimal variation of v.
f()	mathematical function.
F(n_i)	Lagrange function applied to the chemical equilibrium.
La()	Lagrange function.
n, *N*	total number of moles.
n_i, N_i	number of moles of component I in tow successive iterations
nEl	total number of elements (types of atoms).
NG, *NS*, *NL*	total number of gaseous (respectively solid, liquid) species in a mixture.
n_{il}	number of moles of species i in phase l.
n_{iT}	total number of moles of species i (in all phases).
nSp	total number of species (products).
N_v	number of composition vectors.
q	integer larger than 1.
Q(n_i)	Taylor approximation of the G(n_i).
T, dT	temperature (K) and infinitesimal variation of T
T(x,f(x*))	tunneling function of f around the fixed variable x*.
X	vector of unknowns (linear programming).
x_{il}	molar fraction of species i in phase l.
λ_j	Lagrange multipliers.
Δ	average gap between two successive values of n_i (MCGE method).
δ_{ij}	Binary interaction parameter in the Peng Robinson equation of state.
$\varepsilon_j(N_i)$	constrains in the Lagrange function.
p	the number of "mixed" phases.
c	subscript for "condensed"
w	a constant coefficient for the RAND method.
N_V	a given number of composition vectors.

thermodynamic parameters

μ^*	chemical potential at the reference pressure P* (J/mole).
μ_i	chemical potential of species i in the reaction conditions (J/mole).
μ_i^0	standard chemical potential (of formation) of species i (pure in J/mole).
A, dA	Helmholtz energy of a system (free internal energy in J) and infinitesimal variations of A.
Cp	specific heat at constant pressure (J/K/mole).
f	Fugacity.
f_i	fugacity of component i (pure) at T and P.
G, d*G*	Gibbs energy of a system (free enthalpy in J) and infinitesimal variations of G.
G^0	Gibbs formation energy of the system (J).
G^E	Gibbs excess energy of the system (J).

G^{mix}	Gibbs mixing energy of the system (J).
H, dH	enthalpy of a system (J) and infinitesimal variations of H.
U, dU	Internal enegy of a system (J) and infinitesimal variations of U.
H^0_{fi}, h^0_{fi}	enthalpy (respectively molar enthalpy) of formation of species i in the standard conditions (1 bar, 298K).
h_i	molar enthalpy of species i (J/mole) in the conditions of the reaction (P and T).
h_i	reduced chemical potential of species i in the mixture (=μ_i/RT).
P	absolute pressure (usually in bar in the thermodynamic functions and Pa with the equation of state).
Pc	critical pressure (K).
P_r	reduced pressure $P/P_{c.}$
P_{rs}^{sat}	reduced saturated pressure for a solid gas equilibrium $P_{sat}/P_{c.}$
Q, δQ	amount of heat exchanged between a system and its surroundings (J) and infinitesimal variation of Q.
R	perfect gas constant.
S, dS,	entropy of a system (J/K) and infinitesimal variations of S.
s_i	molar entropy of species i (J/K/mole) in the conditions of the reaction (P and T).
$s_i^{departure}$	departure part of the molar entropy of species i (J/K/mole) in the conditions of the reaction (P and T).
Tc	critical temperature (K).
T^n	estimator of T at iteration n.
T_r	reduced temperature $T/T_{c.}$
T_{ref}	reference temperature (usually 298 K).
T_b	boiling temperature.
T_m	melting temperature.
U, dU	internal energy of a system (J) and infinitesimal variations of U.
v	volume (m^3).
v_m	molar volume (m^3/mole).
W, δW	amount of work exchanged between a system and its surroundings (J) and infinitesimal variation of W.
$\hat{f}_i$	partial fugacity of component i in the mixture at T and P.
$\hat{\varphi}_i$	fugacity coefficient of component i in the mixture at T and P.
φ	fugacity coefficient.
φ_i	fugacity coefficient of component i (pure) at T and P.
γ_i	activity coefficient of species i in the mixture.
vc	critical volume (m^3).
G_f	Gibbs free energy of formation.
a	parameter of heat capacity.
H_{fusion}, ΔH_{fus}	enthalpy of fusion;
H_{vap}	enthalpy of vaporization; k A and B are dynamic viscosity.
Pi	Partial pressure of species i.
T_f	Temperature of fusion.
T_{eb}	Boiling temperature.
Hf°	gas-phase enthalpy of formation at T = 298.15.
Cp	heat capacity.
φ^{sat}	fugacity of the saturate vapor for the liquid.
P^{sat}	saturation pressure.

UNIFAC

a_{mn}	interaction parameter between the groups m and n (expressed in temperature units).
Q_k	surface area of subgroup k.
γ_i^c	combinatorial activity coefficient of molecule i
γ_i^r	residual activity coefficient of molecule i in the mixture.
ϕ_i	relative volume of the molecule i in one mole of mixture.
q_i	molar surface area.
θ_i	relative surface of the molecule i in one mole of mixture.
x_j	molar fraction of molecule i in the mixture.
Lj	function of ri and qi.
v_k^i	kth functional group count in the molecule i.
R_k	volume of subgroup k.
Γ_k	residual activity coefficient of subgroup k in the mixture.
Γ_k^i	residual activity coefficient of subgroup k in the pure molecule i.
Ψ_{mk}	function of a_{mn} and T.
X_m	mole fraction of group m in the mixture.

EoS

a, a_i	energy parameter in the Peng Robinson equation of state (respectively of species i in a mixture)
b, b_i	Co-volume parameter in the Peng Robinson equation of state (respectively of species i in a mixture)
λ, A_v, A_m	fitting parameters in the LCVM equation of state
κ	constant in the Peng Robinson equation of state
ω	acentric factor (Peng Robinson equation of state)
$h_i^{departure}$	departure part of the molar enthalpy of species i (J/mole) in the conditions of the reaction (P and T)
Z	compressibility factor
β	isothermal compressibility coefficient of a fluid
α(Tr,ω)	dimensionless energy parameter.
α(T_c)	dimensionless energy parameter.

Kinetics

Ea	activation energy for the reaction.
k	Reaction rate.
A	pre-exponential factor.
N	reaction order.

Content

1 Introduction

Nowadays, numerical modeling can be a great help in research and development activities to guide technical choice and/or to better interpret the experimental data.

Thus, in many industrial fields, the spreading of powerful and lost cost computer resources is massively used to foster the innovation process across many industrial fields[1]. It is true also for the chemical industry where they are used for example to predict toxicity [2], combustion[3], even some complex catalytic reactions[4]. A rather recent branch is molecular modeling which, based an improved understanding of microscopic and molecular behavior, could help designing new molecule and predicting some of their properties via an ab-initio approach [5; 6].

If the industrial aspect of processes in which chemical reaction occurs is considered, there is a need to be able to foresee the evolution of the chemical reaction (yield, heat releases…) as a function of the process conditions (temperature, pressure…). When the variability of the components and reaction conditions are to be considered, the reality of the reaction may be rather complex including not only the chemical reactions with multiple components but also phase changes, energy considerations. Thus, the modeling may prove difficult.

In this domain, significant efforts were deployed since at least one century based on the resources of modern thermodynamics and many software were developed over the last decades (since the seventies), some being public such as those presented in the table below but many others are in-house made to better fit with some specific applications because the available codes suffer from significant limitations as shown in this memory. Most of them are based on

the principle that the Gibbs free energy should be minimum at equilibrium, at least for a reaction occurring at constant temperature and constant pressure. To do this, a list of the potential products has first to be defined from the database of the code and a step by step minimizing technique is used to find the composition producing the smallest value of the Gibbs free energy. One of the acknowledged difficulty is to be able of accounting for several phases, one reason being that the Gibbs free energies (or to be more precise, the chemical potentials) of a compound available in two phases are the same when the phase equilibrium is reached so that it is difficult to distinguish their respective contribution in the Gibbs free energy (and mass) balance. Also, the availability and accuracy of the thermodynamic data may be a limitation in the predictability of the software.

Some description of typical commercially of freely available software is given in **Table** 1.1, with indications and limitations.

Table 1.1. Commercially or freely available software to calculate chemical equilibrium.

Code	Gibbs energy minimization method	Indications	Limitations	Database	Advantage	Disadvantage
Aspen (Commercialized)	RAND method to solve the Lagrange equation+ splitting phase[7].	Prediction of gas and/or liquid reactions.	Difficulties with solids. In multiphase may not converge to the absolute minimum.	A build in database.	Wide empirical database completed by some calculated properties using the group contribution theory.	Only existing and registered products can be used.
HSC (Commercialized)	RAND method to solve the Lagrange equation[8].	Gas phase.	Mono phase	A build in database.	Wide empirical database completed by some calculated properties using the group contribution theory (Benson for H, S, and G).	Only existing and registered products can be used.
CEA (free)	Gordon and Mc Bride method to solve the Lagrange equation.[9]	Gas phase + added solids. Very efficient.	Does not always converge with solids. The choice of the solids to	A build in database.	Over 2000 species are contained in the wide and empirical database.	Only existing and registered products can be

			appear is left to the user.			used.
GASEQ (free)	Morley method to solve the Lagrange equation[10].	Gas phase. Efficient.	Monophase.	Use multiple thermodynamic files in a standard NASA polynomial format.	A small database with no possibility to extend it.	Only existing and registered products can be used.
MINEQL (Commercialized)	Constant equilibrium method.[11]	Multiphase. Very efficient	The reaction has to be known. The reaction constant has to be available in the database.	It contains over 145 ions which can be combined to form species.	Ice, water and mineral system. But no possibility generates totally new molecules themselves.	Only existing and registered products can be used.
TIGER And CHEETAH	Simplified Lagrange Gibbs energy minimization method solved using a Newton-Raphson technique[12].	The reactions are proposed by the code. Converges very quickly for gases.	May converge to a local minimum.	Has a "closed" reactant database containing most frequently used explosives and binders.	Supports multiple product libraries. The user cannot modify the database.	Only existing and registered products can be used.
FREZCHEM	Gibbs energy minimization method combined with the PITZER method to calculate the equilibrium.[13].	For some special system such ice water and mineral.	May converge towards a local.	Built in database of Ice water and mineral system.	The database has ice water and mineral system. The user cannot modify the database.	Only existing and registered products can be used.

Clearly, the existing codes seem to have a limited range of application and there is a need for further work in this domain. Especially, it seems particularly challenging to account for multiphase chemical equilibrium. This shortcoming can be a significant limitation in chemical processes involving heterogeneous catalysis for instance. The second important aspect is about the extent of the database which, if not enough comprehensive, may not be exhaustive and flexible enough to accommodate for brand new chemical processes, in which potential new molecules and by-products may appear.

Thus, this research work is intended to contribute to the improvement of the prediction of

chemical reactions yields (e.g., final composition and the products, pressure, temperature and energy exchanges) in industrial processes. The circumstances in which the chemical reactions may occur (isothermal, adiabatic, at constant pressure or volume…) need to be accounted for since the latter may greatly affect the final outcome.

The first chapter is devoted to the fundamentals of thermodynamic equilibrium and to the presentation of the state of the art of the methods/codes traditionally used to calculate this equilibrium by minimizing the Gibbs energy.

The limitations are discussed and tested by the present author in the second chapter. As the reader will realize, three of them are particularly important: the mathematical methods, from which the convergence problems quoted in **Table** 1.1 result, the accuracy, or more precisely the consistency of the thermodynamic data used and the exhaustivity/relevancy of the final list of products chosen to run the calculation.

To overcome these limitations, a brand-new Gibbs energy minimization method was devised and computed into a new code. This code is named CIRCE and is described in the third chapter. Many other innovations were tested. For instance, to limit the incidence of the inconsistencies linked to the thermodynamic properties, all the thermodynamic data are calculated using the same molecular descriptors. Further, to limit the incidence of the exhaustivity of the final list of products, a routine was devised to generate automatically all the possible and realizable products as a function of the atomic composition of the reactants and a method to sort the products likely to appear is tentatively proposed.

The performances and capabilities of the code are investigated in the last chapter.

Examples are also given corresponding to practical industrial configurations in chemical engineering. The code works as intended but certainly needs further improvements as explained in the conclusions.

2 Analysis of existing methods to predict chemical equilibria

Classically two methods are used to calculate a thermodynamic chemical equilibrium. The law of mass action can be implemented according to which the concentrations of the reactants and products are related via a constant, provided the stoichiometric coefficients of the reaction are known. Several reactions can be chained. The method is reasonable, appealing and, at least conceptually simple, but is very dependent on the chemical reactions chosen and on the values of the equilibrium constants[14; 15]. Besides, it is not adapted to very complex problems where the details of the chemistry are not known. The second method involves the well-established concept elaborated by Gibbs[16], according to which the "Gibbs free energy" (free enthalpy) should have reached a minimum at the thermodynamic equilibrium. There is no need to know the details of the chemical reactions, only the energy and molecular composition of the reactants and of the chemicals likely to be present in the final products.

In the following, the theoretical grounds about this second method are first recalled. Then the various ways available in the literature to solve it and the associated difficulties are highlighted.

2.1 Fundamentals

2.1.1 State functions

Thermodynamics developed at the end of the eighteenth century and expanded very

significantly at the turn of the nineteenth and twentieth century[17; 18]. In particular, the fundamentals of the chemical equilibrium date back from this last period following the discoveries of eminent scientists like Gibbs, De Donder, and Planck…, only the main aspects are dealt with below.

According to the first principle, the total energy of a system is conserved when switching from a first (stable) state to a second (also stable) state. When the system exchanges heat Q and mechanical work W with the outside, its internal energy, U, changes accordingly (δ means infinitesimal changes of Q, W…):

$$\delta U = \delta Q + \delta W \tag{2.1}$$

Where:

$$\delta W = -PdV \tag{2.2}$$

The state function U depends only on the state variables of the systems (mass, Temperature, Pressure, composition…). The work can also be expressed in terms of state variables and if Q would also then a complete description of the evolution of the system could be drawn. Carnot suggested that it could be the case only when the differences in the temperature (and pressure) between the system and the outside were negligible. This notion defines the limiting case of "reversible processes". Using this assumption, Carnot demonstrated that:

$$\oint \left(\frac{\delta Q}{T}\right)_{Reversible\_cycle} = 0 \tag{2.3}$$

And equivalently (between two states A and B):

$$\int_A^B \left(\frac{\delta Q}{T}\right)_{R_1} + \int_B^A \left(\frac{\delta Q}{T}\right)_{R_2} = 0 \tag{2.4}$$

Since $\left(\frac{\delta Q}{T}\right)$, in the reversible situation, is only determined by the state variables of A and B of the systems, it can be associated with a new state function which Clausius called "entropy"

such that :

$$\Delta S = \int_A^B \left(\frac{\delta Q}{T}\right)_{reversible} \quad (2.5)$$

But, in the real world, the transformations can never be reversible. For instance, a difference in temperature is required for Q to flow between the system and the outside so that equality (2.5) cannot be satisfied anymore. It can be shown that in any real transformation:

$$dS - \frac{\delta Q}{T} \geq 0 \quad (2.6)$$

This is the second law of thermodynamics.

One important implication is that, as long as a system change, its entropy increases when the contribution of heat exchanges is removed.

A number of useful state functions were derived from U and S like the enthalpy H, the Helmholtz (free) energy A and the Gibbs (free) energy G :

$$H = U + PV \quad (2.7)$$

$$A = U - TS \quad (2.8)$$

$$G = H - TS \quad (2.9)$$

By differentiating (2.9) and using (2.7) and (2.1), the following relationship is obtained:

$$dG = dU + PdV + VdP - TdS - SdT$$

Thus:

$$dG - VdP + SdT = \delta Q - TdS$$

If now equation (2.6) is considered, then the following important conclusion is obtained :

$$(dG)_{T,P} \leq 0 \quad (2.10)$$

Meaning that a transformation of a system occurring at constant pressure and temperature produces a decrease of the Gibbs energy. This property is used in most chemical equilibrium software. The chemical equilibrium is reached when the Gibbs energy is minimum.

But all systems do not evoluate at constant pressure and temperature. Consider for instance the differentiation of equation ((2.9) and using (2.7) and (2.1), the following relationship is obtained:

$$dA = dU - TdS - SdT = dU + PdV - TdS - PdV - SdT$$

Thus:

$$dA + PdV + SdT = \delta Q - TdS$$

If now equation (2.6) is considered, then the following important conclusion is obtained:

$$(dA)_{T,V} \leq 0 \qquad (2.11)$$

Meaning that a transformation of a system occurring at constant volume and temperature produces a decrease of the Helmholtz energy. The chemical equilibrium is reached when the Helmholtz energy is minimum. This variation can be found in some specific softwares[19].

2.1.2 Molecular interactions

In the present context, the evolution of the Gibbs energy in a multicomponent mixture is to be calculated. The independent variables are T, P, n_1, n_2...n_{nSp} (where n_i is the number of mole of species i with 1<i<nSp, nSp is the total number of products) so that $G = G(T, P, n_1, n_2, \dots, n_{nSp})$. The differential expression of G reads then:

$$dG = \left(\frac{\partial G}{\partial T}\right)_{P,n_i} dT + \left(\frac{\partial G}{\partial P}\right)_{T,n_i} dP + \sum_{i=1}^{nSp} \left(\frac{\partial G}{\partial n_i}\right)_{T,P,n_i} dn_i \qquad (2.12)$$

Where:

$$\left(\frac{\partial G}{\partial n_i}\right)_{T,P,n_i} = \mu_i \qquad (2.13)$$

is the “chemical potential of species i in the mixture.

In a pure mixture containing only the species i, the chemical potential is the Gibbs energy of formation at T and P of this species (μ_{io}). In an ideal mixture, the chemical potential of species i is given by:

$$\mu_i = \mu_{i0} + R \cdot T \cdot ln(x_i) \text{ With } x_i = \frac{n_i}{\sum_i n_i} \quad (2.14)$$

The mixture is rarely ideal because of intermolecular interactions. This is accounted for by replacing the mixture fraction x_i in the logarithm by the "activity" of species i, a_i, in the mixture. Formally, a_i and x_i are related using the coefficient of activity γ_i so that:

$$a_i = \gamma_i \cdot x_i \text{ and } \mu_i = \mu_{i0} + R \cdot T \cdot ln(\gamma_i \cdot x_i) \quad (2.15)$$

In classical thermodynamics, the reference situation is that of the "ideal" component, often a perfect gas, having no molecular interactions. The coefficient of activity can be calculated by performing a virtual transformation from the ideal component to the real component situation.

From the pioneering work of Van der Waals, it was shown a relationship exists, at least for fluids (liquids and gases), between P, V and T. This is the "equation of state" (EoS) of the fluid which can be described by a Taylor expansion Kamerlingh-Onnes [20] in which the coefficients B, C,… depends on the chosen EoS and nature of the fluid :

$$Pv_m = RT + BP + CP^2 + \cdots \quad (2.16)$$

An isothermal and reversible transformation of the mixture is considered so that dG=V.dP. The chemical potential of the fluid at *T* is given by integration :

$$\mu(T,P) = \int v_m dP = \int \left(\frac{RT}{P} + B + CP + \cdots\right) dP = RT \ln P + BP + \frac{C}{2}P^2 + \cdots + I(T) \quad (2.17)$$

The constant I(*T*) depends only on the temperature. When *P* is small enough, the above equation reduces to:

$$\mu(T,P) = RT\ln P + I(T) \qquad (2.18)$$

In the same *P* and *T* conditions, the ideal gas approximation reads:

$$\mu(T,P) = \mu^*(T) + RT\ln\left(\frac{P}{P^*}\right) \qquad (2.19)$$

Where P* is a reference pressure. If P is sufficiently small, the real fluid behaves like the ideal gas, so that (2.19) equates (2.18), and I(T) is obtained:

$$I(T) = \mu^*(T) - RT\ln P^* \qquad (2.20)$$

substituting into (2.17) gives:

$$\mu(T,P) = \mu^*(T) + RT\ln\left(\frac{P}{P^*}\right) + BP + \frac{C}{2}P^2 + \cdots (2.21)$$

By definition, the Taylor term is expressed as:

$$BP + \frac{C}{2}P^2 + \cdots = RT\ln\varphi \qquad (2.22)$$

Where φ is the coefficient of fugacity and $f = \varphi.P$ the fugacity of the fluid, as kind of "effective pressure":

$$RT\ln f = RT\ln P + BP + \frac{C}{2}P^2 + \cdots \qquad (2.23)$$

Lnφ corresponds to the deviation from the ideal gas situation. When $P \to 0$, $\varphi = 1$, f = P. Note that Lnφ is clearly linked to the "residue" of the equation of state (eq (2.16)) seen as the difference between the integrals of the real EoS and the ideal gas law, so that finally:

$$\ln\varphi = \ln\frac{f}{P} = \frac{1}{RT}\int_0^P \left(v - \frac{RT}{P}\right)dP = \int_0^P \frac{Z-1}{P}dP \qquad (2.24)$$

Here the compressibility coefficient *Z* was introduced. For the ideal gas, *Z* is 1. For a liquid Z is typically on the order of 0.1 whereas for a real gas it is about 0.9.

In a mixture, the coefficient of activity can be linked to the coefficients of fugacity since:

- For the pure component i $\mu_{i0}(T,p) = \mu_i{}^*(T) + RT\ln\left(\frac{f_i^0}{P^*}\right)$

- In the mixture $\mu_i(T,p) = \mu_i^*(T) + RT \ln\left(\frac{\hat{f}_i}{P^*}\right)$

Where f_i^0 and $\hat{f}_i$ are respectively the fugacity of the pure component i at *T* and *P* and the partial fugacity of the same component in the mixture at the same *P* and *T*. The difference between these expressions gives:

$$\mu_i = \mu_{i0} + R \cdot T \cdot ln\left(\frac{\hat{f}_i}{f_i^0}\right) = R \cdot T \cdot \ln(\gamma_i \cdot x_i) \qquad (2.25)$$

So it is clear that the knowledge of the equations of state for the pure components and for the mixture opens the possibility to calculate the coefficients of activity tacking into account of the process conditions (Appendix F). Important EoS is discussed below.

2.1.3 Equations of state

The ideal gas equation of state was established empirically and theoretically mainly during the 18th and 19th century. It is assumed that molecules are infinitely small and that their interactions are of mechanical nature. The resulting EoS is well-known:

$$\mathrm{PV} = \mathrm{nRT} \qquad (2.26)$$

In 1893, Van der Waals defined the real gases based on two grounds :

(i) The volume occupied by the molecules is not zero and should be subtracted from the total volume to retrieve the real free volume.

(ii) Molecules interact with various forces which change their velocities, and thus the pressure and a correction term should be added. The final formulation (see Appendix B) is:

$$\left(P + \frac{a}{v_m^2}\right)(v_m - b) = RT \qquad (2.27)$$

Where a and b are constants (v_m is the molar volume). The constant 'b' is related to the volume occupied by the gas molecule ("co-volume" $m^3 \cdot mol^{-1}$) while 'a' is related to the influence of the molecular interaction (energy term in $Pa \cdot m^6 \cdot mol^{-2}$). Equation (2.27) is a "cubic" equation since it has three characteristic roots when the temperature and pressure are varied. It can be demonstrated that a and b are related to the "critical" parameters Pc, Tc, and Vc of the fluid (the pressure, temperature and specific volume of the fluid at the point where the liquid and vapor phases merge). Qualitatively at least, the Van der Waals equation can predict the gas and liquid behavior including phase changes.

The ideal gas can be considered as a limiting case of the van der Waals equation of state when P tends to zero since in such conditions v_m tends to infinity in such a way that the correction terms are negligible. This remark is used to calculate the "departure function" as shown later.

It was recognized that although being a significant progress, the van der Waals equations is deficient in many aspects and alternative EoS, based on a very similar formulation, were proposed later like the RK equation,[21] the SRK[22] EoS and the well-known Peng-Robinson EoS.[23] The latter, detailed below, is particularly efficient in predicting liquid densities and vapor pressures even on the saturation line and was implemented in this work (under the form of the LCVM model as detailed after).

$$P = \frac{RT}{v-b} - \frac{\alpha(T)}{v(v+b)+b(v-b)} \tag{2.28}$$

Where for a pure component:

$$\alpha(T) = \alpha(T_C) \cdot \alpha(T_r, \omega) \tag{2.29}$$

Where $\alpha(T)$ is the energy parameter of equation (2.28), $\alpha(T_r, \omega)$ and $\alpha(T_c)$ are dimensionless, depending on the critical parameters, acentric factor ω and reduced temperature ($T_r=T/T_c$):

$$\alpha^{1/2}(T_r, \omega) = 1 + \kappa\left(1 - T_r^{1/2}\right) \tag{2.30}$$

$$\kappa = 0.37464 + 1.54226\omega - 0.26992\omega^2 \tag{2.31}$$

$$\alpha(Tc) = 0.45724\,\frac{R^2 T_c^2}{P_c} \tag{2.32}$$

And the co-volume parameter b is a constant given by:

$$b(Tc) = 0.07780\,\frac{RTc}{P_c} \tag{2.33}$$

Note that the critical parameters *Tc*, *vc*, *Pc* and acentric factor can be derived from the "group contribution" method as detailed later in this work. The PR EoS is valid both for liquid and gases and is applied in exactly the same way for liquids and gases. To make a distinction between the phases, which is required in the context of this work, the empirical criterion devised by Poling et al.[24] was implemented. The use of the isothermal compressibility coefficient is prescribed.

For example, for the Equation of state of Peng Robinson:

$$P = \frac{RT}{(v-b)} - \frac{a}{v(v+b)+b(v-b)} \tag{2.34}$$

This coefficient is:

$$\beta = -\frac{1}{v}\left(\frac{\partial v}{\partial P}\right)_T = \frac{RT}{v^2} - \frac{2a(v+b)}{v[v(v+b)+b(v-b)]^2} \tag{2.35}$$

When the pressure is in atmospheres, the Poling criteria for deciding whether a calculated saturated volume is that of a liquid or vapor phase are: for a liquid phase, $\beta<0.005$/atm, for a vapor phase, $0.9/P < \beta < 3/P$. Although these rules are not rigorous, they are claimed to be valid over wide ranges of temperature and pressure.

Note that if liquids, gases, and even supercritical fluids can be handled this way, provided the EoS is well chosen, this does not hold for solids, and a specific method is implemented in this particular case as shown in section 4.2.4.

As outlined in the preceding section and as detailed in appendix E, since the EoS accounts for the intermolecular interactions even in mixtures if proper "mixing rules" are implemented, the cubic EoS, open the possibility to calculate the fugacities and derive the activity coefficients provided a proper thermodynamic transformation is applied from the ideal states to the real states. The methodology described in Appendix E.

For instance, the following mixing rules are suggested with the PR EoS:

$$\alpha = \sum_i \sum_j x_i x_j \left(1 - \delta_{ij}\right) \alpha_i^{1/2} \alpha_j^{1/2} \tag{2.36}$$

$$b = \sum_i x_i b_i \tag{2.37}$$

Where δ_{ij} is some empirically determined binary interaction coefficient between component i and component j. This is the primary deficiency of this method which is particularly acute when interactions are strong like with polar molecules, electrolytes …

To overcome this deficiency, Vidal in 1978[23] coupled the Peng-Robinson equation to activity coefficients appearing in the expression of G^E which is the "excess" Gibbs energy term appearing in the total Gibbs energy (as explained in the next section) and incorporating the non ideality effects. The criterion is that G^E derived from the EoS should be equal to that obtained from an independent explicit formulation of the activity coefficients (like UNIFAC…) at some reference pressure. If $\hat{\varphi}_i$ is the fugacity coefficient of component i in the mixture, and φ_i that of the pure compound i, the excess Gibbs energy, G^E is :

$$\frac{G^E}{RT} = \sum_i n_i \ln \frac{\hat{\varphi}_i}{\varphi_i} = \sum_i n_i \ln \gamma_i \tag{2.38}$$

So that:

$$\ln \gamma_i = \ln \frac{\hat{\varphi}_i}{\varphi_i} = \left(\frac{\partial G^E}{\partial n_i}\right)_{T,P,n_{j\neq i}} \tag{2.39}$$

In Huron-Vidal-Wong-Sandler approach, the reference pressure to which this applied equality is infinity whereas for PSRK models the reference pressure is zero.

The LCVM[25] method (LCVM stands for Linear Combination of the Vidal and Michelsen mixing rules) is more flexible since it does not specify any specific pressure. For this, another type of Peng-Robinson EoS is implemented as:

$$P = \frac{RT}{v-b} - \frac{a}{v(v+b)+b(v-b)} \tag{2.40}$$

With:

$$\alpha(T) = \alpha(T_C) \cdot \alpha(T_r, \omega) \tag{2.41}$$

The covolume parameter is that of the standard Peng Robinson EoS but the energy term is modified : $\alpha(T_c)$ is the energy parameter given by equation (2.32) but $\alpha(T_r, \omega)$ is different :

$$T_r = \frac{T}{T_c} \tag{2.42}$$

$$\alpha(Tc) = 0.45724 \frac{R^2 T_c^2}{P_c} \tag{2.43}$$

If ($T_r \leq 1$):

$$a(T_r, \omega) = \left[1 + c_1\left(1 - \sqrt{T_r}\right) + c_2\left(1 - \sqrt{T_r}\right)^2 + c_3\left(1 - \sqrt{T_r}\right)^3\right]^2 \tag{2.44}$$

If ($T_r \geq 1$):

$$\alpha(T_r, \omega) = \left[1 + c_1\left(1 - \sqrt{T_r}\right)\right]^2 \tag{2.45}$$

Coquelet et al.[26] proposed a method to generate the parameter of c1, c2 and c3 automatically:

$$c_1 = 0.1316\omega^2 + 1.4031\omega + 0.3906 \quad (2.46)$$

$$c_2 = -1.3127\omega^2 + 0.3015\omega \pm 0.1213 \quad (2.47)$$

$$c_3 = 0.7661\omega + 0.3041 \quad (2.48)$$

In this version of the PR EoS, all the required parameters can by derived from the group contribution theory. It is believed to be more accurate than the version presented above (equations (2.28) to (2.33).

In LCVM approach, a linear combination of the mixing rules of Huron and Vidal, and Michelsen is implemented, which does need a reference pressure and has been proved[27; 28] to be superior to the other EOS/g^E models. But the innovation is in the formulation of the energy parameter a.

$$\frac{a}{b \cdot R \cdot T} = \lambda \cdot \left(\frac{1}{A_v} \cdot \frac{g^E}{RT} + \sum x_i \frac{a_i}{b_i \cdot R \cdot T}\right) + (1-\lambda) \cdot \left(\frac{1}{A_M} \cdot \left[\frac{g^E}{RT} \times \sum x_i \ln\left(\frac{b}{b_i}\right)\right] + \sum x_i \frac{a_i}{b_i \cdot R \cdot T}\right) \quad (2.49)$$

Where the terms g^E/RT is calculated using the UNIFAC model ($\frac{g^E}{RT} = \sum_i x_i \ln \gamma_i$), the terms $\sum x_i \ln\left(\frac{b}{b_i}\right)$ and $\sum x_i \frac{a_i}{b_i \cdot R \cdot T}$ come from the Peng Robinson Equation of state, and A_M, A_V are constant coefficients proposed respectively by Michelsen and Vidal ($A_M = -0.52$, and $A_V = -0.623$). Coefficient λ is a sort of relaxation parameter and its value was selected empirically to obtain the best fit. When the original UNIFAC approach is chosen, the "best" value for this coefficient is 0.36 and this value was kept in the following.

Note that, for any pure component, the LCVM EoS is "naturally" reduced to the PR EoS.

2.1.4 Mathematical formulation of the Gibbs minimization problem

It is assumed that a chemical reaction occurs between nSp molecules (each is indexed "i") composed of nEl atoms (each indexed "j"). If a_{ij} is the number of atom j in the molecule i (available in n_i moles in the mixture), then the conservation of mass reads (b_j is the total number of atoms j in the initial mixture):

$$\varepsilon_j = \sum_{i=1}^{nEl} a_{ij} \cdot n_i - b_j = 0 \quad for\ 1 < j < nEl \tag{2.50}$$

At constant temperature and pressure, the chemical equilibrium is reached when the Gibbs energy of the mixture is minimum. Using the formalism given above, it comes:

$$G^0 = \sum_{i=1}^{NS} n_i \cdot \mu_{i0} + \sum_{i=1}^{NL} n_i \cdot \mu_{i0} + \sum_{i=1}^{NG} n_i \cdot \mu_{i0} \tag{2.51}$$

$$G^{mix} = \sum_{i=1}^{NL} n_i \cdot R \cdot T \cdot ln\left(\frac{n_i}{\sum_i^{NL} n_i}\right) + \sum_{i=1}^{NG} n_i \cdot R \cdot T \cdot ln\left(\frac{n_i}{\sum_i^{NG} n_i}\right) \tag{2.52}$$

$$G^E = \sum_{i=1}^{NL} n_i \cdot R \cdot T \cdot ln(\gamma_i) + \sum_{i=1}^{NG} n_i \cdot R \cdot T \cdot ln(\gamma_i) \tag{2.53}$$

$$G = G^0 + G^{mix} + G^E \tag{2.54}$$

Where *NS*, *NL*, and *NG* stand respectively for the number of solid, liquid and gaseous species (*nSp=NS+NL+NG*). The Gibbs energy of the mixture is expressed as the sum of the contributions of the Gibbs energies of formation of each pure species G^0, of the mixing of the species G^{mix} (increase of the entropy) and of the non-ideality G^E ("excess Gibbs energy") caused by the intermolecular forces in the real mixture. Note that for solids, it is assumed that the chemical potential depends mostly on the temperature, not from the other compounds and that they do not produce a mixing entropy (so they formally do not mix…).

2.2 Solving the Gibbs minimization problem

As it stands, the first difficulty is mathematics. The conservation of the species and G^0 expressions are linear functions of n_i but G^E is not, and G^{mix} is strongly nonlinear. Consider the case where n_i is very small, but not exactly zero. Because of the logarithm, G^{mix} may vary in enormous proportions even for tiny variations of n_i and convergence might be very difficult. In the following, several "popular" strategies employed are described and analyzed.

2.2.1 Mathematical methods to minimize the Gibbs energy

2.2.1.1 Lagrange multipliers" methods

Various numerical methods exist to minimize the Gibbs energy. Most of them were developed based on the Lagrange Multipliers method. This mathematical technique is meant to minimize the Gibbs energy while satisfying the conservation laws. The most renown chemical equilibrium codes (CEA from NASA[29] and ASPEN[30]) use it, but other techniques were proposed.

Morley, Gordon and Mc Bride use the "Lagrange multipliers" method[31] aiming at minimizing a function *f* knowing that constraints applied to the N variables. The constraints (1<j<p constrains) are represented by:

$$\varepsilon_j(N_i) = 0 \tag{2.55}$$

The Lagrange function is defined as:

$$La = f(N_1, N_2 \dots N_n) + \sum_{j=1}^{P} \lambda_j \times \varepsilon_j$$

Where λj are the "Lagrange multipliers" which are calculated at the same time than the n variable of the problem. The minimum point satisfying the constraints is obtained as (1<i<n) :

$$\frac{\partial La}{\partial N_i} = 0 \Leftrightarrow \frac{\partial f}{\partial N_i} - \sum_{j=1}^{p} \lambda j \times \frac{\partial \varepsilon_j}{\partial N_i} = 0 \qquad (2.57)$$

In the present context f=G, N_i=n_i, N=nSp, p=nEl and the constraints are the conservation of the species. Equation (2.57) provides N relationship whereas $N+p$ unknowns are looked for (n_i and λj). The p conservation laws (2.55) are needed to be solved at the same time. However, the derivatives of G depend very significantly on n_i (especially G^{mix}) so that the resolution can only be a very progressive, nonlinear, step-by-step approach. An additional difficulty is that the problem is fully implicit, the researched values n_i being intricate into other variables like G. To solve the problem some explicit formulation needs to be defined. The way of doing so makes differences between the various "Lagrangian methods".

Morley method (GASEQ, FREZCHEM[13])

A technique proposed by Morley [10] (GASEQ software) is a sort of modified Newton-Raphson method in which a first order Taylor development of the function $\partial La/\partial n_i$ as a function of n_i is applied to approximate the next value of this function. Morley considered only ideal mixtures so that G^E=0 containing gases. Let F(n_i) be the Lagrange function applied to the chemical equilibrium. Note that often μ_i^o is replaced by μ_i^o/R.T.

$$\mathrm{F}(n) = \sum_{i=1}^{nSp} n_i \left(\frac{\mu_i^0}{RT} + \ln\frac{ni}{\sum ni} + \ln P\right) - \sum_{j=1}^{nEl} \lambda_j \sum_{i=1}^{nSp} \left(a_{ij} n_i - b_i\right) \qquad (2.58)$$

The solutions correspond to situations where when F is a minimum for all i from 1 to nSp meaning that:

$$\frac{\partial F}{\partial n_i} = \frac{\mu_i^0}{RT} + \ln\frac{n_i}{\sum n_i} + \ln P + n_i \frac{\partial \ln n_i}{\partial n_i} - \sum_{k=1}^{nSp} n_k \frac{\partial \ln \sum n_i}{\partial n_i} - \sum_{j=1}^{nEl} \lambda_j a_{ij} = 0 \qquad (2.59)$$

It can be verified that the terms $n_i \frac{\partial \ln n_i}{\partial n_i} - \sum_{k=1}^{nSp} n_k \frac{\partial \ln \sum n_i}{\partial n_i}$ is zero so that:

$$\frac{\partial F}{\partial n_i} = \frac{\mu_i^0}{RT} + \ln \frac{n_i}{\sum n_i} + \ln P - \sum_{j=1}^{nEl} \lambda_j a_{ij} = 0 \tag{2.60}$$

Then a first order Taylor expansion of $\partial \mathrm{F}/\partial \mathrm{n_i}$ is applied. In the following n_i is the searched value of ni and Ni is the initial value.

$$\frac{\partial F}{\partial n_i} \approx \left(\frac{\partial F}{\partial x_i}\right)_{at\ n_i = N_i} + \sum_{k=1}^{nSp} \left(\frac{\partial}{\partial n_k}\left(\frac{\partial F}{\partial n_i}\right)\right)_{at\ n_i = N_i} (n_i - N_i) \tag{2.61}$$

Where:

$$\frac{\partial^2 F}{\partial n_k \partial n_i} = -\frac{1}{\sum N_i} \qquad \text{When } i \neq k$$
$$= \frac{1}{N_i} - \frac{1}{\sum N_i} \text{ When } i = k \tag{2.62}$$

Substituting into (2.61):

$$\frac{\partial F}{\partial n_i} \approx \frac{\mu_i^0}{RT} + \ln \frac{N_i}{\sum N_i} + \ln P - \sum_{j=1}^{nEl} \lambda_j a_{ij} + \frac{1}{N_i}(n_i - N_i) - \sum_{k=1}^{nSp} \frac{1}{\sum N_i}(n_i - N_i) = 0$$
$$\frac{\partial F}{\partial n_i} \approx \frac{h_i}{N_i} - \sum_{j=1}^{nEl} \lambda_i a_{ij} + \frac{n_i}{N_i} - \frac{\sum n_i}{\sum N_i} = 0 \tag{2.63}$$

Where:

$$h_i \equiv N_i \left(\frac{\mu_i^0}{RT} + \ln \frac{n_i}{\sum N_i} + \ln P\right) \tag{2.64}$$

Equation (2.63) provides *nSp* equations and (2.50) *nEl* equations whereas the number of unknowns are nSp and nEl (respectively n_i and λ_j). The system is closed. Note however that equation (2.63) is a transcendent function of n_i which may be difficult to solve. The technique is to note that if λ_j and $\frac{\sum n\mathrm{i}}{\sum N\mathrm{i}}$ are chosen as unknowns then n_i is obtained from equation (2.63):

$$n_i = -h_i + N_i \times \left(\frac{\sum n_i}{\sum N_i} + \sum_j \lambda_j \times a_{ij}\right) \tag{2.65}$$

Summing up equation ((2.65) for all n_i provides:

$$\sum_{\mathrm{i}=1}^{\mathrm{nSp}} h_\mathrm{i} = \sum_{\mathrm{j}=1}^{\mathrm{nEl}} \lambda_\mathrm{j} \sum_{\mathrm{i}=1}^{\mathrm{nSp}} N_\mathrm{i} a_\mathrm{ij} \tag{2.66}$$

Substituting ((2.65) into (2.50) provides a set of *nEl* equations:

$$\sum_{i=1}^{nSp}\left(-a_{ij}h_i\right)+\sum a_{ij}x_j+\frac{\sum n_i}{\sum N_i}\sum_{i=1}^{nSp}N_i a_{ij}+\sum_{j=1}^{nEl}\lambda_k\sum_{i=1}^{nSp}a_{ik}a_{ij}N_i-b_j=0 \qquad \text{for j=1 to nEl} \qquad (2.67)$$

The equation (2.67) and (2.66) are equations nEl+1 with unknowns λ_j and $\sum n_i/\sum N_i$. When the latter are known, it is sufficient to replace the obtained values in (2.65) to find all the values of n_i. Since the relationships (2.66) and (2.67) are linear functions of the unknown, equations (2.66) and (2.67) constitute a matrix

((**2.66**)–(2.67)) $\begin{bmatrix}\sum_i^{nSp}N_i\times a_{ij} & 0\\ \sum_{i=1}^{nSp}a_{i,j}a_{i,j}\times N_i & \sum_{i=1}N_i\times a_{i,j}\end{bmatrix}\times\begin{bmatrix}\lambda_j\\ \frac{\sum n_i}{\sum N_i}\end{bmatrix}=\begin{bmatrix}\sum_i h_i\\ b_j+\sum_i a_{i,j}\times h_{ij}\end{bmatrix}$

Figure 2.1) involving a constant column vector (containing the chemical potentials and the total number of atoms) equated to the unknown column vector (containing λ_j and $\sum n_i/\sum N_i$), multiplied by a matrix (containing the coefficients calculated as a linear combination of the previously estimated number of moles and of the atomic composition of the products). The solution is obtained by inverting the matrix:

$$(2.66)\\(2.67)\begin{bmatrix}\sum_i^{nSp}N_i\times a_{ij} & 0\\ \sum_{i=1}^{nSp}a_{i,j}a_{i,j}\times N_i & \sum_{i=1}N_i\times a_{i,j}\end{bmatrix}\times\begin{bmatrix}\lambda_j\\ \frac{\sum n_i}{\sum N_i}\end{bmatrix}=\begin{bmatrix}\sum_i h_i\\ b_j+\sum_i a_{i,j}\times h_{ij}\end{bmatrix}$$

Figure 2.1. The matrix of resolution of equations(2.66) and (2.67)

The method looks simple: from an initial guess of n_i, the derivatives are estimated, new values of n_i are found and the process loops until convergence but:

- as defined, the system of equations does not impose a "realizability" criterion telling that only positive values of n_i are relevant. When negative values occur, logarithms are undefined, and the calculation fails (the logarithmic term in the calculation of h_i generates an error). A potential solution

is to test the values of n_i and when they are negative, to replace them with a value close to 0. Nevertheless, doing so, convergence problems may arise since the corresponding logarithms may vary in large proportions for tiny variations of n_i;

- as acknowledged by the author, it is difficult to run the method when solids are added into the products, which is a severe limitation.

The software CHEETAH[32], using the same principle as TIGER, resembles the Morley method in its resolution method.

Gordon and Mc Bride method (CEA code)

A significant improvement of the robustness (and simplicity) of the Morley method was proposed by Gordon and Mc Bride (thus applicable to perfect gases and non-miscible condensed materials). They used again the Newton-Raphson principle, but instead of using a first order Taylor expansion of $\frac{\partial F}{\partial n_i}$ as function of n_i, the (Taylor) expansion is performed against $C_i = ln(n_i)$ and $D = ln\left(\sum_i^{NG} n_i\right)$ which fits much better with the evolution of G for gases, especially to tackle the evolutions of G_{mix}. This method is implemented in CEA, the thermochemical equilibrium code developed by NASA and in many comparable codes aiming at predicting the composition of gaseous combustion products. Note also that doing so, the increments in n_i are necessarily positive. A further advantage is that when n_i becomes very small, $\ln n_i$ is large so that limiting the increment on $\ln n_i$ instead of n_i limits the risk of divergence.

The starting equation is the same than for Morley (2.60). For the gaseous phase, the Lagrange function derivatives reads (given later for solids):

$$\frac{\partial F}{\partial n_i} = \frac{\mu_i^0}{RT} + \ln\frac{n_i}{\sum n_i} + \ln P - \sum_{j=1}^{nEl} \lambda_j a_{ij} = 0 \qquad (2.68)$$

And the first order Taylor expansion in C_k and D around N reads:

$$\frac{\partial F}{\partial n_i} = \frac{\mu_i^o}{R \cdot T} + ln(N_i) - ln\left(\sum_i^{NG} N_i\right) + \ln(P) - \sum_j \lambda_j \times aij + \sum_k \frac{\partial\left(\frac{\partial F}{\partial Ni}\right)}{\partial Ck} \times \Delta ln(n_k) + \sum_k \frac{\partial\left(\frac{\partial F}{\partial Ni}\right)}{\partial D} \times \Delta ln\left(\sum_i^{NG} n_i\right) = 0 \quad (2.69)$$

$$\frac{\partial\left(\frac{\partial F}{\partial N_i}\right)}{\partial C_k} = 1 \text{ for k=i and zero otherwise and } \frac{\partial\left(\frac{\partial F}{\partial N_i}\right)}{\partial \mathrm{D}} = -1 \quad (2.70)$$

Substituting the equation (2.70) into (2.69), and setting $\frac{\mu_i}{RT} = \frac{\mu^\circ i}{R \cdot T} + ln(N_i) - ln\left(\sum_i^{NG} N_i\right) + \ln(P)$:

$$\frac{\partial F}{\partial n_i} = \frac{\mu_i}{RT} - \sum_j \lambda_j \times a_{ij} + \Delta ln(n_i) - \Delta ln\left(\sum_i^{NG} n_i\right) = 0 \quad (2.71)$$

The mass conservation equation (2.50) is reconsidered separating the gases and the condensed part (the solids are labeled from *i=NG+1* to nSp):

$$\sum_{i=1}^{NG} a_{ij} \times N_i + \sum_{i=NG+1}^{nSp} a_{ij} \times N_i = b_j$$

A differential version of this equation can be written (for the gases $N_i \times \Delta \ln(n_i) = \Delta n_i$):

$$\sum_{i=1}^{NG} a_{ij} \times N_i \times \Delta \ln(n_i) + \sum_{i=NG+1}^{nSp} a_{ij} \times \Delta n_i = \Delta b_i \approx b_j - \sum_{i=1}^{nSp} a_{ij} \times N_i \quad (2.72)$$

The expression for $\Delta \ln n_i$ obtained from equation (2.70) is substituted into the equation (2.72) so that:

$$\sum_j^{nEl} \sum_i^{NG} a_{ij} \times a_{ij} \times N_i \times \lambda_j + \sum_{i=NG+1}^{nSp} a_{ij} \times \Delta n_i + \left(\sum_i^{NG} a_{ij} \times N_i\right) \times \Delta \ln\left(\sum n_{igaz}\right) = b_k - \sum_{i=1}^{nSp} a_{ij} \times N_i + \sum_{i=1}^{NG} a_{ij} \times N_i \times \frac{\mu i}{RT} \quad (2.73)$$

The last step of the mathematical development consists in differentiating the total number of moles of gas:$N = \sum_{i=1}^{NG} N_i$, in the following way:

$$N - \sum_{i=1}^{NG} N_i + dN - \sum_{i=1}^{NG} dN_i = 0$$

As above a transformation of *dN* into *dlnN* is proposed:

$$\sum_{i=1}^{NG} N_i \Delta \ln n_i - N \Delta \ln n = N - \sum_{i=1}^{NG} N_i \quad (2.74)$$

The expression of $\Delta \ln n_i$ from expression (2.70) is introduced in (2.74) to obtain a conservation law:

$$\sum_{j}^{nEl} \sum_{i}^{NG} a_{ij} \times N_i \times \lambda_j + \sum_{i=1}^{NG} (N_i - N) \times \Delta \ln(N) = N - \sum_{i=1}^{NG} N_i + \sum_{i=1}^{NG} N_i \times \frac{\mu i}{R \times T} \quad (2.75)$$

And for (non miscible) condensed material, equation (2.68) reduces to:

$$\sum_{j}^{nEl} a_{ij} \times \lambda_j = \frac{\mu i}{R \times T} \quad (2.76)$$

A system of 4 sets of equations (2.73), (2.75) and (2.76) is obtained which can be presented as a matrix containing as unknown the Lagrange multipliers, the increments of moles of each condensed material and the increment of the logarithm of the total number of moles in the gaseous phase. Note that once the latter parameters and the Lagrange multipliers are known, $\Delta \ln n_i$ can be calculated using (2.71).

$$\begin{matrix} (2.76) \\ (2.75) \\ (2.73) \end{matrix} \begin{bmatrix} 0 & a_{ij} & 0 \\ a_{ij} & \sum_{i}^{NG} a_{ij} \times a_{ij} \times N_i & \sum_{i=1}^{NG} a_{ij} \times N_i \\ 0 & \sum_{i}^{NG} a_{ij} \times N_i & \sum_{i}^{NG} \left(N_i - \sum_{i}^{NG} Ni \right) \end{bmatrix} \times \begin{bmatrix} \Delta n_{icond} \\ \lambda_j \\ \Delta \ln \left(\sum_{i}^{NG} n_{igaz} \right) \end{bmatrix} = \begin{bmatrix} \frac{\mu i}{R \times T} \\ b_j - \sum_{i=1}^{nSp} a_{ij} \times N_i + \sum_{i=1}^{NG} a_{ij} \times N_i \times \frac{\mu i}{R \times T} \\ N - \sum_{i=1}^{NG} N_i + \sum_{i=1}^{NG} N_i \times \frac{\mu i}{R \times T} \end{bmatrix}$$

Figure 2.2 Coefficient matrix of 'CEA' method.

Although this method can be seen as progress as compared to the Morley one, especially regarding robustness and computer efficiency, problems remain such as:

- in the case of a phase change, the variations of the Gibbs energy near the equilibrium are such that dG tends towards 0 so that $\frac{\partial F}{\partial N_i} and \frac{\partial G}{\partial n_i} \rightarrow 0$ and consequently the Lagrange multipliers should tend to zero also (see equation (2.57)). Then, because of the truncation errors, the mathematical problem becomes indeterminate.

- the coexistence of mixtures (especially gases) with solids is difficult to handle because primarily

the variations of G with n_i is linear for the solids and largely logarithmic for gaseous mixtures. If the existence of a solid is postulated which should not be present, the minimization process may produce negative values of n_i for the condensed phase, and the algorithm fails.

Rand and some others tried to improve the convergence of the Lagrange multipliers method.

Rand method (ASPEN, HSC, TEA code)

In Aspen software, the RGIBBS module minimizes the Gibbs free energy of a system using the RAND technique proposed by Gautam et al. in 1979[7]. HSC[21] and TEA[33] codes use the same technique.

The "N vector" contains guessed values of the number of moles of compound i in phase l (n_{il}) at equilibrium (p phases). Equation (2.54) is differentiated analytically with the specific assumption that $\partial\gamma_{il}/\partial n_{il} = 0$, and a quadratic 'Taylor development is used to approximate the Gibbs free energy at the **n** vector, a vector of mole numbers in close proximity to the N vector. Note that contrary to the QASEQ and CEA code, non-ideal mixtures can be computed:

$$G = \sum_{i=1}^{NS} \mu_i{}^{\circ} n_i^c + \sum_{i=NS+1}^{nSp} \sum_{l=1}^{p} \mu_{il} n_{il} \qquad (2.77)$$

Where p is the number of "mixed" phases (i.e., having a contribution in G^{mix} and G^E either in a vapor, liquid or solid phase), and *NS*, non-mixed condensates, usually solids (non-mixed condensates are from i=1 et *NS*). Parameter μ_{il} is the chemical potential of component i in phase l (for solids $\mu_i{}^{\circ}$ is the Gibbs energy of formation in the conditions of the reaction). Note that the superscript "c" is used to identify the number of moles of solids in the equations. The second order truncation reads:

$$Q(n_1, n_2, \dots, n_n) = G(N_1, N_2, \dots, N_n) + \sum_{i=1}^{NS} \frac{\partial G}{\partial N_i^C}\left(n_i^C - N_i^C\right) + \sum_{l=1}^{p} \sum_{i=NS+1}^{nSp} \frac{\partial G}{\partial N_{il}}(n_{il} - N_{il}) + \frac{1}{2}\sum_{i=1}^{NS} \frac{\partial^2 G}{\partial N_i^{c2}}\left(n_i^C - N_i\right)^2 + \frac{1}{2}\sum_{l=1}^{p} \sum_{i=NS+1}^{nSp} \sum_{i'=NS+1}^{nSp} \frac{\partial^2 G}{\partial N_{il}\partial N_{i'l}}(n_{il} - N_{il})(n_{i'l} - N_{il}) \qquad (2.78)$$

N is computed at minimum **Q** subject to the atom balance constraints. An unconstrained objective function, using Lagrange multipliers, $\lambda_j (j = 1, 2...nEl)$.

$$F\{n_1, n_2, \dots, n_n\} = Q\{N_1, N_2 \dots, N_n\} + RT \sum_{j=1}^{nEl} \lambda_j \left[b_j - \sum_{i=1}^{NS} a_{ij} n_i^c - \sum_{l=1}^{p} \sum_{i=\mathrm{NS}+1}^{nSp} a_{ij} n_{il}\right] \quad (2.79)$$

Is minimized using:

$$\frac{\partial F\{n\}}{\partial n_i^c} = \frac{\partial F\{n\}}{\partial n_{il}} = \frac{\partial F\{n\}}{\partial \lambda_j} = 0 \quad (2.80)$$

Equation (2.80) can be written:

$$\frac{\partial F\{n\}}{\partial n_i^c} = \frac{\partial^2 G}{\partial {n_i^c}^2}(n_i^c - N_i^c) + \frac{\partial G}{\partial n_i^c} + RT \sum_{j=1}^{nEl} \lambda_j \left[a_{ij}\right] = 0 \quad (2.81)$$

$$\frac{\partial F\{n\}}{\partial n_{il}} = \frac{\partial^2 G}{\partial {n_{il}}^2}(n_{il} - N_{il}) + \frac{\partial G}{\partial n_{il}} + RT \sum_{j=1}^{nEl} \lambda_j \left[a_{ij}\right] = 0 \quad (2.82)$$

$$\frac{\partial F\{n\}}{\partial \lambda_j} = RT\left[b_j - \sum_{i=1}^{NS} a_{ij} n_i^c - \sum_{l=1}^{p} \sum_{i=NS+1}^{nSp} a_{ij} n_{il}\right] = 0 \quad (2.83)$$

Because by definition,

$$\frac{\partial^2 G}{\partial {n_i^c}^2} = 0; \frac{\partial G}{\partial n_i^c} = \mu_i^0; \frac{\partial^2 G}{\partial {n_{il}}^2} = 0; \frac{\partial G}{\partial n_{il}} = \mu_{il}; \quad (2.84)$$

This problem, including the species conservation (2.50), also reduces to a matrix representation:

(2.83)

错误! 未找到引用源。)

(2.82)

$$\begin{bmatrix} \sum_{i=\mathrm{NS}+1}^{nSP} a_{ij} & a_{ij} & 0 \\ 0 & 0 & \sum_{j=1}^{nEl} a_{ij} \\ 0 & 0 & \sum_{j=1}^{nEl} a_{ij} \end{bmatrix} \times \begin{bmatrix} n_{il} \\ n_i^c \\ \lambda_j \end{bmatrix} = \begin{bmatrix} b_j \\ -\frac{\mu_i^o}{RT} \\ -\frac{\mu_{il}}{RT} \end{bmatrix}$$

Figure 2.3. Coefficient matrix, 'RAND' method.

Solving this system provides n. In the RAND method, the new "guessed" value of the *n* vector, called *n'*, is not automatically *n* because, as shown by Morley, negative values of the

number of moles can appear. n' is obtained as follows. Let Δ be the molar gap between N and n:

$$\Delta = (n_1, n_2, \dots, n_n) - (N_1, N_2, \dots, N_n) \tag{2.85}$$

n' is obtained as a fraction of Δ added to n via a constant coefficient w:

$$n' = N + w\Delta \tag{2.86}$$

w is chosen to provide a smaller Gibbs energy (than at n) and to avoid negative values of n'_{jl} and n'^{C}_{j}. This latter condition is reached when w is between w_{max}, (maximum value such that $N' \geq 0$) and w_{min} (minimum value such that $N' \geq 0$). dG/dw is computed as:

$$\frac{dG}{dw} = \sum_{i=1}^{NS} \frac{\mu_i^o}{RT} \Delta_i^C + \sum_{i=NS+1}^{nSp} \sum_{l=1}^{p} \mu_{il} \Delta_{il} \tag{2.87}$$

(because $\partial \gamma_{jl}/\partial w$ = zero) and μ_{il} calculated at n'. Beginning with $w = w_{max}$, w, is reduced by 0.1 w_{max} until a negative slope is obtained; if not found for $w > 0$, a similar search is conducted for $w_{min} \leq w < 0$. With the value of w thus estimated, the new guessed value of $n = n'$ is used and the process is looped. The RAND method is as significant improvement as compared to the Morley method, in particular when looking for phase equilibrium, but nevertheless is not universally valid:

- When a mixed phase l is postulated at the starting point which cannot exist in the starting conditions, the Rand method deceases rapidly its concentrations of the component in the "illegal phase" to zero. This causes the lines and columns associated with this "illegal phase" in the coefficient matrix to approach zero and singularities to develop which impedes the inversion of the matrix. The technique to avoid this is to eliminate this phase (remove the corresponding lines and columns from the matrix). But when phases are removed, the minimum Gibbs free energy is searched in a restricted domain so that the minimum is constrained and may not be the absolute one [34].

- For the solid phase, a similar difficulty as for the Morley and Gordon/Mc Bride methods is found. If the solid phase is not likely to exist at equilibrium, values of n_j^c become easily negative, values

of w becomes infinitesimal, and the code does not converge.

Additional techniques proposed to help to find the absolute minimum

The main drawback of the Lagrange method is that because the calculation has to start from an initially guessed value, there is a risk to go toward a local (constrained) minimum. Gautam et al. at 1979[35] devised the 'splitting phase' method to solve this difficulty. The principle of the method is, at a given point in the calculation, to split a phase into two trial phases and to use this new configuration in the minimization process if the Gibbs energy was effectively reduced. Only vapor (V) and liquid phases (L) can be split (V becomes V+L, L becomes V+L or L becomes L_1+L_2). Specific rules, and in particular the same activities of the species in two different phases, are applied to split the phases so that they are, before the minimization process, not too unrealistic (otherwise it would be rapidly eliminated by the RAND method). This method is implemented in ASPEN. As compared to the simple use of the RAND method as in HSC, the "phase splitting" technique seems a significant improvement but is not a panacea. First, as admitted by Gautham, it does not always avoid the constrained minimum and, even, may provide wrong results as when the source phase is, before splitting, already close to the equilibrium composition of the phase[36]. Nevertheless, this method is implemented in ASPEN. Later, Michelsen et al. [37; 38] attempted to apply the phase stability criterion initially developed by Gibbs to identify more robustly the situations in which a phase splitting should be applied. But it does not ensure a constrained minimum will not be reached. Levy and Montalvo[39] proposed the "tunneling" method. It is a succession of minimization cycles (with the RAND method for instance) and "tunneling" phases. Suppose a given

objective function, f(x) to minimize and having several local minima. Starting the first minimization phase at the point $x_1°$, the first local minimum to be found (**Figure 2.4**) is x_1*. The Tunneling Function reads:

$$T\big(x, f(x^*)\big) = f(x) - f(x^*) \tag{2.88}$$

x is increased (or decreased) starting from $x1*$ and T is calculated along the trajectory until T is negative. The point corresponding to T=0 is a new starting point $x_2°$. And the minimization process is restarted to reach a second local minimum x_2*. And so on until T is always positive. The last minimum is the absolute one x_G*. Note that this method is applicable primarily to the minimization problem of the Gibbs functions if the constraints (mass balance) are ignored. It is known that the minimum Gibbs point in a thermochemical problem is not the absolute one because of the mass balance constraints. So the tunneling technique may be better suited to phase changes where dG=0 as the equilibrium. On that aspect, it may help to decide if phase splitting is required.

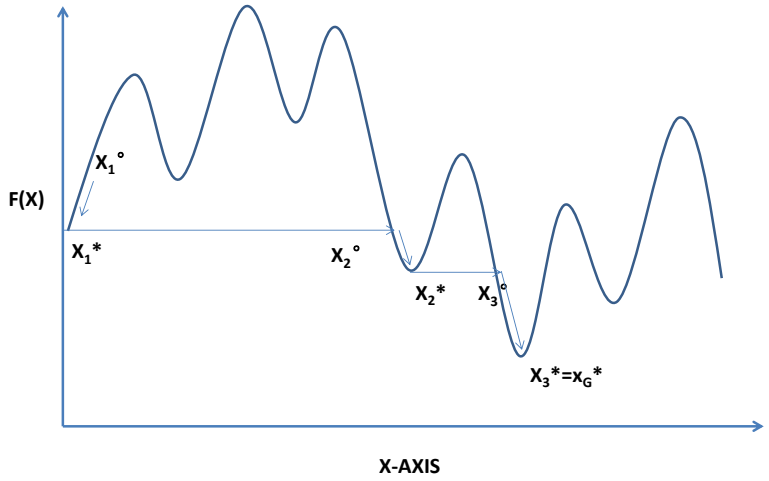

Figure 2.4. Illustration of the tunneling method.

The development of the Lagrange based algorithm is a significant breakthrough and allowed the development of numerically efficient computer codes to find thermochemical

equilibria by minimizing the Gibbs free energy. Nevertheless, many issues remain. The first one is that because it is an iterative process starting from an initial guess of the final composition, the algorithm may find a local minimum which may be far from the absolute one. Despite that some techniques were proposed to avoid this, this issue is not solved. The second issue is that the Gibbs function has to be linearized to solve the Lagrange problem. Necessarily the physical representatives are challenged (notably, the influence of the variations of the activity coefficients on G^E is ignored), and the truncation errors may jeopardize the convergence. This is the case when solid is to be considered in the mixture.

Recently some further developments were proposed[40],[41],[42] but these methods are still model-dependent, may require problem reformulation or significant computational time for multi-component systems.

Some other techniques not using the Lagrange theorem were proposed to avoid the relevant mentioned difficulties.

2.2.1.2 Other methods

The linear optimization

"Linear programming" has been extensively used in economics where it is often desired to minimize a cost of production, accounting for various constrains like the fixed and variable costs. Mathematically, the problem is as follows:

$$\text{Min } (C.X)$$

$$A \cdot X = B$$

$$X \geq 0$$

Where X is the vector of the variables. A, B, and C are matrices (B is a vector) with constant coefficients. $C \cdot X$ is the objective function to be optimized. The equation $A \cdot X = B$ defines a set of intersecting hyper planes in the space (order n) of the variables X. It can be shown that the optimized solution is located on one summit of the polyhedron defined by the intersection of these hyper planes. In 1947, Danztig[43] introduced an algorithmic method to find this optimum: the well-known "simplex method" aiming at systematically going from one summit to another and calculating the objective function there. Later other techniques were proposed. The resemblance of the equations above, with the problem of minimizing the Gibbs free energy (2.54) under the constraints of species conservation (2.50) and positivity of the number of moles ($n_i \geq 0$), is striking. Nevertheless, for the "linear programming" to work, it is essential for the objective function to be a linear function of the variables. For the specific case of ideal mixtures (formulation used in GASEQ and CEA), Dantzig proposed a linearization strategy of G. More recently Rossi et al.[44] used a similar methodology incorporating nonidealities. The authors proposed a methodology which was applied using the software 'GAMS'. 2.5 ("General Algebraic Modeling System"), using the CPLEX solver which can do the linear optimization. This method transforms the non-linear problem into a set of linear problems. Nonetheless, although the authors are not explicit on that aspect, many calculated values of G at different preselected compositions need to be provided to represent the G function conveniently by a set of linear approximations. The calculations are tedious and long. In practice, the cost of the calculations seems prohibitive especially when the number of species

is above 4.

Genetic algorithm:

Genetic algorithm[40] is a search heuristic algorithm for solving optimization problem. It is used in artificial intelligence. It is a kind of evolutionary algorithm. It is a kind of evolutionary algorithm. Evolutionary algorithms were firstly developed for many phenomena in biology, including inheritance, mutation, natural selection, and hybridization. The genetic algorithm can be divided into three steps: initialization, iteration, and selection.

In the initialization stage, the problem is translated in "genetic" terms. In the present context of Gibbs Energy minimization where $G(x_i) = \mu_i^o + RT(f_i/f°)$ and x_i is varying between 0 and 1 (a mole fraction for instance), the actual solution space ("phenotype" space) is composed of a set of x_i satisfying the mass conservation. This solution space should be encoded in "chromosomes" to define the "genotype" space where the genetic operations described in the iteration step could be performed. The "genes" describing the "chromosomes" is the binary code representing x_i in the computer language. If a two digits precision after the decimal is expected for x_i, then x_i will be encoded using seven binary numbers. The binary string represents the chromosome. To apply the Genetic Algorithm to phase equilibrium calculations for instance, instead of using n_{il} (for i = 1, 2, …, nSp; l= 1,2, …,p) as solution variables in the optimization, variables x_{il} (for i=1,2,…,nSp; l=1,2;…; p) varying in the range [0,1] have to be defined and employed as decision variables:

$$n_{il} = x_{il}\left(n_{iT} - \sum_{k=1}^{l-1} n_{ik}\right) \quad l = 1,2,\dots,\mathrm{p}-1 \tag{2.89}$$

Where n_{il} is the variation range of the mole number of species i in phase l. The mass conservation equation results in:

$$n_{ip} = \left(n_{iT} - \sum_{\iota=1}^{p-1} n_{il}\right) \quad (2.90)$$

For i=1, 2... nSp, the benefit of this modification is that all generated candidate solutions will be feasible which promotes an easy and efficient implementation of GA. Since GA can only handle maximization problems, the "fitness value" F is taken as the opposite of the Gibbs energy. Therefore, the minimization of Gibbs energy can be reformulated as:

$$\text{Maximize } F = -G(x_{il}),\ i = 1,2,\dots,nSp;\ l = 1,\dots p \quad (2.91)$$

$$\text{Subject to } 0 \leq x_{ik} \leq 1 \quad (2.92)$$

The function F is used to evaluate the quality of the points on which a selection will be performed the initial population is generated by choosing the genes randomly.

The iteration step is performed in three stages: selection, crossover, and mutation. Different types of Genetic algorithms exist[45]. A first technique is to choose randomly a couple of parents, to break their chromosome string as some predefined location and to rearrange them to form the chromosomes of the children (2.5). In this new population, some random mutations are allowed which consists of exchanging two genes chosen randomly in the chromosome string.

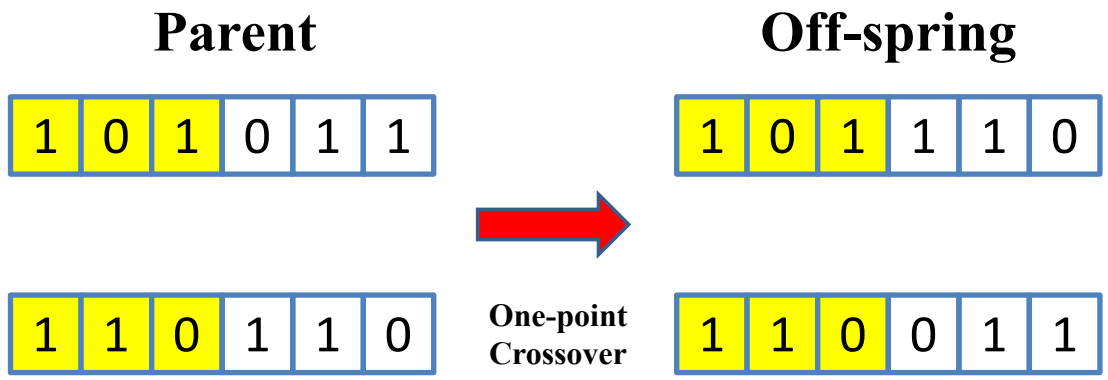

Figure 2.5. Illustration of the crossover stage.

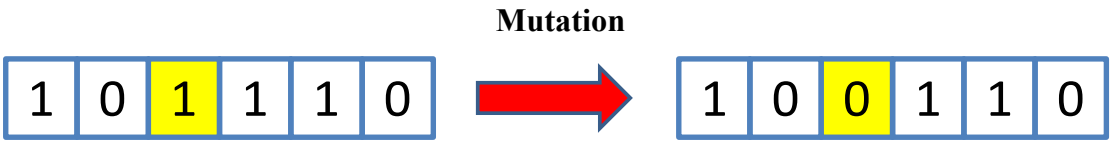

Figure 2.6. Illustration of the mutation stage.

A selection in the parent/child population is operated (so that the total number of individuals is constant) based on the fitness function according to which the "weaker" parents are replaced by the "stronger "children. In another technique, the fittest couple of parents are selected by groups of 4, and their genes are mixed according to arbitrary rules to produce two children. Similarly for the mutation stage (2 genes changed randomly, Figure **2.7**). The new population replaces the previous one. After many generations of evolution, the population satisfies the optimal requirements, and the chromosomes are the same. The convergence is reached and the iteration stops.

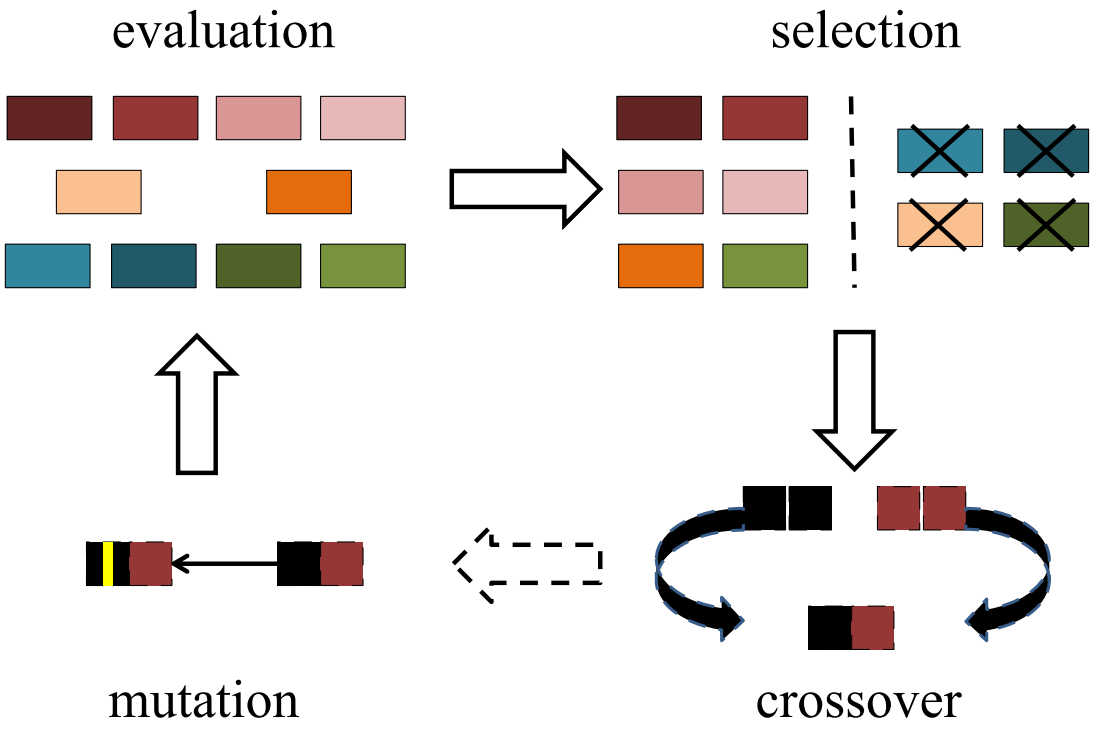

Figure 2.8. Illustration of the acceptance stage.

The example[46] of a binary system of n-butyl acetate and water is one of the most extensively studied examples in the literature. This method is very demanding in computing resources as recognized by the authors. It is doubtful this technique can handle many components. Furthermore, there is no guaranty that the global optimum can be found[40].

3 Illustration of some limitations

In everyday practice, software like CEA and Aspen are still of wide use because there are very efficient and fast in finding the Gibbs energy minimum even if many species are required.

Nevertheless, limitations exist and deserve special attention. In the present work, some of them were studied with more details.

3.1 Mathematical modeling aspects

The first difficulty is that solids introduce instabilities in the simulations because the risk of finding negative values for the related n_i variables is very high. Second, a local minimum may be reached instead of the global one because of the step by step approach. There is this no guarantee that the correct minimum can be found, and this is even more likely when multiphase reaction chemistry is expected. These aspects are the logical conclusions from the preceding chapter and will not be illustrated further.

Another limitation, developed below, is simplifications/linearization of the Lagrange problem is required which may affect the physical meaning of the Gibbs energy.

The distillation of a binary water-ethanol mixture is considered. The experimental data from Dortmund Data Bank[47] are used for comparison. In the simulations, the experimental condition is an adiabatic distillation at constant pressure (1atm). The initial enthalpy of the mixture is chosen inside the distillation peninsula (**Figure 3.1**). Iterating produces the equilibrium.

With the Gordon and Mc Bride method (**Figure 3.1**), the vapors keep the composition of

the original mixture. No ethanol is found in the liquid phase. One of the main reasons lies in the fact that the intermolecular forces are neglected especially in the condensed phase for which, also, the mixing entropy is neglected. It is also difficult to obtain a solution (convergence).

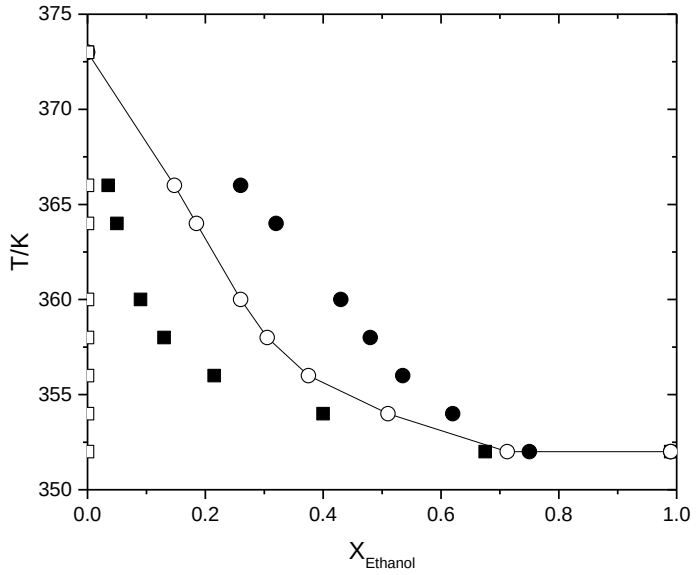

Figure 3.1. Distillation of an ethanol-water mixture. Comparison of the simulations using the Gordon and Mc Bride method (from CEA code) and experimental data (Dortmund Data Bank[47]). The points correspond to the % (in mole) of ethanol in the corresponding phase (ex 30% in the liquid phase means 30% of a mole of the liquid phase is ethanol) simulations-vapor,○; experiments-vapor,●; simulations-liquid,□; experiments-liquid,■.

The results obtained using the module RGIBBS (Rand Method) from ASPEN suite are shown in **Figure 3.2** and **Figure 3.3** using two different options to model the non-ideality of the fluids. The simulation can be much closer to the experiments but the accuracy depends significantly on the simulation choices.

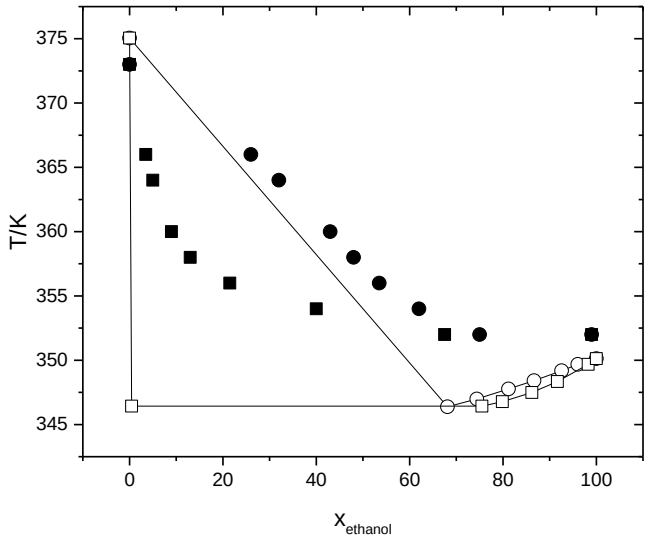

Figure 3.2. Distillation of an ethanol-water mixture. Comparison of the simulations using the rand method (ASPEN-RGIBBS with Peng Robinson Equation of state) and experimental data from Dortmund Data Bank[47]. Simulations-vapor, ○; Experiments-vapor, ●; Simulations-liquid, □; Experiments-liquid, ■.

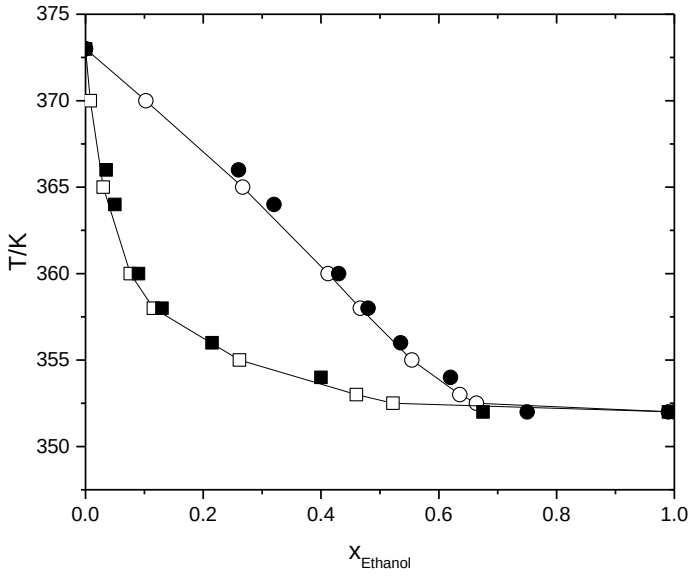

Figure 3.3. Equilibrium phase diagram of the ethanol-water mixture. Comparison of the simulations using the ASPEN RGIBBS Unifac method and experimental data from Dortmund Data Bank[47]. Simulations-vapor, ○; Experiments-vapor, ●; Simulations-liquid, □; Experiments-liquid, ■.

3.2 Physical modeling aspects: influence of the accuracy of the thermodynamic data

3.2.1 Analysis

The input thermochemical data are the chemical potentials of the pure components (at ambient pressure and temperature of the equilibrium) and the activity and fugacity coefficients which describe the departure from the ideal mixtures (i.e. the incidence of the molecular interactions).

Considering a three components mixture (n_1, n_2 and n_3) with one product (n_3) being a diluent (no variation of its number of moles). The atom balance (2.50) between n_1 and n_2, imposes a relationship which can be written as below:

$$n_2 = C - A \cdot n_1 \tag{3.1}$$

Where C and A are constants. In the presence context where n1 turns into n_2, typically for a phase change which is considered here, A is unity. Equation (3.1) can be inserted in (2.51) to (2.54) and the only dependent variable is n_1 since n_3 is constant. The minimum of G is obtained when $\frac{dG}{dn_1} = 0$. If we consider that n_1 is a liquid and n_2, n_3 gases, after some straightforward calculations (Appendix A), the final expression reads:

$$0 = \mu_{10} - A \cdot \mu_{20} - A \cdot R \cdot T \cdot ln(x_2) - A \cdot R \cdot T \cdot \left[ln\gamma_2 + \frac{d\gamma_2}{dx_2} \cdot \frac{(1-x_2)\cdot x_2}{\gamma_2} + \frac{d\gamma_3}{dx_2} \cdot \frac{(1-x_2)^2}{\gamma_3}\right] \tag{3.2}$$

Where x_2 is the molar fraction of component 2 in the gaseous phase (containing only components 2 and 3) and is the eigenvalue parameter of this problem. The contribution of the formation energies of the components on one end and of the molecular interactions are now rather explicit.

The influence of the accuracy chemical potential of the pure components is illustrated first setting the fugacity coefficients equal to 1 (ideal mixtures). Then (3.2) reduces to:

$$\ln(x_2) = \frac{\mu_{10} - A \cdot \mu_{20}}{A \cdot R \cdot T} \tag{3.3}$$

This equation suggests that the accuracy of the determination of the chemical potentials should be smaller than R.T or, more accurately, that the method used to determine the chemical potentials should not generate deviations from one component to another comparable to R.T, and thus should typically be smaller than 1kJ/mole. This finding challenges the use of thermochemical data from different sources in which the uncertainties associated with the chemical potentials amount several kJ/mole at least .

Now, the question of the accuracy of the activity coefficients is addressed. From equation (3.2), the deviation of the molar fraction of component 2 from the ideal mixture case (given by equation (3.3) reads:

$$ln\left(\frac{x_2}{x_{2\_id}}\right) = -\left[ln\gamma_2 + \frac{d\gamma_2}{dx_2} \cdot \frac{(1-x_2)\cdot x_2}{\gamma_2} + \frac{d\gamma_3}{dx_2} \cdot \frac{(1-x_2)^2}{\gamma_3}\right] \tag{3.4}$$

A graphical representation is proposed (**Figure 3.4**) in which the ideal mixture case is compared to a constant (γ_2=2) and a variable activity coefficient (γ_2=2 and $1/\gamma_2 \cdot d\gamma_2/dx_2 = 1/\gamma_2 \cdot d\gamma_3/dx_2 = 1$) case, which is more realistic. Note that both the coefficient of activity chosen and its variations are typical orders of magnitude encountered in real systems.[48]

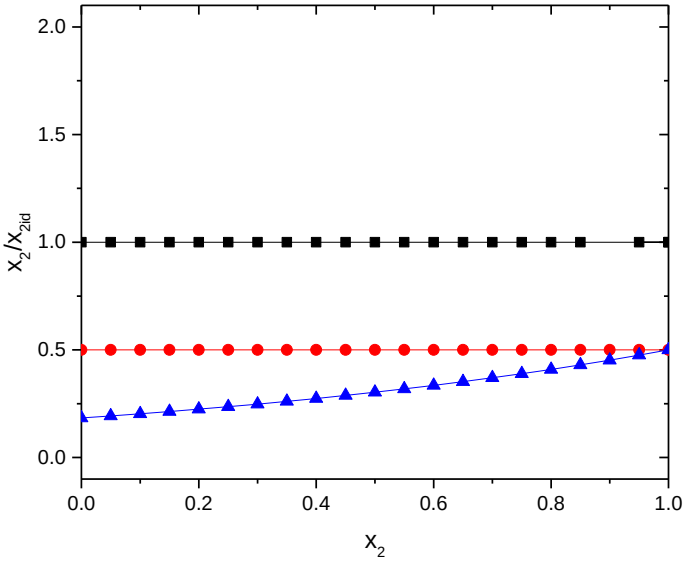

Figure 3.4. Ideal mixtures approximation as compared to a constant (γ_2=2 and d γ_2/dx_2= dγ_3/dx_2=0) and a variable coefficient of activity (γ_2=2 and $1/\gamma_2$.d γ_2/dx_2=$1/\gamma_2$.d γ_3/dx_2=1). The latter case is labeled "real mixture". ideal mixture, ■; constant act. Coeff, ●; real mixture, ▲.

It appears that a significant deviation is possible, within the ratios of 2 to 4, when the details of the variations of the coefficient of activity are ignored. Even a quasi-constant approximation (with $d\gamma_2/dx_2$=0) may not be satisfactory.

The last point deals with the representativity of the list of the chosen final products. A similar methodology as above is used to show this. A two components one phase mixture (n_1, n_2) is considered (polymerization for instance). The mixture is ideal (activity coefficients=1). The atom balance between n_1 and n_2, gives again:

$$n_2 = C - A \cdot n_1 \qquad (3.5)$$

Where C and A are constants. Equation (3.5) can be inserted in (2.50) to (2.54), and the only dependent variable is n1. The minimum of G is obtained when $dG/dn_1 = 0$. After some straightforward calculations, the final expression reads:

$$0 = \mu_{10} - A \cdot \mu_{20} - A \cdot R \cdot T \cdot ln(1 - x_1) + R \cdot T \cdot ln(x_1) \qquad (3.6)$$

Where x_1 is the molar fraction of component 1 is the eigenvalue parameter of this problem. Clearly, x_1 depends significantly on the "balance" of chemical potentials. ((3.6) reduces to:

$$\ln\left(\frac{(1-x_1)^A}{x_1}\right) = \frac{\mu_{10}-A\cdot\mu_{20}}{R\cdot T} \tag{3.7}$$

$$\frac{(1-x_1)^A}{x_1} = e^{\frac{\mu_{10}-A\cdot\mu_{20}}{R\cdot T}}$$

The evolution of x_1 as a function of the relative "balance" of chemical potentials is shown in **Figure 3.5**.

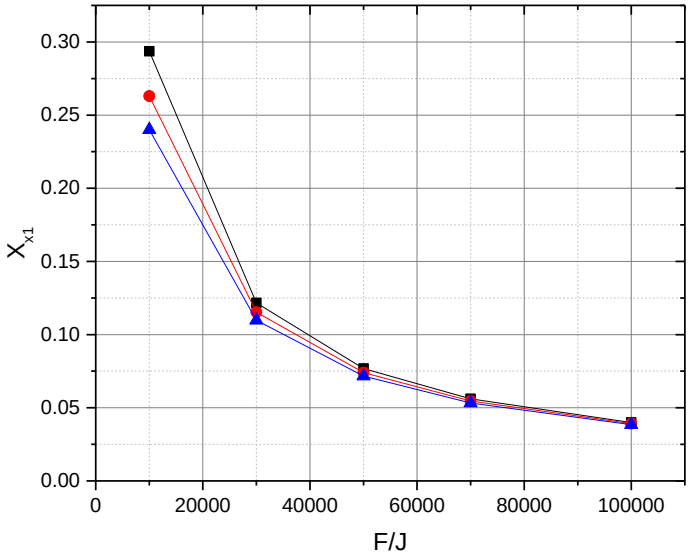

Figure 3.5. The variations in x_1 when A change from 1 to 2. $F = \mu_{10} - A \cdot \mu_{20}$, x_{x1} is the molar fraction of x1. A=1, ■; A=1.5, ●; A=2, ▲.

It appears that variations in x_1 seem to become significant (by 20% typically) as soon as the "balance" of chemical potentials is shifted by more than 10%. For many organic molecules, the individual chemical potentials are on the order of 100 kJ/mole, so that inserting or removing one component with a typical standard Gibbs energy of formation of tens of kJ is likely to impair the predictions not only from the relevancy point of view of the reaction but also for numerical reasons.

3.2.2 Illustrations

An illustration of the influence of the accuracy of the thermodynamic data (enthalpy of formation) is proposed for a 5 components chemical reaction consisting in a water gas shift simulation (C, CO, CO_2, H_2O, H_2). In this kind of reactions, the amount of produced CO is seen as a sensitive indicator of the global reaction since it is produced by the C/H_2O reaction and consumed in the CO/H_2O reaction. The evolution of the CO molar fraction as a function of the pressure and temperature of the reactions is shown in **Figure 3.6** knowing that all components (except C) are perfect gases. In this simulation, the standard enthalpy of formation of CO is 110 kJ/mole.

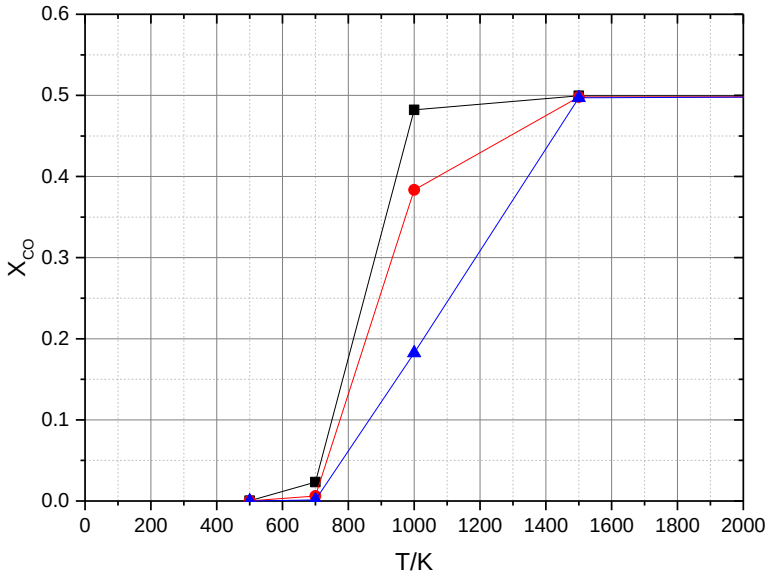

Figure 3.6. CO volumetric fraction in a 5 components water shift reaction as a function of the pressure and temperature of the reaction under the assumption of perfect gases-reference cases. 10kPa, ■; 100kPa, ●; 1Mpa, ▲.

The changes in the CO volumetric fraction are shown in **Figure 3.7** when the standard enthalpy of formation of CO is changed by ±1%, ±5% or ±10%.

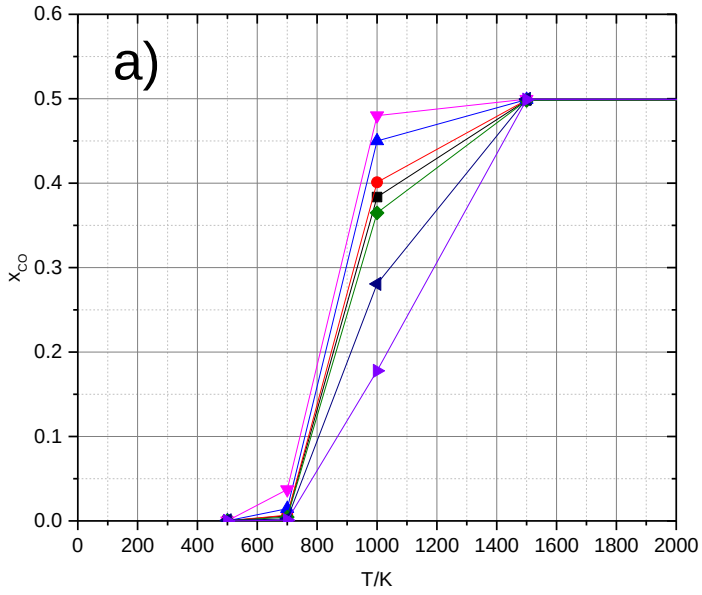
a)
0.6
0.5
0.4
0.3
0.2
0.1
0.0
x_{CO}
0
200
400
600
800
1000
1200
1400
1600
1800
2000
T/K

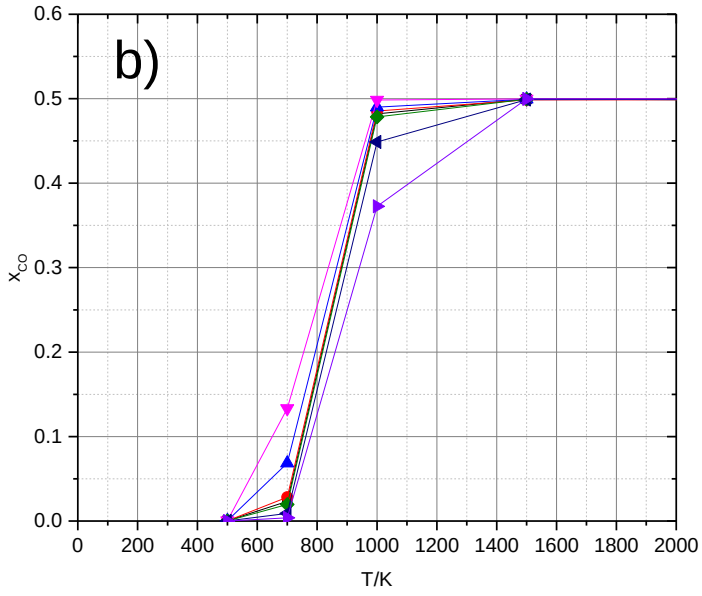
b)
0.6
0.5
0.4
0.3
0.2
0.1
0.0
x_{CO}
0
200
400
600
800
1000
1200
1400
1600
1800
2000
T/K

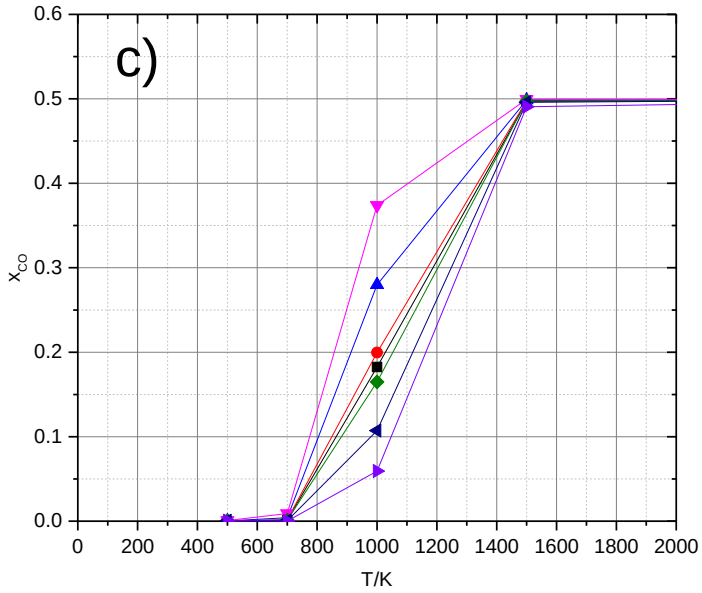

Figure 3.7. CO volumetric fraction in a 5 components water shift reaction as a function of different pressure a) 100kPa, b) 10kPa and c) 1MPa and temperature of the reaction under the assumption of the perfect gas. Influence of the accuracy of thermochemical data (variation of the standard enthalpy of formation of CO). Reference case at 100kPa,■; Hf_{CO}+0.01Hf_{CO}, ●; Hf_{CO}+0.05Hf_{CO}, ▲; Hf_{CO}+0.1Hf_{CO}, ▼; Hf_{CO}-0.01Hf_{CO}, ◆; Hf_{CO}-0.05Hf_{CO}, ◀; Hf_{CO}-0.1Hf_{CO}, ▶.

This example shows a clear influence on the values of the thermochemical data and in particular of the Gibbs energy of formation of the components (in which the standard enthalpy of formation is the main aspect). The pressure influences the evolution of the entropy. Globally a 10% change in the standard enthalpy of formation of CO, i.e. ±10 kJ/mole, produces erratic results. Perhaps ±1% variations, ±1 kJ/mole, would seem more acceptable.

An illustration of the influence of the intermolecular forces estimation is presented below about the distillation of ethanol-water mixtures at atmospheric pressure (**Figure 3.8**). Clearly assuming ideal mixtures provides results rather far from the reality. In textbooks, the activity coefficients of ethanol and water are respectively on order 2 so that the real concentrations in the gaseous phase should be about twice smaller. However, even doing this correction, the agreement would remain poor (not shown on the figure). The variations of the activity

coefficient with the compositions should be included. This is done, partly at least, when using the RAND method for which a quadratic Taylor approximation of G is performed to be able to run the step by step algorithm. However, this Taylor approximation removes the derivatives of the activity coefficients. It can be seen in **Figure 3.8** (right) that even when using very accurate data (UNIFAC activity models) some deviations from the experiments are visible.

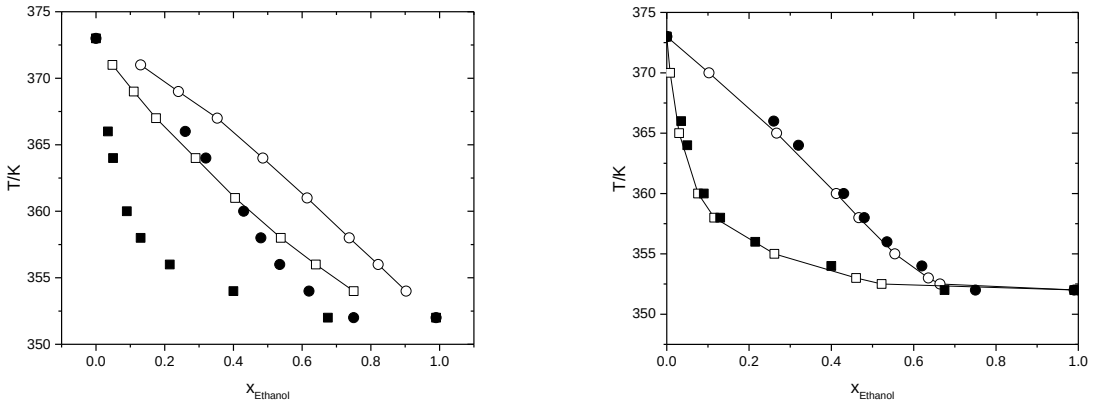

Figure 3.8. Simulation (ASPEN-RGIBBS) of the water-ethanol equilibrium (atmospheric pressure) using the ideal mixtures approximation (left) and UNIFAC (right).

3.3 Chemical modeling aspects: influence of the relevancy of the list of products

Before running a simulation, the list of the products expected to be present at the thermodynamic equilibrium should be established. This choice is sensitive.

To analyze this, the reader is referred again to expression (3.7) and to **Figure 3.5**. The chemical potential balance can not only be impaired by numerical uncertainties affecting each chemical potential but even more by the omission (or undue incorporation) of a species. The balance would easily be switched by tens of kJ so that a severe impact on the reaction yield may

appear.

A typical illustration of the influence of the representativity of the list of products is presented below again with the 5 components chemical reactions consisting in a water gas shift simulation (C, CO, CO_2, H_2O, and H_2). In this kind of reactions, the amount of CO produced can be seen as a sensitive indicator of the global reaction since it is produced by the C/H_2O reaction and consumed in the CO/H_2O reaction. In this case, the evolution of the H_2 molar fraction is chosen and shown in **Figure 3.9** as a function of the pressure and temperature of the reactions.

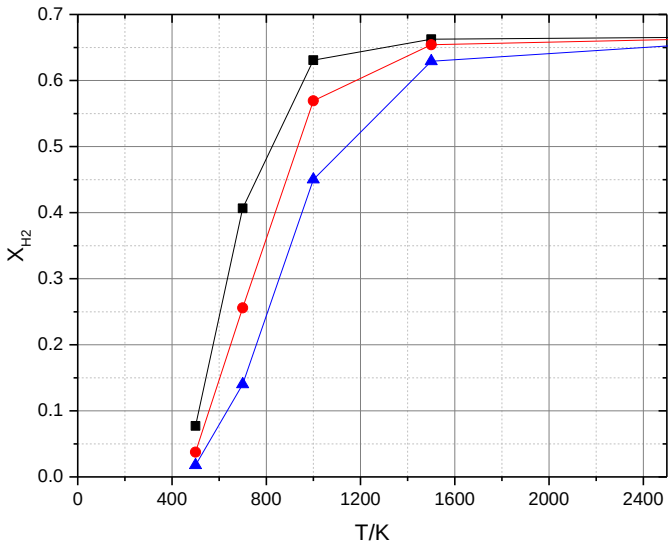

Figure 3.9. H_2 volumetric fraction in a water shift reaction as a function of pressure and temperature of the reaction under the assumption of the perfect gas. Reference case: 10kPa, ■; 100kPa, ●; 1Mpa, ▲.

In **Figure 3.10**. The calculations are reprocessed by removing CO. Very clearly the results are significantly different, not only about the maximum H_2 yield (70% when CO is removed as compared to 50%), but also the evolutions as a function of the temperature.

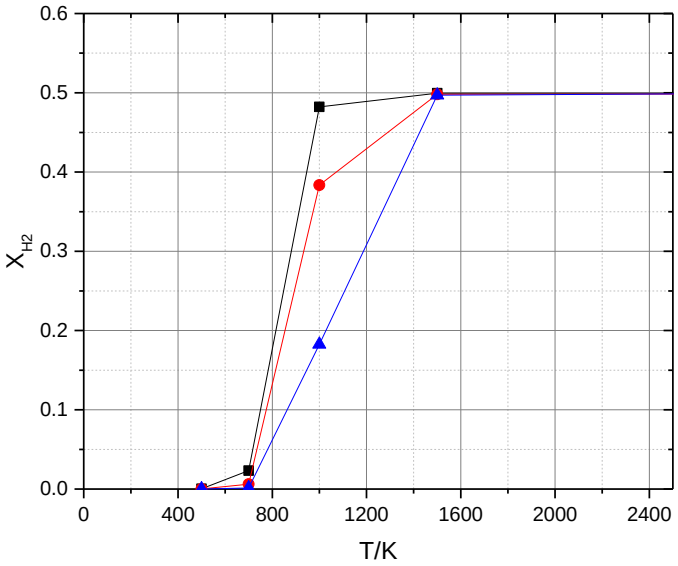

Figure 3.10. H_2 volumetric fraction in a water shift reaction as a function of pressure and temperature of the reaction under the assumption of perfect gas without considering CO. 10kPa, ■; 100kPa, ●;1Mpa ▲.

3.4 Synthesis

Great progress was made in the second half of the 20th century when numerical method attempting to calculate the minimum of the Gibbs energy function were developed to determine the thermodynamic equilibrium of a complex multiphase, multispecies transformation. Most of them are based on the Lagrange multipliers method (LM), a powerful mathematical method particularly efficient computationally speaking. More exotic techniques were tested like the global optimization (SIMPLEX), genetic algorithm but which do not really solve the difficulties associated with the use of the Lagrange multipliers technique.

Among them, the necessity to linearize the Gibbs function locally (with is strongly nonlinear) and the step by step approach limit the predictability. At best, the closest minimum to the initial “guess” is found. For multiphase reactive mixtures, and non-ideal mixtures, the Gibbs function may be strongly nonconvex exhibiting a multitude of local minima. A new

method to solve this is presented in the next chapter.

Other difficulties were identified such as the accuracy of the thermodynamic data (enthalpy/entropy of formation). It was shown above that wrong results may be obtained if the relative accuracy of the thermochemical data is lower than typically 1kJ/mole. A systematic bias would not a problem, but scattering/inconsistencies between the data sources for the components would easily produce larger relative uncertainties. A similar finding was obtained as for the activity coefficients. A potential solution would be to estimate all the thermochemical properties for the pure components and the intermolecular forces in a coherent way, or in other words, based on the same physical principles. A solution is presented in the next chapter.

It was also demonstrated that it is of paramount importance to select from the beginning, the relevant list of final products. The first difficulty is to be exhaustive enough and the second one to sort the list of products as a function of the targeted reaction conditions. Routes to achieve this are suggested in the next chapter.

4 Development of alternative methods and implementation in a new software: CIRCE

Solutions to the previous problems were investigated one by one. They are presented in the sections 3.1, 3.2 and 3.3. There were bridged together into a new thermodynamic code, named CIRCE, to challenge the relevancy of these solutions. The latter code is described in section 3.4.

4.1 The MCGE (Monte Carlo + Gaussian Elimination) method

Because the mathematical problem is not convex in general, and because it can be highly nonlinear, especially when multiphase mixtures are concerned, the Lagrange method coupled with some Newton-Raphson technique cannot guarantee a correct result.

The principle of the proposed method is to calculate the Gibbs energy of a “large enough” number of composition vectors chosen in the “realizable” space, i.e., fulfilling the species conservation. Then the global optimum can easily be found using traditional spanning techniques. There is no need to linearize the problem nor to guess a starting point. The two major drawbacks of the Lagrange/Newton-Raphson methods can thus be avoided if the MCGE method is applied. But other difficulties may appear like the minimum number of composition vectors required to ascertain that the global optimum was found, the accuracy of the solution and the costs of the calculation.

The MCGE procedure is a combination of a Monte Carlo heuristic search method and of a Gaussian Elimination technique. To the knowledge of the present author, it is new in the context of chemical equilibrium simulation.

4.1.1 Monte Carlo step

Once a total number of composition vector N_v is chosen, the species compositions in each vector are chosen randomly. This technique is typically derived from the Monte Carlo method[49] invented in the late 1940s by Stanislaw Ulam (One of his colleagues suggested using the name Monte Carlo[50]). One advantage of the Monte Carlo method as compared to a systematic "meshing" of the composition space is that for a given number of composition vectors Nv, two different minimization exercises of the same problem would provide different minima if Nv is not large enough. This is also faster and ensures intrinsically an equal probability of appearance of each composition vector in the realizable space.

The Monte Carlo method may be used abruptly. Composition vectors are produced randomly and then only the "realizable" composition vector, i.e., those satisfying the mass conservation (equation (2.50)), are conserved. To make this method more efficient, a first level of constraining can be applied to the random choice methodology. Consider for instance a specific product "i" with an elementary composition a_{ij} (1<j<nEl). The number of moles of this product should satisfy:

$$n_i \leq n_{imax} = min_j \left(\frac{b_j}{a_{ij}}\right) \tag{4.1}$$

Let Rand () be the mathematical function of the computer generating an arbitrary number between 0 and $RAND_{max}$ ($RAND_{max}$=32767) with equal probabilities, then Rand ()/$RAND_{max}$ is an arbitrary number between 0 and 1. The number of moles of species "i" is estimated as:

$$\frac{n_i}{n_{imax}} = \frac{Rand\ ()}{RAND_{max}} \tag{4.2}$$

Let Δ be the average gap between two successive values of n_i/n_{imax}. Between 0 and 1, there are $1/\Delta$ possible values of n_i/n_{imax} so that for a composition vector containing nSp components, a total number of composition vectors produced arbitrarily amounts$(1/\Delta)^{nSp}$.

But only a fraction of them can satisfy the *nEl* atom conservation laws. Because of the average gap between two consecutive component mole fractions, each conservation law can only be satisfied to within ± Δ at best. There is a considerable probability that none of the Nv composition vectors satisfies strictly the atom balance. Some "acceptance criterion" should be settle: for instance, it can be stated that the atom balance would be judged fulfilled if the total number of atoms j (in an accepted composition vector) is not different from b_j by more than ± q.Δ (with q> 1) for all j. Starting from a composition vector satisfying the atom conservations laws to within ± q.Δ, all the composition vectors satisfying this can be derived by reasoning by pairs of components. If the number of atom j of component i (a_{ij}) is decreased by δ_j, the number of atom j of component i+1 is increased by δ_j. The δj is linked with Δ and a_{ij} (also note that since all conservation laws are interlinked, the acceptance criterion for a given atom j is automatically valid for the other atoms). Based on this reasoning, the number of composition vectors satisfying the atom conservation laws within the relative accuracy ± q.Δ reads:

$$2 \cdot q \cdot (nSp - 1) \cdot \left(\frac{1}{2 \cdot \Delta}\right) \tag{4.3}$$

If a minimum of 1000 “realizable” composition vectors (i.e., satisfying the atom balances) is needed to find the Gibbs energy minimum for nSp=3 and q=1, then (4.3) equals 1000 and gives $\Delta=1/500$ meaning 500^3 initial composition vectors….

So, this method is very unproductive and can hardly be envisioned in practice. Furthermore, the imperfect satisfaction of the atom balance renders the final result of the Gibbs minimization exercise inaccurate especially for phase changes.

4.1.2 Gaussian elimination step

The idea is to limit the use of the Monte Carlo method to the minimum number of species and to derive the quantities of the remaining species using the atom balance by implementing the “Gaussian elimination method”.

Consider, for instance, six species U, V, W, X, Y, Z composed of three different atoms E1, E2, E3 (**Table** 4.1). The unknown variables are the mole’s numbers u, v, w, x, y, z whereas the total numbers of atoms NE1, NE2, NE3 are known so as the atomic composition of U, V, W, X, Y, Z (a_i, b_i, c_i are the number of atoms of respective elements E1, E2 and E3 in molecule i).

Table 4.1“coefficient” matrix of the products U, V, W, X, Y, Z

Elements↓/molecules→	U	V	W	X	Y	Z	Totals
E1	a1	a2	a3	a4	a5	a6	NE1
E2	b1	b2	b3	b4	b5	b6	NE2
E3	c1	c2	c3	c4	c5	c6	NE3

This “coefficient” matrix of the products is a problem with six unknowns and three equations. To solve it, u, v and w are chosen randomly as shown in the section above whereas

x, y and z are calculated using a Gaussian elimination method as explained below. As a first step, the atom balance is written as:

$$a_4 \cdot x + a_5 \cdot y + a_6 \cdot z = N_{E1} - a_1 \cdot u - a_2 \cdot v - a_3 \cdot w = R_{E1} \quad (4.4)$$

$$b_4 \cdot x + b_5 \cdot y + b_6 \cdot z = N_{E2} - b_1 \cdot u - b_2 \cdot v - b_3 \cdot w = R_{E2} \quad (4.5)$$

$$c_4 \cdot x + c_5 \cdot y + c_6 \cdot z = N_{E3} - c_1 \cdot u - c_2 \cdot v - c_3 \cdot w = R_{E3} \quad (4.6)$$

The objective of the method is to eliminate x from the second equation and w, y from the third one so that z could be calculated then y and lastly x. This is done by applying a series of linear combinations of the atom balance equations.

The first equation is kept as such whereas x is eliminated from (4.5) and (4.7) using a linear combination with (4.8) : (b_4·(4.4)-a_4·(4.5))=(4.7) and c_4·((4.4)-a_4·(4.6))=(4.8):

$$a_4 \cdot x + a_5 \cdot y + a_6 \cdot z = R_{E1} \quad (4.4)$$

$$(a_5 \cdot b_4 - b_5 \cdot a_4) \cdot y + (a_6 \cdot b_4 - b_6 \cdot a_4) \cdot z = b_4 \cdot R_{E1} - a_4 \cdot R_{E2} \quad (4.9)$$

$$(a_5 \cdot c_4 - c_5 \cdot a_4) \cdot y + (a_6 \cdot c_4 - c_6 \cdot a_4) \cdot z = c_4 \cdot R_{E1} - a_4 \cdot R_{E3} \quad (4.10)$$

Lastly, a linear combination of ((4.9) and (4.10) is applied to eliminate y. The final system reads:

$$a_4 \cdot x + a_5 \cdot y + a_6 \cdot z = R_{E1} \text{ ((4.4)}$$

$$(a_5 \cdot b_4 - b_5 \cdot a_4) \cdot y + (a_6 \cdot b_4 - b_6 \cdot a_4) \cdot z = b_4 \cdot R_{E1} - a_4 \cdot R_{E2} \quad (4.11)$$

$$[(a_5 \cdot c_4 - c_5 \cdot a_4) \cdot (a_6 \cdot b_4 - b_6 \cdot a_4) - (a_5 \cdot b_4 - b_5 \cdot a_4) \cdot (a_6 \cdot c_4 - c_6 \cdot a_4)] \cdot z =$$

$$(a_5 \cdot c_4 - c_5 \cdot a_4) \cdot (b_4 \cdot R_{E1} - a_4 \cdot R_{E2}) - (a_5 \cdot b_4 - b_5 \cdot a_4) \cdot (c_4 \cdot R_{E1} - a_4 \cdot R_{E3})$$

(4.12)

The mole number z is deduced from (4.12), then y is deduced from (4.11), and then x is calculated from ((4.4).

The method is efficient as long as the multipliers of x, y and z are not zero and when the number of species is larger than the number of atom types.

The first situation above may arise for instance for purely numerical reasons. A simple remedy is to reorganize the "coefficient" matrix so that the multipliers calculated after having applied the Gaussian elimination method are not zero anymore. It may also arise when two chemically identical compounds (isomers or identical product in two different states) are present in the mixture. To solve this difficulty, it is essential that one of the "isomer" is part of the components selected using the Monte Carlo method and thus is withdrawn from the Gaussian elimination step.

The second situation is usually derived from the previous one. Consider for instance, the distillation of a binary mixture (4 products) with 3 elements (ex: water and ethanol: **Table 4.2**). If the preceding method is applied, U is chosen using the Monte Carlo method, and then the Gaussian elimination method is applied.

Table 4.2. "Coefficient" matrix for a binary distillation.

Elements↓/molecules→	U	V	W	X	totals
E1	a1	a2	a1	a2	NE1
E2	b1	b2	b1	b2	NE2
E3	c1	c2	c1	c2	NE3

At the end of the process the atom balance equations read:

$$a_2 \cdot v + a_1 \cdot w + a_2 \cdot x = R_{E1} \tag{4.13}$$

$$(a_1 \cdot b_2 - b_1 \cdot a_2) \cdot w + (a_2 \cdot b_2 - b_2 \cdot a_2) \cdot x = b_2 \cdot R_{E1} - a_2 \cdot R_{E2} \tag{4.14}$$

$$[(a_1 \cdot c_2 - c_1 \cdot a_2) \cdot (a_2 \cdot b_2 - b_2 \cdot a_2) - (a_1 \cdot b_2 - b_1 \cdot a_2) \cdot (a_2 \cdot c_2 - c_2 \cdot a_2)] \cdot x = (a_1 \cdot c_2 - c_1 \cdot a_2) \cdot (b_2 \cdot R_{E1} - a_2 \cdot R_{E2}) - (a_1 \cdot b_2 - b_1 \cdot a_2) \cdot (c_2 \cdot R_{E1} - a_2 \cdot R_{E3}) \tag{4.15}$$

In equations (4.14) and (4.15), the multipliers of x are equal to zero. The system has solutions only if u is chosen so that the right-hand side of (4.15) is also zero. Then, the value

taken by x can be chosen randomly provided the calculated value of v remains positive which complicates somewhat the manipulation of the Gaussian elimination method.

To solve this, the "isomers" are grouped into a single “composite” product of the same elementary composition (u with w and v with x) so that the right and left members of equation are zero which is logical. Then the Gaussian Elimination step is applied and values for (u + w) and (v + x) are obtained. Then the Monte Carlo method is used again to generate values of u, w, v, and x the sums (u + w) and (v + x) obtained during the preceding Gaussian elimination step.

So, provided some precautions are taken to organize the “coefficient” matrix, the association of the method of Gaussian elimination makes it possible to limit "naturally" the application of the Monte Carlo method to the field of compositions respecting the conservation of the mass.

4.2 Improving the robustness of the thermodynamic database

There is a need to find a way to estimate all the thermochemical properties for the pure components and the intermolecular forces in a “coherent” way. A systematic bias may not be so problematic, since the absolute value of G is not looked for but only its minimum, but scattering/inconsistencies between the data sources for the components would easily produce large uncertainties. A common route/model for estimating the chemical potentials/intermolecular effects should be looked for, or in other words, based on the same physical principles. Possibilities are presented hereafter.

4.2.1 Implementing the "group" contribution theory

Expression (2.54) contains both an historical and a conceptual vision of thermodynamics. Historically, pure and ideal mixtures where considered at first (G^0 and G^{mix}) and conceptually since real fluids and mixtures (G^E) are approached as deviations for the ideal cases, which can be calculated via some virtual transformation.

So, what is needed is a common set of descriptors enabling the estimation of the enthalpy/entropy of formation of the pure ideal components, of the real fluid "transformation" via the equation of state of the fluid and the activity coefficients.

As explained in textbooks, many attempts were made along the last century to connect some "relevant" molecular descriptors to thermodynamic properties of species. The simplest and perhaps the first attempt is to use the property and number of each atom and to add up each atomic contribution to the searched property for the molecule (additivity rule), just as what is done to calculate the molar mass of a molecule. But even for this simple property, careful verification shows that the contribution of a given type of atom also depends on the neighboring atoms. The extent of this effect depends upon the importance of the outer valence electrons. A refinement is to consider the various types of bonds (ex for carbon: carbon-carbon, carbon-oxygen, carbon-nitrogen,..) rather that the atoms alone. But this adds many complications. A medium way is to consider groups of atoms from which most molecules are made of and correlate the thermodynamic properties of molecules (and mixtures) to the number of each group. To some extent, such groups have built-in information on the valence structure

associated with a significant proportion of the atoms present. This is the "group contribution" theory and is widely and successfully used at least in organic chemistry.

Perhaps, the most developed side of the group contribution theory appears in the determination of the activity coefficient via the well-known UNIFAC method[51]. Today, in organic chemistry, UNIFAC incorporates about 54 main groups and about 113 subgroups (**Table 4.3**) from the DDBST[47] database (Appendix C). It is recalled that "main groups" are groups of atoms ("subgroups") sharing the same interaction effects with the other groups of atoms. The "subgroups" describe the interactions of the molecule into the mixture. Using UNIFAC the activity coefficients at 1 bar can be calculated.

But the group contribution theory can also be used very satisfactorily to derive most of the important thermodynamic parameters like those for the equation of state of each component from which the real fluid behavior can be calculated following the pioneering work of Lydersen method.[52] The latter method provides the critical parameters, temperature Tc, pressure Pc and volume Vc from the group contribution theory enabling the derivation of the "covolume" and "energy" parameters of the equation of state. An extension was proposed by Gani-Constantinou[53] about the "acentric factor" of the equation of state. Joback's[54] method also uses the group contribution theory to derive the standard enthalpy, entropy of formation,… of the ideal gas form of the components. Further refinements were proposed by Klincewicz,[55] Ambrose [56]...

Thus, the group contribution theory seems to offer the possibility to obtain all the required thermodynamic parameter from the same set of molecular descriptors which, at least in

principle, could provide the expected self-consistency of the thermodynamic database. The chosen method and its adaptation are described below.

4.2.2 Extracting thermodynamic parameters using the "group contribution" approach

The following parameters are needed to run a calculation by CIRCE: standard formation enthalpy, standard entropy, heat capacities at specific temperatures for extrapolation purposes (typically at 290 K, 1000 K, 2500 K, 3500 K, 5000 K), critical parameters (vc, Tc, Pc), acentric factor.

The molecular descriptors chosen in the present work are those from UNIFAC. Methods both using these descriptors and providing the required thermodynamic parameters were selected in the literature at detailed hereafter.

The ideal gas thermodynamic data (standard enthalpy and entropy of formation, heat capacity,…) and real fluid parameters (acentric factor, critical parameters,…) were extracted from the works of Joback,[54] Constantinou[53], and Kolska et al.[57].

The Joback's method uses a group contribution theory (not the version implemented in UNIFAC) as an extension of the pioneering work of Parks and Huffmann[58]. Note that Joback assumed no interactions between the groups so that only linear combinations are considered. The used data were obtained from the literature. Critical property values, Tc, Pc, and vc, were obtained from Ambrose[59; 60] and Reid et al.[61]. Values for the thermodynamic properties such as standard enthalpy and Gibbs energy of formation of each species (perfect gas state) and

specific heat (C_p^0) were obtained from Reid et al.[55] and Stull et al.[62]. Multiple linear regression techniques were employed by these authors to determine the group contributions for each structurally-dependent parameter (**Table 4.3**). The acentric factor correlation was obtained by Constantinou[51]. Some performances of this technique are presented in **Table 4.3**.

Table 4.3. The different parameters for Joback.

Property*	Symbol	Estimation equations
Critical Temperature	Tc	$T_c = T_b\left\{0.584 + 0.965\left[\sum_k^N N_k(t_{ck})\right] - \left[\sum_k^N N_k(t_{ck})\right]^2\right\}^{-1}$ (4.16)
Critical Pressure	Pc	$\mathrm{P_c} = \left\{0.113 + 0.0032 \times \mathrm{N_{atomes}} - \sum_\mathrm{k}^N \mathrm{N_k(p_{ck})}\right\}^{-2}$ (4.17)
Critical volume	Vc	$\mathrm{V_c} = 17.5 + \sum_\mathrm{k}^N \mathrm{N_k(v_{ck})}$ (4.18)
Fusion temperature	Tf	$\mathrm{T_f} = 122 + \sum_\mathrm{k}^N \mathrm{N_k(t_{fk})}$ (4.19)
Boiling point	Teb	$\mathrm{T_{eb}} = 198 + \sum_\mathrm{k}^N \mathrm{N_k(t_{ebk})}$ (4.20)
enthalpy of gas-phase formation at T = 298.15	$\mathrm{H_f^o}$	$\Delta_\mathrm{f}\mathrm{H_g^o} = 68.29 + \sum_\mathrm{k}^N \mathrm{N_k(d_f h_k)}$ (4.21)
Standard Gibbs energies of formation	$\Delta_\mathrm{f}\mathrm{G_g^o}$	$\Delta_f G_g^o = 53.88 + \sum_k^N N_k\left(d_f g_k\right)$ (4.22)
heat capacity, ideal gas	$\mathrm{c_p^o}$	$\mathrm{c_p^o} = \sum_\mathrm{k}^N \mathrm{N_k(c_{Ak})} - 37.93 + \left[\sum_\mathrm{k}^N \mathrm{N_k(c_{Bk})} + 0.210\right]\mathrm{T} + \left[\sum_\mathrm{k}^N \mathrm{N_k(c_{Ck})} + 3.91 \times 10^{-4}\right]\mathrm{T}^2 + \left[\sum_\mathrm{k}^N \mathrm{N_k(c_{Dk})} + 2.06 \times 10^{-7}\right]\mathrm{T}^3$ (4.23)
enthalpy change of fusion	$\Delta\mathrm{H_{fus}}$	$\Delta\mathrm{H_{fus}} = -0.88 + \sum_\mathrm{k}^N \mathrm{N_k(dh_{fusk})}$ (4.24)
Enthalpy of vaporization at $\mathrm{T_b}$	$\Delta\mathrm{H_{vap}(T_{eb})}$	$\Delta\mathrm{H_{vap}(T_{eb})} = 15.30 + \sum_\mathrm{k}^N \mathrm{N_k}\left(\mathrm{dh_{vapk}}\right)$ (4.25)

*Parameters t_{ck}, P_{ck}, v_{ck}, t_{fk}, t_{bk}, d_fh_k, d_fg_k, c_{Ak} to c_{Dk}, dh_{fusk}, dh_{vapk} are the fitted contributions to Tc, Pc, vc, T_f, T_{eb}, $H°_f$, $\Delta_fG°_g$, Cp, ΔH_{fus}, ΔH_{vap}respectively corresponding to by the k-th functional group (N_k the number of the functional groups of type k). N_{atomes} is the number of atoms of the molecule.

Table 4.4. Statistical summary of the regression work (after Joback[54])

Property	No. of compounds used	Average absolute error	Standard deviation	Average per cent error
Tb (Boiling point)	439	12.9K	17.9K	3.6
Tf (Fusion temperature)	388	22.6K	24.7K	11.2
Tc (Critical Temperature)	409	4.8K	6.9K	0.8
Pc (Critical Pressure)	392	2.1bar	3.2bar	5.2

Vc (Critical volume)	310	7.5cm^3/mole	13.2cm^3/mole	2.3
$\Delta H^0_{f,298}$(enthalpy of gas-phase formation at T = 298.15)	378	8.4kJ/mole	18.0kJ/mole	-
$\Delta G^0_{f,298}$ (Standard Gibbs energies of formation)	328	8.4kJ/mole	18.3kJ/mole	-
$\Delta H_{v,b}$ (Enthalpy of vaporization at T_b)	368	1.27kJ/mole	1.79kJ/mole	3.9
ΔH_f (enthalpy of fusion)	155	2.0kJ/mole	2.8kJ/mole	39

Note however that the "groups" considered by Joback are not those from UNIFAC (**Table 4.5**) and some adaptations are required which were done in this work.

Table 4.5. groups considered by Joback[54].

Non-ring Groups	Ring Groups	Halogen Groups	Oxygen Groups	Nitrogen Groups	Sulfur Groups
$-CH_3$	$-CH_2-$ (ring)	$-F$	$-OH$(alcohol)	$-NH_2$	$-SH$
$-CH_2-$	$>CH-$ (ring)	$-Cl$	$-OH$(phenol)	$>NH$(non $-$ ring)	$-S-$ (non $-$ ring)
$>CH-$	$>C<$ (ring)	$-Br$	$-O-$ (non ring)	$>NH$(ring)	$-S-$ (ring)
$>C<$	$=CH-$ (ring)	$-I$	$-O-$ (ring)	$>N-$ (non $-$ ring)	
$=CH_2$	$=C<$ (ring)		$>C=O$(non $-$ ring)	$-N=$ (non $-$ ring)	
$=CH-$			$>C=O$(ring)	$-N=$ (ring)	
$=C<$			$=CH-$ (aldehyde)	$=NH$	
$=C=$			$-COOH$(acid)	$-CN$	
$\equiv CH$			$-COO$(ester)	$-NO_2$	
$\equiv C-$			$=O$(alcohol)		

Since the interactions between groups are ignored (in Joback's work), the groups used by Joback were simply added to retrieve the UNIFAC groups. For instance, -CH_2Cl subgroup from UNIFAC is the sum of -CH_2- and -Cl groups from Joback. The details are presented in Appendix C. Verification was performed on typical molecules (**Table 4.6**) for which accurate

thermodynamic data are available: methanol, ethanol, formic acid, acetaldehyde. The agreement is reasonable and in accordance with the previous findings (**Table 4.4**).

Table 4.6. Comparison of the JOBACK method with experimental data[54].

	T_b(K)	T_c(K)	P_c(bar)	Vc(cm^3/mole)	$\Delta H^0_{f,298}$(kJ/mole)	$\Delta H_{v,b}$(kJ/mole)
Simulated C_2H_5OH	337.34	499.11	57.57	166.50	-236.84	36.64
Measured C_2H_5OH	351.5	514	63	168	-234	42.3
Simulated CH_3COOH	390.67	587.25	57.31	171.50	-434.88	40.67
Measured CH_3COOH	391.2	593	57.81	170.34	-433	50.3
Simulated CH_3OH	314.46	475.49	66.97	110.50	-216.20	33.91
Measured CH_3OH	337.8	513	81	117	-205	35.21
Simulated CH_3CHO	293.82	465.29	56.03	164.50	-170.19	26.92
Measured CH_3CHO	293.9	466.0	55.7	151.38	-170.7	26.12
Standard deviation	20	20	8	5	2	6

4.2.3 The real fluid behavior: "departure function" and "equation of state"

The properties of each component considered as an ideal gas at the temperature and at the pressure of the reaction can be obtained using the above methodology. But the components are real fluids (gases or liquids) for which the chemical potentials at T and P need to be calculated (to obtain G^0). The nonideality of the components is added under the form of a "departure function[23] which is a "virtual" transformation from an ideal gas to a real fluid. The method is detailed in Appendix E. The resolution highlights the link between the variations of the thermodynamic state function (H, S, G) as a function of the state variables (P, v, and T). For the Gibbs energy:

$$\mathrm{G}(T,P)_{real} - \mathrm{G}(T,P)_{ideal} = \int_{ideal}^{real} v\,dP = \int_{ideal}^{real} d(Pv) - \int_{v=\infty}^{v} P\,dv = (Pv - RT) - \int_{v=\infty}^{v} Pdv \quad (4.26)$$

The Equation of State (EoS) of the fluid is required to compute the departure functions. In the present case, the LCVM[25] method was selected, implementing the original UNIFAC methodology (chapter 2).

4.2.4 The specific case of solids

The EoS/g^E/departure function assembly is attractive and fully applicable to fluids (liquid and gases) even when supercritical but is not valid for solids. For those solids for which the ideal gas state can be defined, the contribution in the Gibbs energy balance of the reaction can be expressed as:

$$H_s = H_{ideal\,gas} + H_{departure} - \Delta H_f + (Cp_{ideal\,gas} - Cp_{solid}) \times \left(T_{fusion} - T\right) \quad (4.27)$$

$$S = S_{ideal\,gas} + S_{departure} + (Cp_{ideal\,gas} - Cp_{solid}) \times \left(\frac{T_{fusion}}{T}\right) \quad (4.28)$$

$$G_s = H_s - TS^{\circ} \quad (4.29)$$

But admittedly this equation is not as accurate as above. Furthermore, some products, like Si and C, do not even have the required critical parameters to implement the EoS in the departure function. In this last situation, the associated EoS is collapsed into the ideal gas law so that the departure functions are zero and the only the incidence of the standard enthalpy of formation, entropy of formation and Cp intervene into the Gibbs energy equation. A consequence is that solids are considered as ideal compounds with no interaction with the other products.

Another method, potentially more accurate, was designed to calculate the real state of solid using: $\widehat{G}_i = \mu^o + RT \times \ln\left(\frac{\hat{f}_{isolid}}{f^{\circ}_{gas}}\right)$, where the $\hat{f}_{isolid}$ is the fugacity of the solid. The $\hat{f}_{isolid}$ can be calculated using this equation: $f^S = \varphi^{sat} P^{sat} \exp(\frac{v^S(P-P^{sat})}{RT})$, where P^{sat} is the saturated

pressure, φ^{sat} is the fugacity of saturated state. But this equation is not universal as the v^S (molar volume of solid) is an empirical parameter.

4.3 Looking for the exhaustivity and representativity of the list of reaction products

As shown in the preceding chapter, it is important, to select from the beginning, the relevant list of final products. As shown, the first difficulty is to be exhaustive enough and the second one to sort the list as a function of the targeted reaction conditions.

4.3.1 Generating an "exhaustive" list of equilibrium products

In practice, this step is often subjective, based on the experience of the practitioner or on a literature review. Notwithstanding that the list might be incomplete, it might also happen that the situation to be modeled has not been thoroughly investigated before so that even some products may not be so well known. It is often the case in accidents involving hazardous substances or fires.

Starting with an elementary composition of the reactant, all the potential but viable products need to be foreseen. The proposed method is derived from Ganis's and Brignole's work[63] which was originally designed to help to choose the fittest molecule to reach some targeted solvent properties. The authors proposed an algorithm to design "realizable" molecules

based on the group typology from UNIFAC. The core of this algorithm is to implement a set of rules enabling only stable molecules to be generated and molecules for which the thermo-physical properties could be reasonably evaluated using the group contribution theory. Thus, only “realizable” molecules are “produced” but perhaps not all the possible molecules. In particular, radicals do not appear. But, in the present context, since the stable final equilibrium is looked for, this last limitation seems acceptable.

The reader is referred to Appendix D for the details about the rules. A molecule is constructed by adding groups progressively. A check of the valence is done and but also some groups are not allowed to bond with some others depending on the topology of the molecule under construction. This method is applied in the present work.

The specificity of the method implemented (in CIRCE code) is pointed out below. The root information is the atomic composition of the reactants: the maximum number of each atom is that contained in the initial mixture. So in the “realizable” molecules, the number of each atom can only be smaller than that in the initial mixture. The affordable groups are selected in the UNIFAC table according to the atoms available in the initial mixture. Only the groups containing the atoms available in the reactants are selected. Groups are sorted into “intermediate” groups (like CH_2), able to participate to the skeleton of the molecules, and into “terminal” group (like CH_3, OH…). The construction of the molecule starts from one intermediate group (selected randomly), and other groups are added (randomly) checking at each step the “realizability” rules and atom balance up to a maximum of 12 groups in a single molecule.

An example of the application of the Brignole's method is presented below about the anaerobic pyrolysis of ethanol at atmospheric pressure between ambient temperature and 1000 K (**Table 4.7**).

Table 4.7. list of realizable products established by CIRCE methodology for the anaerobic pyrolysis of one mole of ethanol.

CH_3OH	C_2H_4	H_2O	CH_3CHO	H_2	CH_4	HCHO
CO	C_2H_6	C_2H_2	$C_2H_5OH_{liq}$	$C_2H_5OH_{vap}$	CO_2	C

Depending on the temperature, the literature[64] provides some indications of what kind of molecules are likely to appear in the present situation. At moderate temperatures (below 700 to 800°C), liquid and vapor ethanol were detected ($C_2H_5OH_{liq\text{-}vap}$), acetaldehyde ($CH_3CHO$), formaldehyde (HCHO), water (H_2O), ethylene (C_2H_4), acetylene (C_2H_2), CO and CO_2. Hydrogen and methane were not detected, but some acetone was. The presence of acetone could not be foreseen here since the pyrolysis of one mole of ethanol only was considered. But globally the prediction seems reasonable.

The same source of information provides data (**Figure 4.1**), on the evolution of the concentration of the various components as a function of the temperature of the pyrolysis (at ambient pressure).

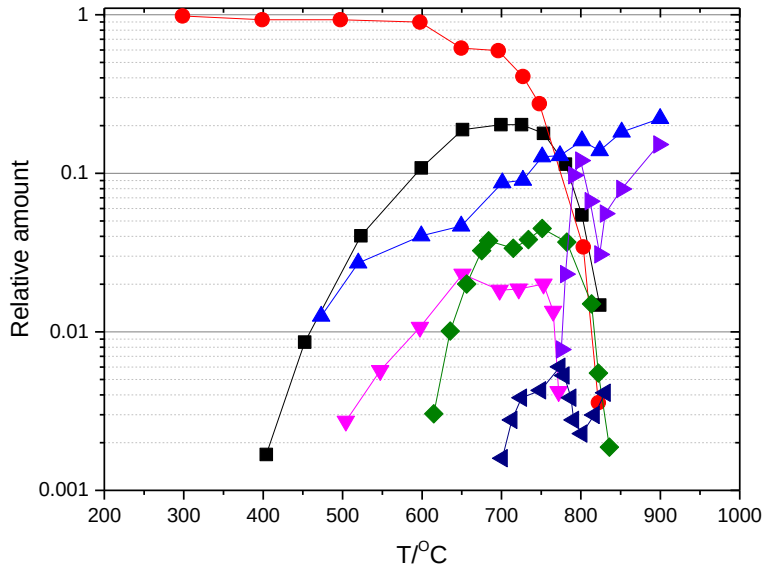

Figure 4.1. Pyrolysis of ethanol, experimental results[64]. CH_3CHO,■; C_2H_5OH,●; H_2O,▲; CH_3COCH_3,▼; $C_2H_4+C_3H_6$,◆; HCHO,◀; $C_2H_2+CO+CO_2$,▶.

The simulation of this pyrolysis was performed using CIRCE software and the list of final potential products given in **Table 4.7**. The results are presented in **Figure 4.2**.

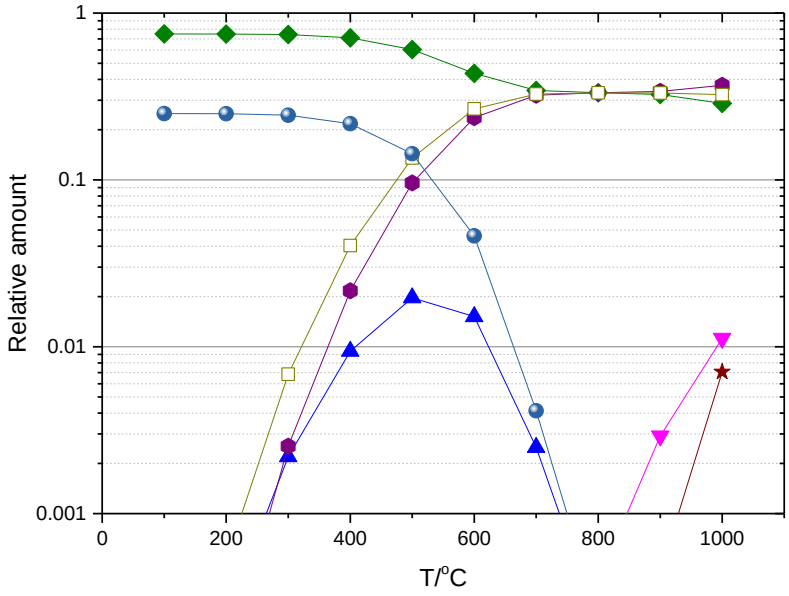

Figure 4.2. Pyrolysis of ethanol, CIRCE simulation results. C_2H_6O,■; CH_3CHO ●; H_2O ▲; C_2H_4,▼; CH_4, ◆; C_2H_6, ◀;CH_2O, ▶; H_2,● ;C_2H_2, ★;CO, □;CO_2 ●;CH_3OH ○.

Clearly, the simulation results shown in **Figure 4.2** are very different from the experimental

results although the list of products, as said above, is reasonable. The thermodynamic system "prefers" CH_4, CO_2, and CO even at a very low temperature (200°C…) which is obviously not realistic. The reason for this trend is the large and low Gibbs free energy values of those components in the Gibbs energy balance.

This comforts the preceding analysis about the choice of the product list which should not only be complete enough but representative of the reaction conditions. Apparently, carbon dioxide cannot be produced immediately from the ethanol molecule but after several reaction steps occurring successively at various temperatures.

Additional considerations are needed to take such reality into account. Possible routes are analyzed below.

4.3.2 Adapting the list of products to the reaction conditions

Incorporating reaction kinetics may be a way. Software like CHEMKIN[65] can do this by providing the available products and chemical information is available in the database of the software. As explained before, when performing simulations in unusual conditions some products may not be well known and hence the kinetic data also. Alternatively, quantum chemistry[66] is potentially capable of providing results in such situations, but the method may be tedious to handle, time-consuming especially when a succession of reactions is to be investigated. Some alternatives may be looked for, as for instance using the Bell-Evans-Polanyi method[66] which may offer a way to estimate the kinetic parameters rapidly avoiding the use of the transition state theory[67].

Nevertheless, if ever demonstrated to apply to the somewhat complicated chemistry targeted to using the Gibbs energy minimization, such theories could be instrumented only if a preliminary method were developed to rank the potential products (determined as detailed above which again contains only stable products) and reactions as a function of the reaction conditions. This last point is addressed in the following.

Again, the anaerobic pyrolysis of ethanol at atmospheric pressure and up to 1000K is considered. The realizable products were given in **Table 4.10**.

To help to organize the succession of reactions, the temperature is supposed to increase gradually. The liquid ethanol first vaporizes and then the gaseous molecules are split into only two molecules respecting the atom balance. Using the products list of **Table 4.7**, the possible combinations are:

$$C_2H_5OH_{liq} \rightarrow C_2H_5OH_{gaz} \quad (4.30)$$

$$C_2H_5OH \rightarrow C_2H_4 + H_2O \quad (4.31)$$

$$C_2H_5OH \rightarrow CH_3CHO + H_2 \quad (4.32)$$

$$C_2H_5OH \rightarrow CH_4 + HCHO \quad (4.33)$$

The first step of the thermochemical analysis of these reactions is to compare their Gibbs energies. Those for which the Gibbs energy is positive are thermodynamically impossible, and among the thermodynamically possible reactions (negative Gibbs energy), those with the smaller Gibbs energy should typically dominate although, admittedly, this may be not a sufficient condition (kinetics need also to be considered). For reactions (4.30) to (4.33) the evolution of the Gibbs energy as a function of the temperature are shown in **Figure 4.3**.

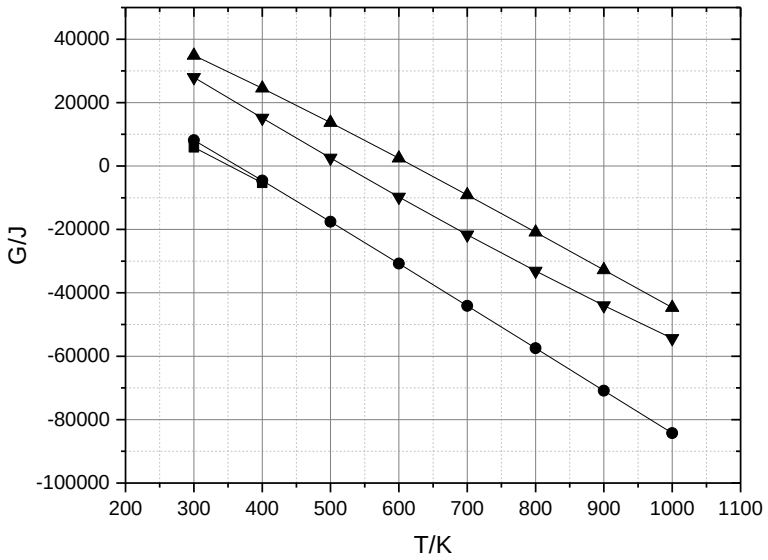

Figure 4.3. Gibbs energy as a function of the temperature for reactions (4.30) to (4.33) (atmospheric pressure-CIRCE code with LCVM). $C_2H_5OH_{liq}$=$C_2H_5OH_{gas}$ (reaction 4.28), ■; C_2H_5OH=C_2H_4+H_2O (reaction 4.29), ●; C_2H_5OH=CH_3CHO+H_2 (reaction 4.30), ▼; C_2H_5OH=CH_4+HCHO (reaction 4.31), ▲.

Below about 350 K only liquid ethanol is possible. Above 350 K and up to 500 K, gaseous ethanol appears but can be dehydrated in ethylene. Above 600 K, ethanol and hydrogen may appear.

The same method can be used to guess the fate of the molecules formed during this first pyrolysis step. CH_4 and H_2O are stable up to 1000 K, and there is no possibility in **Table 4.8** to further decompose HCHO which is then also considered as stable.

Considering ethylene, Brignole's method provides the list of products shown in **Table 4.8**.

Table 4.8. List of realizable products established by CIRCE methodology for the anaerobic pyrolysis of one mole of C_2H_4 by CIRCE.

C_2H_4	C_2H_2	H_2	C

On this basis, the following reactions can be considered:

$$C_2H_4 \rightarrow C_2H_2 + H_2 \quad (4.34)$$

$$C_2H_4 \rightarrow 2C + 2H_2 \quad (4.35)$$

The Gibbs energy of (4.34) and (4.35) as a function of the temperature is shown in **Figure**

4.4, clearly showing that both reactions are not possible in the present temperature range.

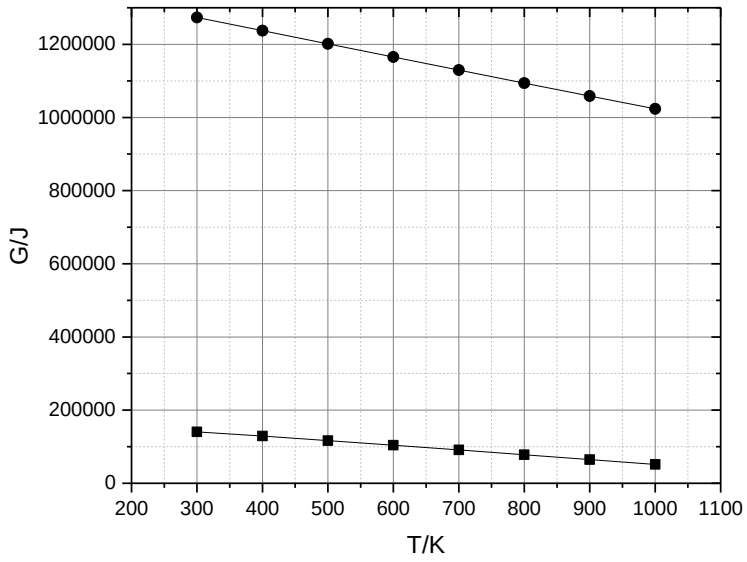

Figure 4.4. Gibbs energy as a function of the temperature for reactions (4.34) and (4.35) (atmospheric pressure-CIRCE code). C_2H_4---C_2H_2+H_2 (reaction 4.32) ■; C_2H_4---2C+2H_2 (reaction 4.33),●.

The same procedure is now applied to acetaldehyde. The list of potential products of decomposition is given in **Table 4.9**. Note the presence of vinyl alcohol which has the same molecular composition than ethanal but a different structure.

Table 4.9. list of realizable products established by CIRCE methodology for the anaerobic pyrolysis of one mole of Acetaldehyde by CIRCE.

CH_3CHO	H_2C=CHOH	CH_3OH	CH_4	HCHO	H_2	CO

On this basis, the chemical process of decomposition would be:

$$CH_3CHO \rightarrow CH_2 = CHOH \quad (4.36)$$

$$CH_3CHO \rightarrow H_2 + C_2H_2O \quad (4.37)$$

$$CH_3CHO \rightarrow CH_4 + CO \quad (4.38)$$

$$CH_3CHO \rightarrow C_2H_2 + H_2O \quad (4.39)$$

The thermodynamic feasibility is studied in **Figure 4.5** shows the evolution of the Gibbs

energy of these reactions as a function of the temperature (**Figure 4.5**).

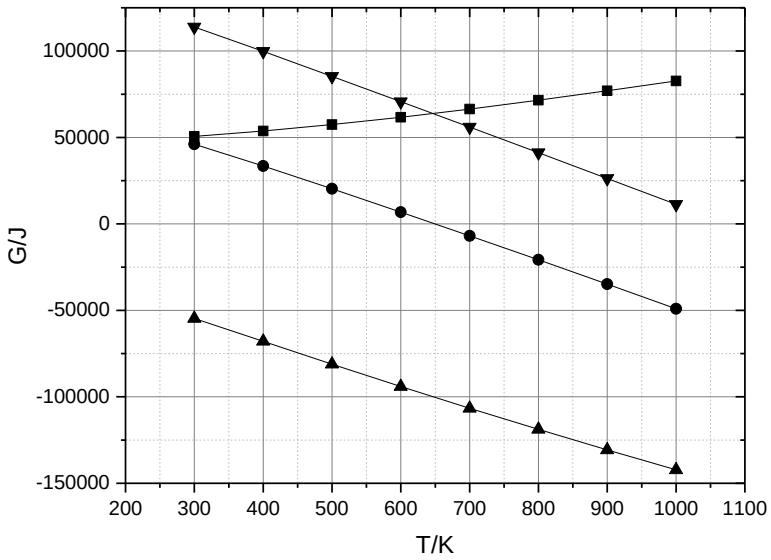

Figure 4.5. Gibbs energy as a function of the temperature for reactions (4.36) to (4.39) (atmospheric pressure CIRCE code with LCVM). Reaction (4.34) CH_3CHO---CH_2=$CHOH$ ■; Reaction(4.35) CH_3CHO---H_2+C_2H_2O ●, Reaction (4.36) CH_3CHO---CH_4+CO ▲; Reaction (4.37) CH_3CHO---C_2H_2+H_2O ▼.

It is clear that reactions (4.36) and (4.39 are not possible, that reaction (4.37) could occur only above 700 K and that, for the entire temperature range, (4.38) is possible.

In the end, the reaction scheme obtained this way is represented in **Figure 4.6**.

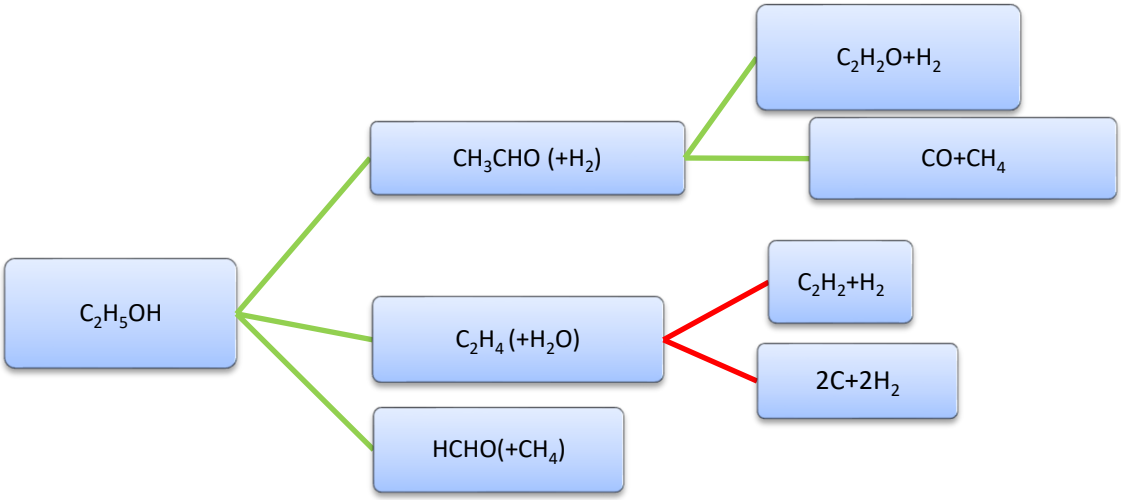

Figure 4.6. The thermal decomposition reaction of C_2H_5OH. The green lines designate the possible reactions, and the red lines are the impossible reactions.

Using these data, it is possible to propose a sort of order of appearance of the identified compounds.

Table 4.10. List of products for the anaerobic pyrolysis of one mole of ethanol.

Temperature		*Proposed products*							
300K	$C_2H_5OH_{liq}$	C_2H_5OH							
350K	C_2H_5OH	*(boiling point)*							
400K	C_2H_5OH	C_2H_4	H_2O						
500K	C_2H_5OH	C_2H_4	H_2O	$HCHO$	CH_4				
600K	C_2H_5OH	C_2H_4	H_2O	$HCHO$	CH_4	CH_3CHO	CO	H_2	
700K	C_2H_5OH	C_2H_4	H_2O	$HCHO$	CH_4	CH_3CHO	CO	H_2	C_2H_2O
800K	C_2H_5OH	C_2H_4	H_2O	$HCHO$	CH_4	CH_3CHO	CO	H_2	C_2H_2O
900K	C_2H_5OH	C_2H_4	H_2O	$HCHO$	CH_4	CH_3CHO	CO	H_2	C_2H_2O
1000K	C_2H_5OH	C_2H_4	H_2O	$HCHO$	CH_4	CH_3CHO	CO	H_2	C_2H_2O

Globally, these products appear in reality but not in the temperature range of the experiment. One reason is undoubtedly the kinetics. An illustration is proposed below concerning reaction (4.31). The kinetic data considered hereafter are those from the NIST website[68] and other sources[69]. Data from the literature are given in **Table 4.11**, knowing that the rate of the reaction is expressed as:

$$\frac{d[reactant]}{[reactant]dt} = k = A \times T^n exp(-E^a/RT)$$

Where k is the rate constant, T is the absolute temperature (in kelvins), A is the pre-exponential factor, a constant for each chemical reaction. According to collision theory, A is the frequency of collisions in the correct orientation. *Ea* is the activation energy for the reaction (in the same units as *R.T*); *R* is the universal gas constant.

Table 4.11. some kinetics parameters according to published data[69].

	A(s^{-1})	N	Ea (J/mol)
C_2H_5OH--C_2H_4+H_2O (2)	2.79E+13	0.09	66136

The analysis reveals that the reaction rate remains very small at 400 K. Other

considerations are needed to define a “practical” temperature threshold for this dehydration reaction. If, for instance, the reaction is to be over within some tens of minutes, the characteristic time scale is 10^{-3} seconds, so that k(T) should be on that order for the reaction to be practically feasible. In that particular case, it means that reaction (4.31) will become detectable when the reaction temperature is above 850 K which seems more in line with the experimental data. Similar consideration would show that reaction (4.31) is extremely slow and will not decompose ethanol. So definitely, kinetic data would also be helpful.

Another reason is the recombination of the products from parallel reactions (for instance the water gas shift reaction). Time was too short to implement this aspect in the method.

4.4 Programming CIRCE

The methods presented in the preceding sections were computed and compiled (C language) into an entire homemade software: CIRCE.

The constraint is that the code should provide a result even if thermodynamic data for some compounds are poorly known (or even missing), if multiphase reaction occurs and under various reaction regimes, not only at constant pressure and temperature as it is usually assumed.

Targeted applications cover naturally standard chemical transformations at constant pressure and temperature to foresee the yield and energetic of in a chemical reactor but also dangerous fast reactions, like fires and explosion, usually occurring adiabatically at constant pressure or constant volume. These functionalities are integrated.

4.4.1 The overall structure of the code

The functional organigram is shown in **Figure 4.7**. The details are given in appendix G.

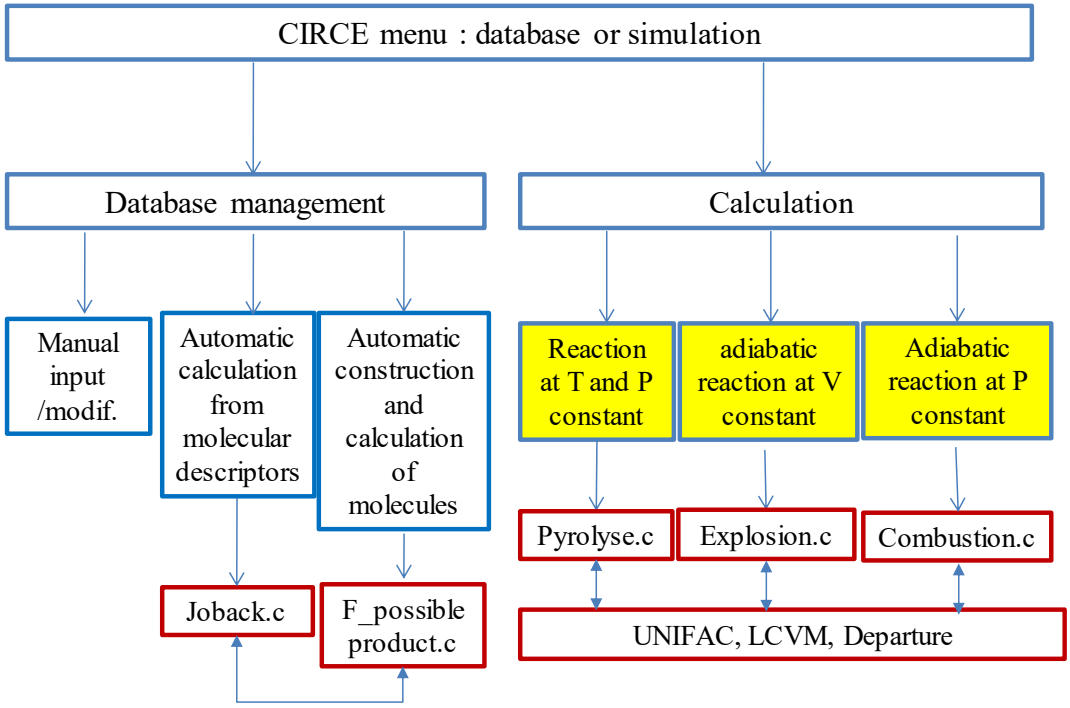

Figure 4.7. Functional structure of the software CIRCE (in red squares: main routines)

CIRCE consists in two separate blocks.

- The database implementation block which offers the user the possibility to introduce, create new components and modify as desired the thermodynamic properties calculated by the code which implements UNIFAC for molecular descriptors, a modified Joback's method and the Constantinou's methods for the ideal gas thermodynamic properties. A "product list generator" is programmed which offers the user the possibility to create new products from the reactants composition.
- The simulation block incorporates 3 separate routines to simulate the various reaction modes: at constant P and T ("pyrolysis"), adiabatic and constant pressure ("combustion") and adiabatic and at constant volume ("explosion"). The common functions are: UNIFAC to calculate the

activity coefficients, the LCVM EoS to calculate the departure functions. The user is asked to select a list of products from the database.

4.4.2 Implementation/management of the database

In the database, all the product/component data required to calculate the thermodynamic equilibrium are saved. It includes (**Table 4.12**): the standard enthalpy of formation, standard entropy of formation, heat capacity at various temperatures, critical temperature, critical pressure, acentric factor and the molecule descriptor to apply UNIFAC.

Table 4.12. The format of the database of CIRCE (files 'donnee.csv' for the gases, 'donneecond.csv' for the liquids and 'donneesolid.csv' for the solids)

Atomic composition	$\Delta H_f°$ (kJ/mol)	$\Delta S_f°$ (J/moleK)	Cp_{300K} (J/moleK)	Cp_{500K} (J/moleK)	…	Pc (bar)	Tc (K)	CH main group		
								CH	CH_2	CH_3
C_2H_6								0		
								0	0	0

This database can be updated using a molecular descriptor routine. To do this, the user describes the molecule in a csv file (**Table 4.12**) which is then used by the codes which implement the modified Joback's method and the Constantinou and Gani's method[53] to add new molecules in the database (donnees.csv).

Table 4.13. How to define the group of a molecule from the database of CIRCE.

Atomic composition	CH main group					
	CH	CH_2	CH_3			
C_2H_6	0	0	2			

The user can also introduce a product manually into the database (the database is a csv file). This is necessary when the group contribution theory cannot be implemented which is the case for mineral molecules for instance but also for solids.

The last choice allows the user to generate the possible product automatically. The user provides an elementary composition of the reactants, all the potential but viable products are foreseen using the Gani and Brignole method.

4.4.3 Simulation blocks

First, the user has to introduce the reactants and to select the potential end product into the database. The software selects the products from the elemental composition of the reagents of the database which contain only the elements of the reagents. Then the user selects manually from the list proposed. In this task, the user can ask the code to provide all the possible products (see above).

The starting point of the simulation is the list of the selected products, the composition of reactants, the initial temperature, pressure, and energy. From this, the code will generate, using the MCGE method, the composition vectors (number selected by the used) satisfying the species conservation.

The root simulation block is then calculating the chemical composition of the end-state system at equilibrium. Consider first that the transformation is supposed to operate at constant temperature and pressure. A typical example is the reaction of pyrolysis. In this case, the total Gibbs energy needs to be minimized. First, the ideal enthalpy and entropy of formation of each

product are calculated using the thermodynamic data from the database (P* is the reference pressure 1 atm):

$$h_i^0(T,P) = h_{fi}^0 + \int C_{pi}dT \text{ and } s_i^0(T,P) = s_{fi}^0 + \int C_{pi}dT + R \cdot ln\left(\frac{P}{P*}\right) \quad (4.40)$$

The various values of Cpi as a function of T, given by the Joback's method, are used to integrate. Then, the departures functions, $h_{ideparture}$, and $s_{ideparture}$, for each pure component are calculated (function PENG_Robinson_for_HSCp) using the PR EoS coefficients for each product and stored in the database.

$$h_i(T,P) = h_i^0(T,P) + h_i^{departure}(T,P) \text{ and } s_i(T,P) = s_i^0(T,P) + s_i^{departure}(T,P) \quad (4.41)$$

From which the Gibbs energy of formation of product i is calculated: $\mu_i(T,P) = h_i(T,P) - T \cdot s_i(T,P)$. Then, for each composition vector, the contribution of each product to the total Gibbs energy is calculated via the functions:

$$Gi(T,P) = \mu_i(T,P) + G_i^{mix} + G_i^E = \mu_i(T,P) + R \cdot T \cdot ln\left(\frac{n_i}{\sum_i n_i}\right) + R \cdot T \cdot ln(\gamma_i) \quad (4.42)$$

For the solid phase, $G^E{}_i$ and G_{mixi} are zero. For each composition vector the total Gibbs energy is calculated using:

$$G(T,P) = \sum_i n_i \cdot G_i(T,P) \quad (4.43)$$

The minimum of the Gibbs free energy can be calculated after comparing all the values of G calculated for all the composition vectors. The final result is the composition vector at the minimum of the Gibbs energy (gases, liquids and solids), the total volume, total number of moles and the total enthalpy.

A variant of this routine is the adiabatic reaction at constant pressure. In this case, the total enthalpy is also conserved so that the temperature may vary significantly between the

initial and final states. Starting from two "guessed" final temperatures typically 100 and 3000 K), T^0_1 and T^0_2, the Gibbs energy is minimized as explained above and the total enthalpies corresponding to these minima are calculated. If both are different from the initial enthalpy of the reactants, a new value of final guessed temperature is calculated from the two formers using the bisection method[70] and the Gibbs energy is minimized again. At iteration number n, the total enthalpy $h_{product}(T^{n+1})$corresponding to the average temperature $T^{n+1} = (T_1^n + T_2^n)/2$ is calculated and used along with $h_{reactants}$, $h_{product}(T_1^n)$ and $h_{product}(T_2^n)$ to compute a temperature step:

$$\Delta T = \text{fabs}\left(\frac{(H_{produits} - H_{reactif})}{\frac{(H_{produits} - H_{reactif})}{(T_2 - T_1)}}\right) \tag{4.44}$$

Then the two subsequent values of the temperature are calculated by adding ΔT to T_{n1} and T_{n2}. The calculation loops until $\Delta T \leq 0.01$.

5 Performances and case studies

The new methods proposed in the preceding chapter were challenged to identify the potentialities and limitations. Further, the applicability of CIRCE to some typical industrial cases was tested.

5.1 Capabilities and limitations of the proposed methods

The challenging points are the performances of the MCGE method in finding the absolute minimum in any circumstances (including multiphase reactions) and the relevancy of the use of "group contribution theory" in terms of predictability.

5.1.1 Performances of the MCGE method

5.1.2 Finding the absolute minimum

Several difficult cases were investigated among those challenging the Lagrangian methods (those implemented in CEA and ASPEN) and the MCGE method.

The first one deals with a coal gasification situation. The experimental data[71] from Yoshida and al. are used. The reaction is pyrolysis in a flow reactor under ambient pressure. The experimental conditions and results are presented in **Table 5.1**. The global reaction (unbalanced) reads:

$$Coal + H_2O \rightarrow H_2 + CO + CO_2 + CH_4 + H_2O + C(s) \qquad (5.1)$$

Table 5.1. Experimental condition of the Texaco entrained-flow gasifiers.

Coal	Illinois no. 6	Illinois no. 6	Wyodak	Illinois	Wyodak	Vaccum Residue
C	71.23	70.96	78.37	69.73	78.06	83.79
H	5.44	5.38	5.81	5.21	5.32	10.5
O	1.97	2.55	3.7	2.7	4.75	0
N	0.74	0.77	0.92	0.8	0.93	0.45
S	1.74	1.63	0	1.38	0.05	5.14
Ash	18.55	18.54	11.05	19.96	10.86	0.12
CFR[c]/kg·h^{-1}	296	342	309	42259	38511	30861
$R_{O2/Coal}$[d]/kg·kg^{-1}	0.812	0.801	0.899	0.803	0.881	1.1
$R_{H2O/Coal}$[e]/kg·kg^{-1}	0.31	0.24	0.318	0.4	0.5	0.35
P[f]/kPa	8280	8280	8280	8280	8280	8280
T[g]/K	1567	1677	1571	1520	1516	1597
Gpr[h]/mol·h^{-1}	30080	33390	34340	4446000	4563000	4302000
Gc[i]/x[a]						
CO	51.88	56.06	53.48	48.53	47.66	45.35
H_2	37.32	37.21	35.72	35.67	34.24	41.37
CO_2	5.24	3.26	4.56	6.18	6.7	4.5
CH_4	0.09	0.05	0.05	0.01	0.01	0.05
H_2O	5.47	3.41	6.2	9.61	11.39	8.73
CC[j]/x[b]	0.981	0.981	0.989	0.994	0.989	0.996

[a] x is the gas composition for each product, x=100 x (mole of chosen gas)/sum of mole for all the gas; [b] x= $[(N_{CO}+ N_{CO2} + N_{CH4})_{outlet}/ N_{Cfeed}]$. [c] CFR is the Coal feed rate; [d] $R_{O2/Coal}$ is the ratio between O_2 and Coal; [e] $R_{H2O/Coal}$ is the ratio between H_2O and Coal; [f] P is pressure; [g] T is temperature; [h] Gpr is the Gas production rate; [i] Gc is gas composition; [j] CC is the carbon conversion rate.

The simulation is performed under the assumption of constant pressure and temperature and the results are presented in **Table 5.2**, **Table 5.3** and **Table 5.4**.

Table 5.2. Coal gasification under the conditions of **Table 5.1** simulated using the RAND method (Aspen-RGIBBS) module).

Gas composition/x[a]	Illinois no. 6	Illinois no. 6	Wyodak	Illinois	Wyodak	Vaccum Residue
CO	54.55	57.81	55.5	50.53	49.64	46.34
H_2	35.96	36.3	34.82	34.44	32.97	40.7
CO_2	2.65	1.7	2.8	4.09	4.82	2.91
CH_4	0	0	0	0	0	0
H_2O	6.84	4.19	6.89	10.93	12.56	10.04
Carbon conversion /x[b]	100	100	100	100	100	100

Table 5.3. Coal gasification under the conditions of **Table 5.1** simulated using the Gordon and Mc Bride method (from CEA code).

Gas composition/x[a]	Illinois no. 6	Illinois no. 6	Wyodak	Illinois	Wyodak	Vaccum Residue
CO	54.4	57.88	55.36	50.12	49.16	46.26
H_2	36.11	36.22	34.95	34.85	33.46	40.79
CO_2	2.79	1.63	2.94	4.5	5.31	3
CH_4	0	0	0	0	0	0
H_2O	6.69	4.27	6.75	10.53	12.07	9.96
Carbon conversion/x[b]	100	100	100	100	100	100

Table 5.4. Coal gasification under the conditions of **Table 5.1** simulated using the MCGE method (CIRCE code).

Gas composition/x[a]	Illinois no. 6	Illinois no. 6	Wyodak	Illinois	Wyodak	Vaccum Residue
CO	54.2	57.14	54.43	49.86	48.95	46.35
H_2	36.25	36.92	35.83	35.06	33.66	40.64
CO_2	3.01	2.37	3.87	4.77	5.52	2.9
CH_4	0.03	0.02	0.02	0.03	0.01	0.02
H_2O	6.52	3.55	5.85	10.28	11.87	10.08
Carbon conversion/x[b]	100	100	100	100	100	100

Globally the results are comparable between the various methods and rather close to the experimental data. Note that this finding may not be so surprising since the major difficulties associated with minimizing the Gibbs energy may appear when phase changes and mixing intervene as shown below.

The distillation of a binary water-ethanol mixture is considered. This case was presented in the first chapter of this memory and is based on the experimental data from Dortmund Data Bank[47]. It was already shown that the Gordon and Mc Bride method just fails and that the RAND method provides a good but nevertheless approximate estimate **(Figure 5.1**). The MCGE method was employed with CIRCE (UNIFAC is used like with ASPEN) and an excellent agreement is now obtained (**Figure 5.2**). This demonstrates that the Taylor truncation adopted in the RAND method may generate some deviations.

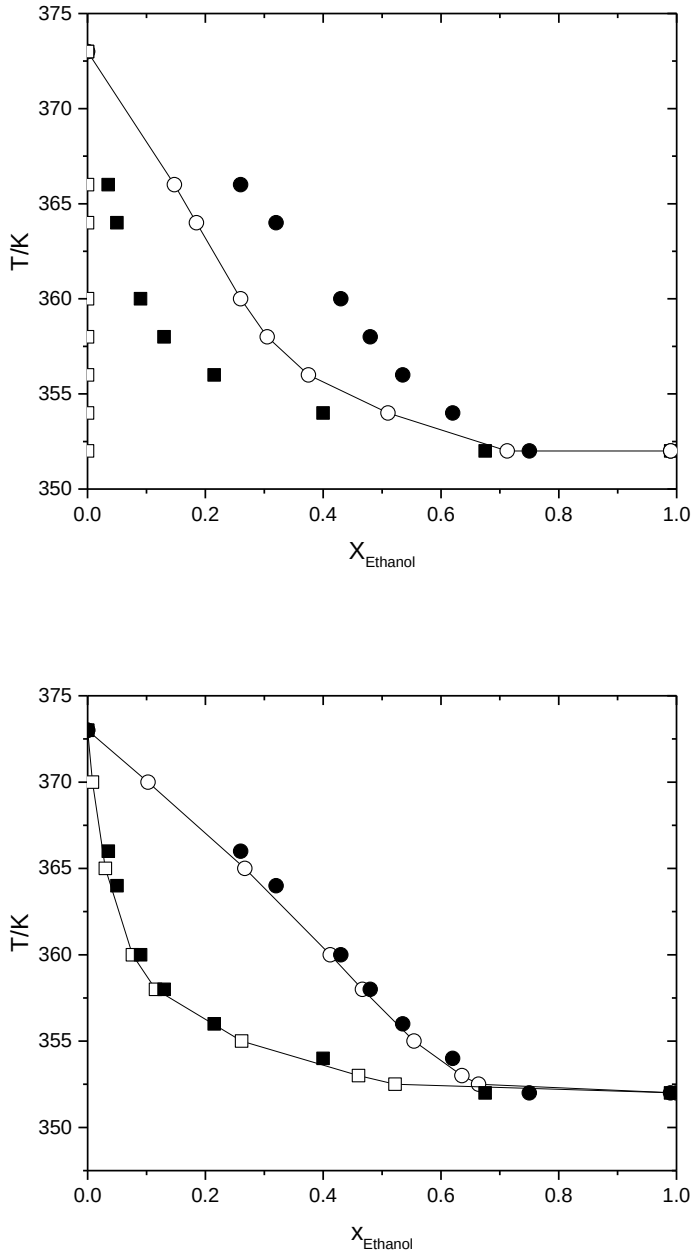

Figure 5.1. Distillation of ethanol-water mixture. Comparison of the simulations using the Gordon and Mc Bride method (from CEA–above and ASPEN-RGIBBS UNIFAC-below) and experimental data (Dortmund Data Bank[47]). The points correspond to the % (in mole) of ethanol in the corresponding phase (ex 30% in the liquid phase means 30% of a mole of the liquid phase is ethanol). Simulations: vapor, ○; experiments: vapor, ●; simulations: liquid, □; experiments: liquid,■.

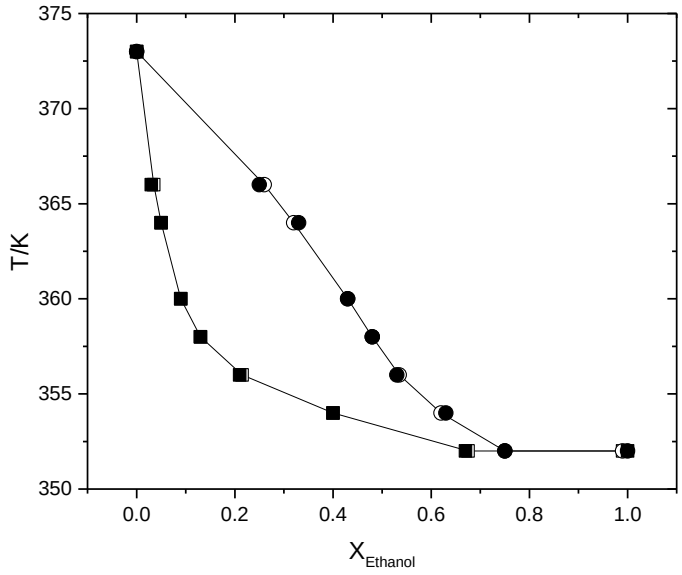

Figure 5.2. Distillation of an ethanol-water mixture. Comparison of the simulations using the MCGE method (CIRCE code with UNIFAC to calculate G^E) and experimental data from Dortmund Data Bank[47]. vapor, ○; experiments: vapor, ●; simulations: liquid, □; experiments: liquid, ■.

.

This last case corresponds to a three-phase equilibrium of biphenyl in CO_2 and is particularly challenging. The experiments were performed by McHugh et al.[72] investigating the extraction of biphenyl using supercritical CO_2. Biphenyl is an aromatic solid (**Figure 5.3**)

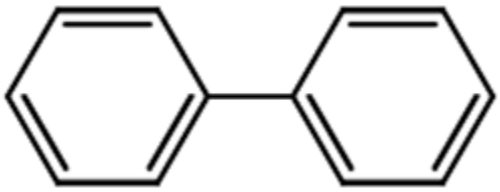

Figure 5.3. The structure of Biphenyl.

The schematic diagram of the experimental apparatus is presented in **Figure 5.4**[72]. After the thermal equilibrium within the constant-temperature bath is reached, the solvent is introduced into the first of two high-pressure equilibrium cells connected in series. Downstream the second column, the saturated solution flows through a high-pressure switching

valve in a small cell where a sample can be isolated for analysis. The volume of carbon dioxide in the sample is determined to within 0.3% by slowly expanding the CO_2 across a valve through a water column. The sampling cell is then flushed with a suitable solvent to recover the solid component.

In parallel with the sample analysis, the continuous stream exiting the switching valve is flashed cross a heated metering valve (Autoclave Engineers, Inc.), and the heavy solute is collected in a cold trap held at ice temperature. Gaseous carbon dioxide is subsequently passed through a bubble meter to determine flow rate. The equilibrium temperature and pressure of the system are measured at the exit of the second equilibrium cell.

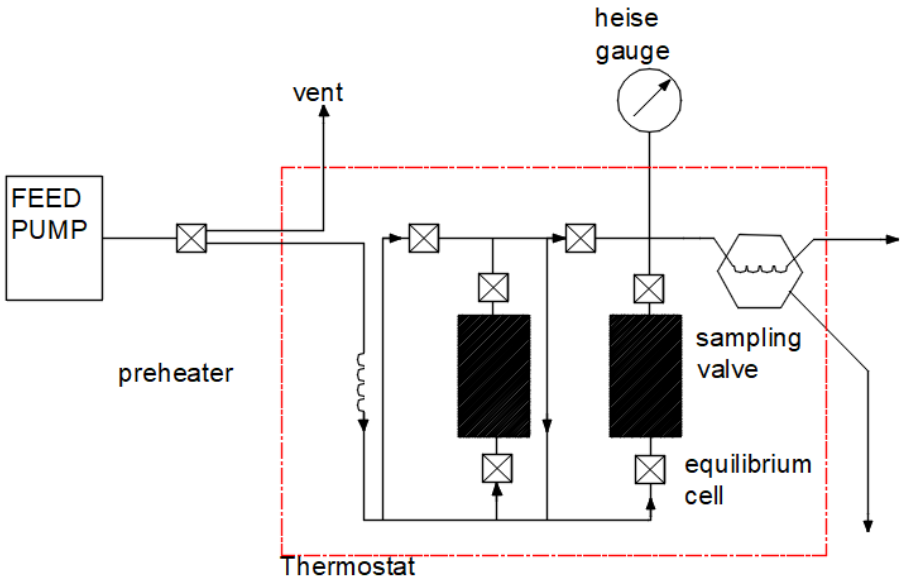

Figure 5.4.the experimental instrument for the equilibria of CO_2 and biphenyl.

Depending on the pressure and temperature three-phases may coexist: vapor as a mixture of CO_2 and biphenyl, liquid as a mixture of CO_2 and biphenyl and solid with biphenyl only. The experimental P, T curve along which the three phases coexist is shown in **Figure 5.5**. The particular case at 48°C (321K) and various pressures are shown on **Figure 5.6** giving the

solubility of biphenyl in CO_2 (vapor and liquid).

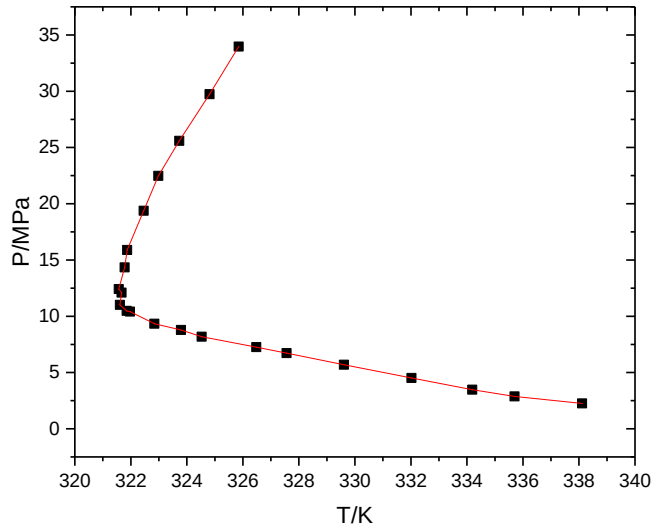

Figure 5.7. phase equilibrium diagram from experiments ■ [81] and simulation using CIRCE —.

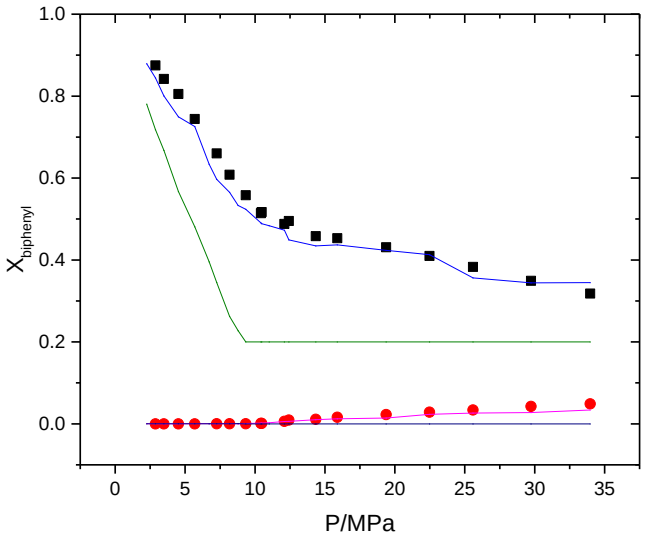

Figure 5.8. solubility curve of biphenyl in liquid and vapor phases. ■ experiment-liquid phase, ● experiment-liquid phase, — simulation for the liquid phase CIRCE, — simulation for the vapor phase CIRCE, — simulation for the liquid phase ASPEN, — simulation for the vapor phase ASPEN/RGIBBS.

The simulation was performed using CEA, ASPEN (RGIBBS) and CIRCE. The results are also shown in **Figure 5.7** and **Figure 5.8**. The initial composition of this simulation was set to 0.8 for CO_2 and 0.2 for biphenyl in a pure liquid phase (the amounts are not critical for the calculations provided saturation of the phase is reached). The transformation is operated at constant pressure and temperature. The reader will realize that no point is shown for CEA and ASPEN-RGIBBS in **Figure 5.8**. The reason is that the Gordon and Mc Bride method (CEA code) systematically diverges and that the Rand method (ASPEN-RGIBBS) is not able to predict a three-phase mixture. In particular, the solid phase never appears. In **Figure 5.8,** it can be realized that ASPEN-RGIBBS provides a liquid-vapor equilibrium only up to 9 MPa. Above this pressure, the code returns the original mixture (pure liquid).

In the same situation, CIRCE does identify the multiphase equilibrium and seems to provide a correct estimate of the VLE. Note however that the cost of the calculation is significant (2 mn for one point….).

5.1.3 Predictability and accuracy

Nevertheless, CEA and ASPEN mathematical methods, although sometimes limited, are known to be computationally very efficient. On that aspect, the MCGE method is clearly behind. One of the difficulties is to set the number of composition vectors required to make sure to converge towards the global minimum.

Two cases were tested: the nearly complete pyrolysis of methane in oxygen (**Table 5.5**)

and the nearly complete condensation of alcohols in water (**Table 5.6**) which are complicated thermodynamic problems for the MCGE method. In both situations, the complexity of the problem was increased gradually by adding more and more components. Thermodynamically, these are transformations at constant pressure and temperature.

Table 5.5. Pyrolysis of methane in the presence of oxygen

Number of components→	4	6	8
Pyrolysis of CH_4 (40%v/v) in O_2 at 1 atm and 2500 K	CH_4 O_2 CO_2 H_20	CH_4 O_2 CO_2 H_20 CO H_2	CH_4 O_2 CO_2 H_20 CO H_2 C(s) OH

Table 5.6. Condensation of alcohols in water

Number of components→		2	4	6	8
Condensation at 1 bar and 250 K	Gas	H_2O	H_2O Ethanol	H_2O H_2O_2 Ethanol	H_2O H_2O_2 Methanol Ethanol
	Liquid	H_2O	H_2O Ethanol	H_2O H_2O_2 Ethanol	H_2O H_2O_2 Methanol Ethanol

In each test case, the number of composition vectors approaching a stable solution was looked for. An example of this procedure is given below. A fixed number of composition vectors is chosen (for instance 10000) and the calculation is performed 10 times to establish some statistics (**Figure 5.**). On **Figure 5.**-a are given the evolution of the number of moles of 6 components resulting for the pyrolysis of methane in oxygen during 10 successive runs (third column of **Table 5.5**. On **Figure 5.**-b is given the evolution of the vapour fraction for the "8 components" condensation case (fifth column of **Table 5.6**). Fluctuations of the final result are visible. This makes a difference with the Lagrangian method, for which provided the starting point is the same, the final result will be identical. It does not mean that the latter will be the

true minimum as shown before and, furthermore, in the specific case of the Lagrangian methods, the accuracy of the result is not really known.

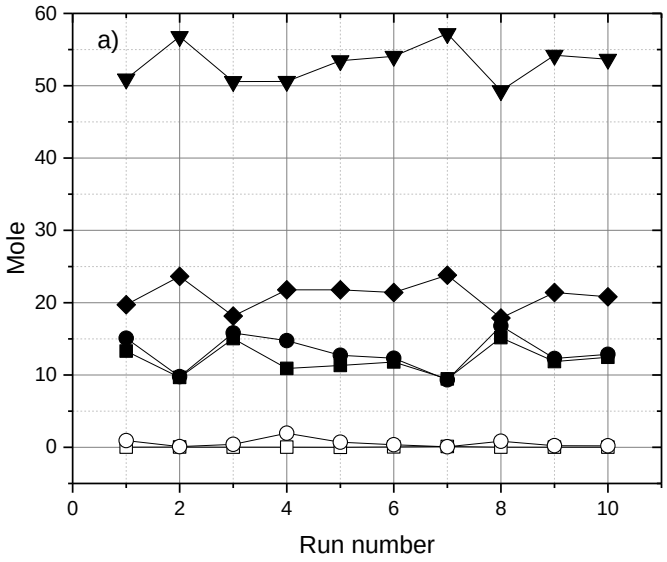

(a)

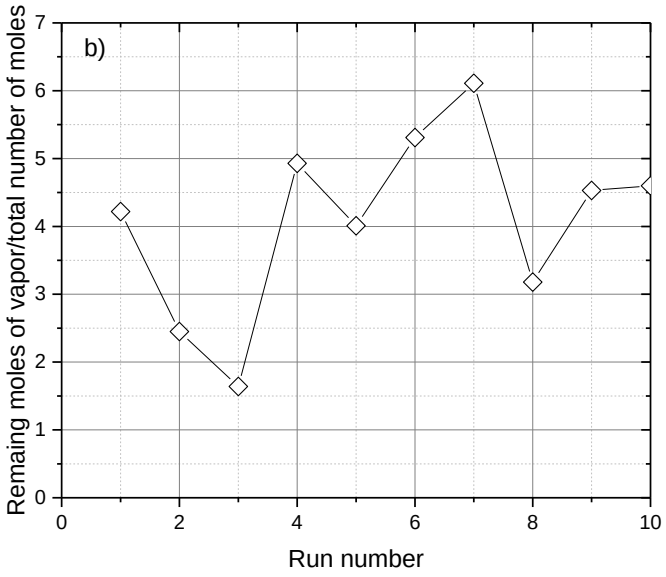

(b)

Figure 5.7. (a) pyrolysis at 2500 K and 1 bar of methane (40% v/v) in oxygen containing 100 moles of reactants (case with 6 components, 10000 composition vectors H_2O, ▼; CO,◆; H_2,●; CO_2,■; O_2,○; CH_4,□); (b) condensation at 1 bar – 250 K of an alcoholic solution containing 100 moles of mixture (case with 8 components; 10000 composition vectors) where N_R is remaining moles of vapor,◇.

It appears (**Figure 5.8**) that the larger the number of composition vectors, the smaller the fluctuations from one run to another. Note that whatever the number of composition vectors those fluctuations always exists even if of decreasing relative value when increasing the number of composition vectors. A direct consequence of this is that with the MCGE method the final composition can be known only within some margin of uncertainty. This effect is particularly marked in the present case which is particularly demanding for the MCGE method. The reason is that the minor species in the product (CH_4 and O_2 for the pyrolysis and % liquid for the condensation) are the major species in the reactants. As a result, the composition space to explore is particularly wide: CH_4 between 0 and 40%, O_2 between 0 and 60%, CO_2 between 0 and 40%, etc.…

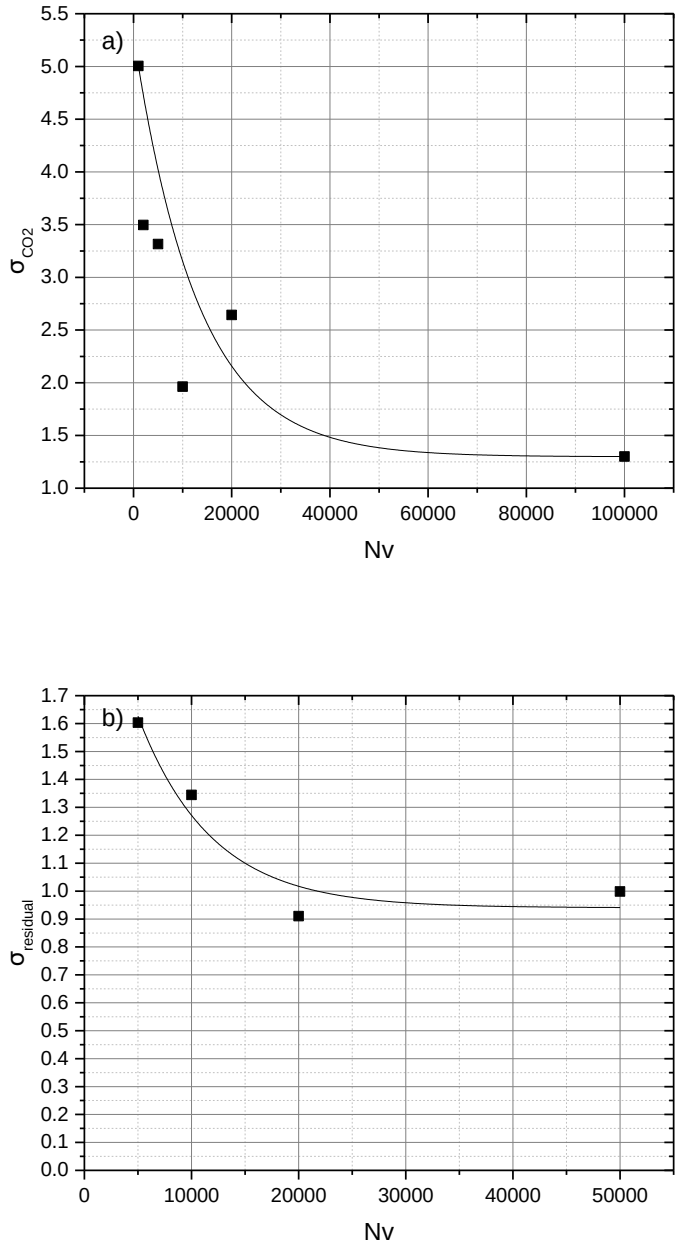

Figure 5.9. standard deviation divided by the mean value calculated on 10 successive runs as a function of the number of composition vectors for the CO_2 concentration in the methane-oxygen pyrolysis case ("8 components case"-top) and for the vapor faction in the condensation case ("8 components case"-bottom), For these two figures, the fitted equation curve is on the form: $y = A_1 \times \exp(-x/t_1) + y_0$.

As shown in these examples, the number of composition vectors needed to reach a given degree of accuracy can be as large as 100000. With a similar complexity, a minimum would be reached using a Lagrangian method by calculating only about 1000 points. But remember that

the accuracy is not clearly known in the latter case. As a consequence, the calculation costs are on average larger with the MCGE method as compared to the standard Lagrangian based techniques. For the specific case of the MCGE method, the calculation costs are presented in **Figure 5.10**. Note that most of the burden of the calculation is due to the calculation of the intermolecular effects. It can be estimated that without accounting for the intermolecular forces the duration of the calculation will be 100 to 1000 times less for the same number of composition vectors.

Moreover, in case the number of products greatly exceeds the number of elements, many of the composition vectors chosen by the Monte Carlo step will be rejected during the Gaussian Elimination step because negative concentrations will appear. A large number of attempts will be required to obtain the desired number of composition vectors.

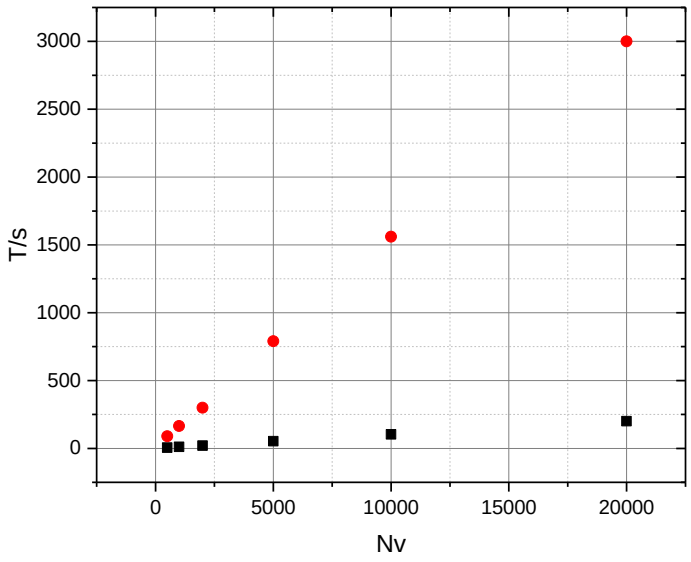

Figure 5.10. duration of a calculation for the 6 components cases of **Table 5.7** and **错误!未找到引用源。** (laptop - Intel(R) Core(TM) i5-4210U CPU - 1.70GHz - 8.00 GB RAM). T is time, and Nv is the number of composition vectors. Distillation,●; Pyrolysis,■.

One of the advantages of the MCGE method is that it avoids a linearization of the Gibbs equations so that the evolutions of the Gibbs energy as a function of the chemical composition (including the effect of the intermolecular forces) can in principle be accounted for accurately.

The polarity effects and pressure effects are nevertheless likely to be challenging situations.

To investigate this, the distillation of an ethanol-water solution can be recalled as being representative of a polar case (**Figure 5.11**). The simulation results are fully consistent with the experimental data, suggesting first that the thermodynamic data are calculated in a relevant manner and second that the minimization technique is able to follow conveniently the variations of the activity coefficients.

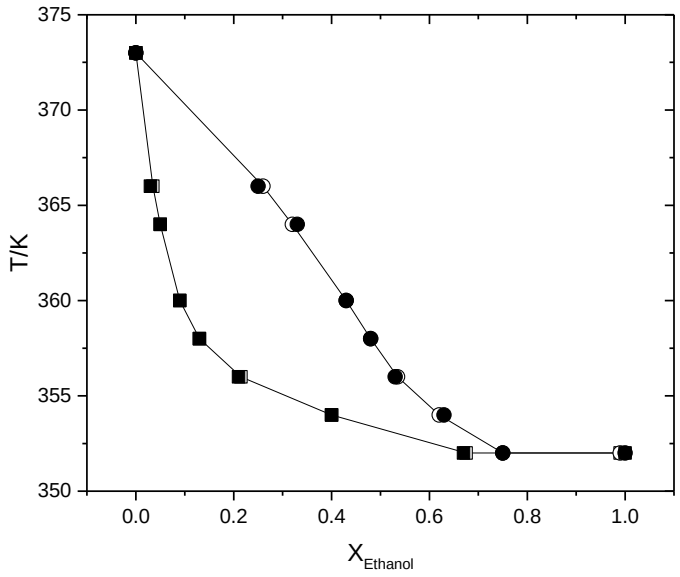

Figure 5.11. Simulation of the water-ethanol equilibrium (atmospheric pressure) as a function of the temperature using the LCVM/departure function/MGCE methods (CIRCE code). Simulations: vapor, ○; experiments: vapor, ●; simulations: liquid, □; experiments: liquid, ■.

To investigate the influence of large pressures, the high-pressure distillation of n-pentane

in propane at 344 K and various pressures (nonpolar system) is investigated[73]. It also shows a satisfactory agreement with available experimental data (**Figure 5.12**).

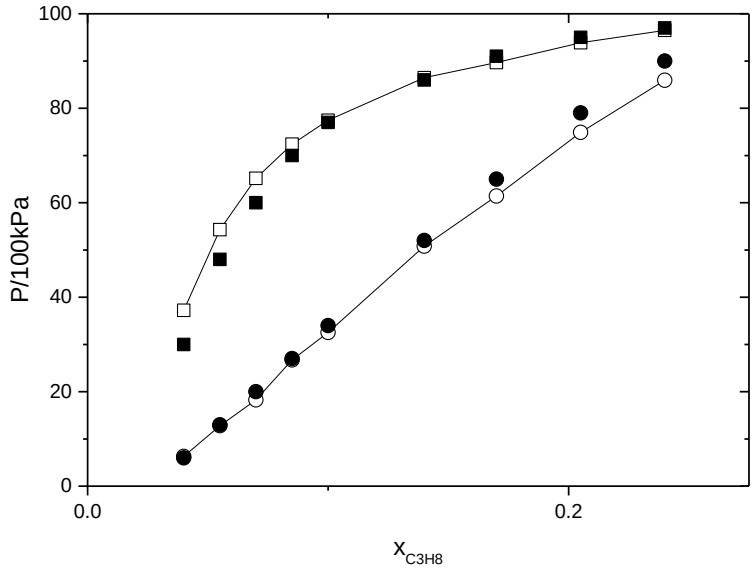

Figure 5.12. Prediction of the P-x-y diagram for the distillation propane/n-pentane at 344.26 K using the LCVM/departure function/MGCE methods (CIRCE code). Experimental data from Knapp et al.(1982)[73]. Simulations: vapor, ○; experiments: vapor, ●; simulations: liquid, □; experiments: liquid, ■.

The distillation of methanol in water at 423 K and various pressures[74] (pressure and polar effects) also shows a satisfactory agreement with available experimental data again (**Figure 5.13**).

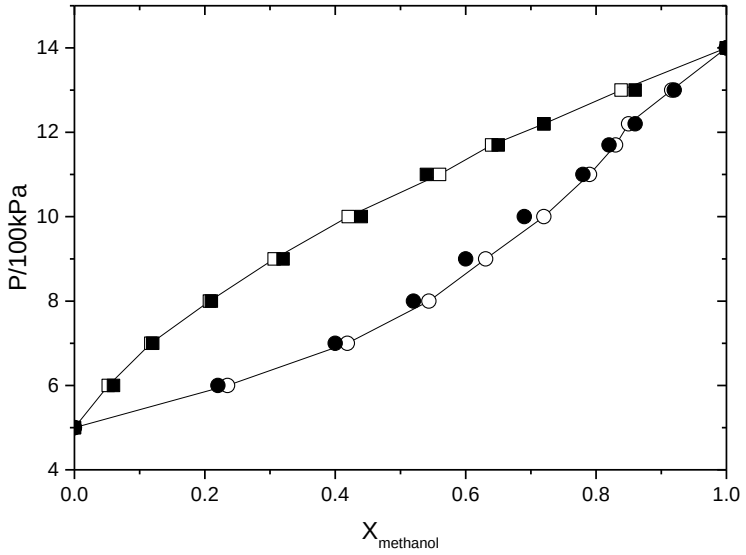

Figure 5.13. Prediction of the P-x-y diagram for the distillation methanol-water at 423 K using the LCVM/departure function/MGCE methods (CIRCE code). Experimental data from Griswold and Wong ENREF[74]. Simulations: vapor, ○; experiments: vapor, ●; simulations: liquid, □; experiments: liquid, ■.

Hence it seems that the various modeling strategies implemented in CIRCE could offer the possibility to cover many situations.

5.2 Case studies

CIRCE is typically a thermodynamic code for chemical engineering. Practical applications cases were done and are presented below as illustrations.

The following case studies correspond to various practical applications covered or addressed in our laboratory: biomass pyrogasification, combustion in burners, safety (explosions) and separation using supercritical “green” fluids. Note that catalysis and “Gibbs energy enhanced processes” like those using microwaves and electrical fields were not addressed yet.

5.2.1 Biomass pyrogasification

Pyrogasification is a rather versatile technique enabling the transformation of various carbonaceous materials into commercial fuels with an optimal yield in mass and energy. The work considered here was performed during the$BioH_2$ program[75] sponsored by Ademe (National Agency for Energy).

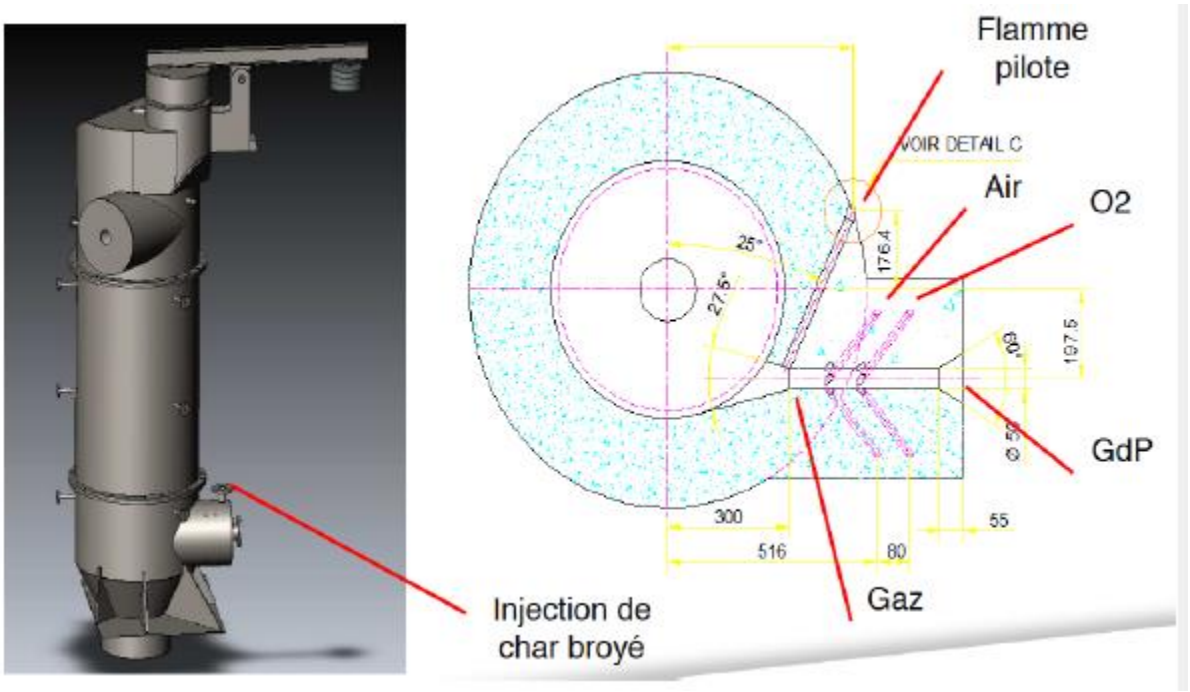

Figure 5.14. The experimental device of pyrolysis.

The experimental device is a rotating oven used under the gasification mode i.e., using a low oxygen flowrate, associated with a gasifier transforming the char issued from the oven into syngas. The pyrolyzed gases produced in the oven are partly burned in the oven, to maintain the required gasification temperature (300-600°C) and partly combusted in the char gasifier for a similar reason (maintain 1000°C). Following, the syngas results only from the char gasification (**Figure 5.15**).

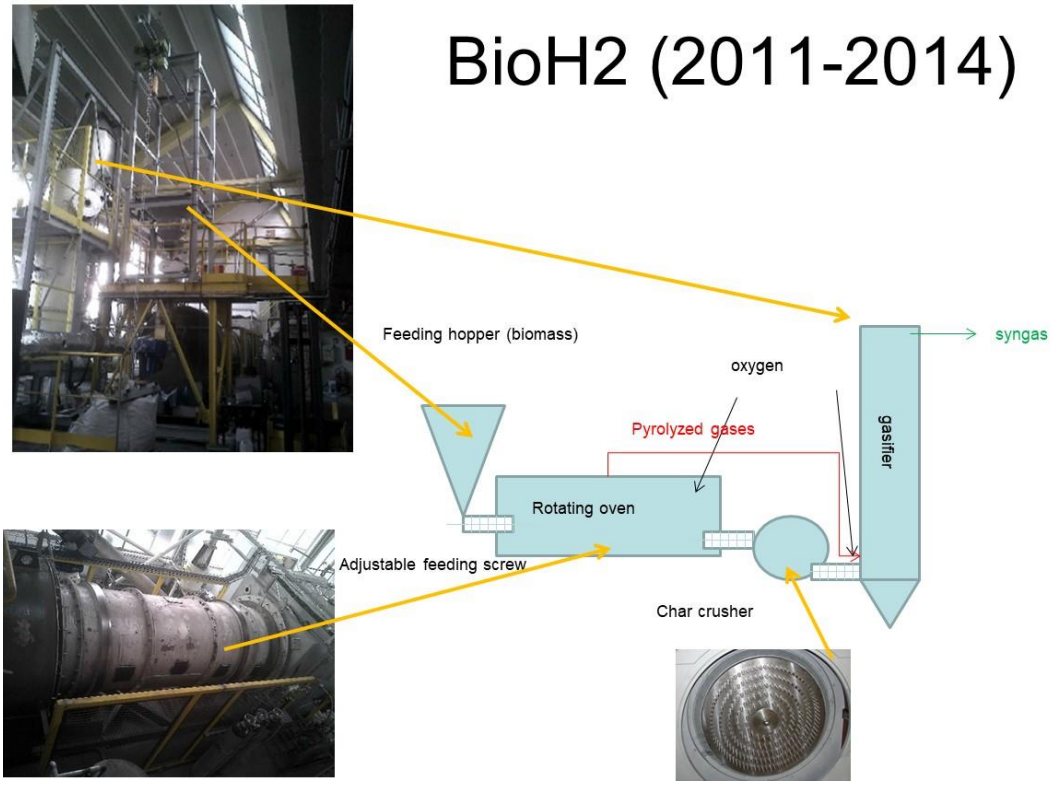

Figure 5.15. the pyrogasification process of $BioH_2$ process.

The pyrolysis reactor is a 4 m long rotating oven, with an internal diameter of 0.80 m. The char is extracted from the exit with a rotating screw and crushed in a mill. The oven is preheated to the pyrolysis temperature using a methane-air burner which is switched off when the pyrolysis is on. Then oxygen is admitted which burns part of the pyrolysis gases to maintain the temperature. Typical pyrolysis temperatures are between 400°C and 700°C.

The gasification reactor is vertical cylindrical with an ortho-radial inlet at the bottom and a tangential outlet on the upper part. At the inlet the pyrolysis gases coming from the oven, the grinded char, oxygen and air are admitted. At the output, syngas is collected. The typical gasification temperature is 1000°C.

The combustible is biomass consisting in a mixture of woods (hardwood and/or resinous) preconditioned in small bits. The "particle" size is 20-30 mm (**Figure 5.16**). The humidity

content is =11.1% m/m on the crude. The elemental analysis on the dry stuff yields: C=51.1%; H=5.76%; N<0.3%; K<0.1%; O=42.7% (m/m %).

Figure 5.16. the biomass sued in BioH_2 project.

Typical experimental conditions are given in **Table 5.8**.

Table 5.8. Temperature in different sections and for different tests (Sxx).

Reference	**S37**	**S47**	**S49**	**S50**	**S51**
Wood feeding/(kg/h)	72	72	72	72	72
O_2 flow rate oven/(kg/h)	19	18	11.5	11.5	11.5
T average oven/(°C)	280-480	440-640	360-580	390-590	340-560
T pyrolysis gases/(°C)	215	300	216	238	207
O_2 gas flow rate/(kg/h)	23	26	23	26.8	27
T average low gasifier/(°C)	950	1300	1200	1260	1260
T medium high gasifier/(°C)	600	1150	1080	1120	1120
T syngas gas outlet/(°C)	400	970	1030	1050	1000
Gas passage time/(s)	11.7	6.2	6.4	6.1	6.3
Dry gas analysis: CO/H_2/(%)	22/12.5	35/32.4	26/27	25/26	28.7/28.2
PCI/(kJ/Nm_3) dry gas	4400	8500	6200	5700	6850

In this work, the mass flowrates were also estimated at different points of the equipment. But only the composition of the syngas and the char were controlled. The results for test S51 are shown in **Table 5.9** and **Figure 5.17**.

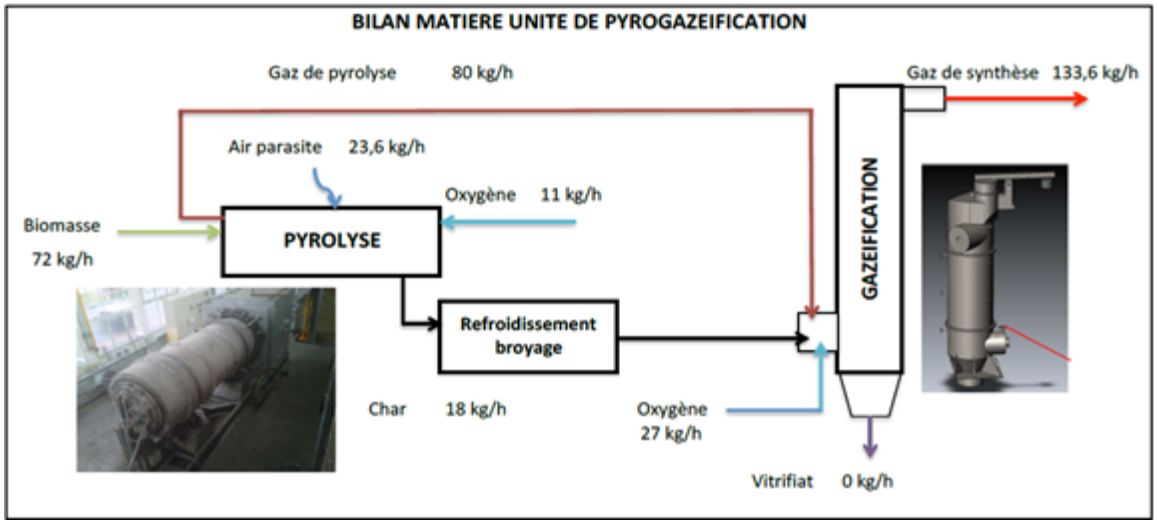

Figure 5.17. typical balance of the flowrates in the process (test S51)

Table 5.9. measured composition of the syngas (in % v/v - test S51)

Syngas		
composition	Dry sample	wet
CO_2(%)	28.70	24.77
CO	28.80	24.85
CH_4	0.48	0.41
H_2	28.20	24.34
N_2	13.82	11.93
O_2	0.00	0.00
H_2O	0.00	13.70
	100.00	100.00
Specific heat (kJ/Nm^3°C)	2.09	2.06
Specific mass (kg/Nm^3)	1.13	1.08
PCI (kJ/Nm^3)	6845	5915
PCI (kcal/Nm^3)	1637	1413
PCI (kJ/kg)	6092	5472

The simulations in the oven (pyrolysis) were performed using CIRCE using the inlet mass proportions of **Figure 5.17** above (wood 72 kg, air 23.6 kg, and oxygen 11 kg corresponding to one hour processing) and the module simulating a reaction at fixed P and T.

The pressure is atmospheric, and the temperature in the pyrolyzer is on average=450°C.

The selected products are H_2, CO, CO_2, H_2O, CH_4, N_2, O_2 and solid carbon to mimic the char (it was analyzed and contains fixed carbon at more than 90%m/m). The results are presented in **Table 5.10**.

Table 5.10. Number of moles and mass of products for the pyrolysis step during one hour of pyrolysis: CIRCE simulations (test S51)

species	C(s)	H_2	O_2	N_2	CO	CO_2	CH_4	H_2O	Total
Number of moles	1756.70	388.54	0.68	642.90	66.81	934.62	321.43	1051.44	5163.10
Mass	19.83	0.78	0.02	18.00	1.87	41.12	5.14	18.93	105.69

From the **Table 5.10**, it can be realized that the simulation results obtained with CIRCE reasonably agree with the values obtained from the experiments: 18 kg of char and 80 kg of gases measured as compared to 20 kg of char and 85 kg of gases (simulated).

More information is available for the gasification step. The simulated pyrolysis gas and char were reacted with additional oxygen (27 kg/h) at 1100°C and atmospheric pressure. The results are presented in **Table 5.11**.

Table 5.11. the experimental and simulation results for the gasification step (test S51).

	Experiment		Simulation	
Composition	Vol%	Mass%	Vol%	Mass%
H_2(g)	24.34		22.28	
CO(g)	24.85		38.67	
CO_2(g)	24.77		14.08	
CH_4(g)	0.41		0.07	
H_2O(g)	13.7		13.71	
N_2(g)	11.93		11.15	
O_2(g)	0		0.04	
Total	100	100	100	

The agreement is not as good showing with an excess of CO detrimental to CO_2 production. Since the other gases are well predicted, this means that the oxygen balance used in the calculation (extracted from the experimental report), may not exactly correspond to the reality.

5.2.2 Combustion in burners

An example of premixed combustion and burnt gases analysis in an atmospheric burner is given. The experiments were performed by Konnov et al.[76]. The concentrations of O_2, CO_2, CO, and NO were measured in the post-flame zone in mixtures of H_2, CO, CO_2 burning in air.

The experimental setup is shown in **Figure 5.18**. The gases (air, CO, CO_2, H_2) were supplied from gas cylinders to the inlet of the burner's plenum chamber in which they mix thoroughly. The flow rates are carefully controlled.

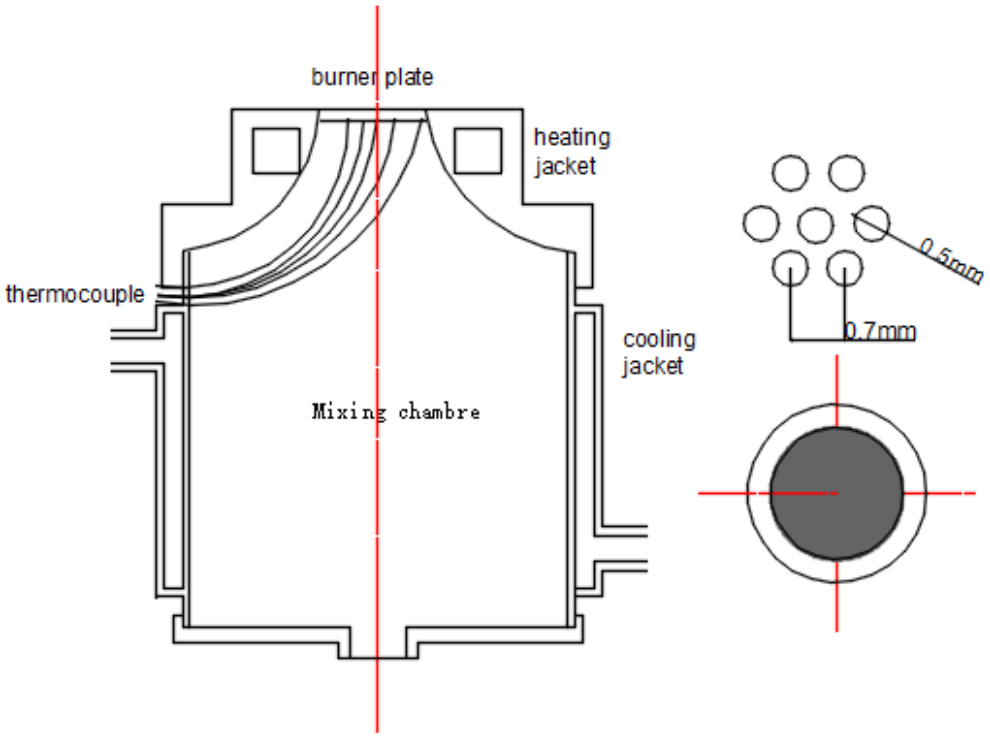

Figure 5.18. the experimental instrument for the combustion burner.

The burner head is mounted on the plenum chamber and is a porous plate (brass plate of 2 mm thickness and 30 mm diameter, perforated with a hexagonal pattern of small holes of 0.5 mm diameter and 0.7 mm pitch). Six copper-constantan thermocouples of 0.1 mm in diameter

are welded into the plate surface at the upstream side and gas samples are sucked via a tiny quartz tube some mms downstream from the flame towards a gas chromatography assembly (CO, CO_2, O_2 and NOx are measured). During the experiments, the temperature was fixed at 353 K and the pressure is atmospheric.

The simulations were performed using the block "adiabatic reaction at constant pressure" and the following list of products: H_2O, H_2, CO, CO_2, NO, N_2, O_2. **Figure 5.19** is plotted the measured and simulated concentrations of O_2, CO_2, CO and NO. Numeric values are listed in **Table 5.12**. Note, the "equivalence ratio" is the ratio of fuel concentration in the actual fuel-air mixture divided by the fuel concentration in the stoichiometric mixture.

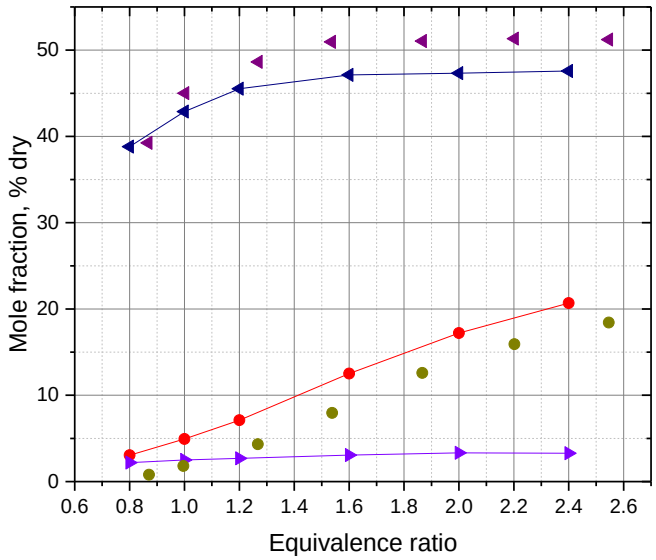

(a)

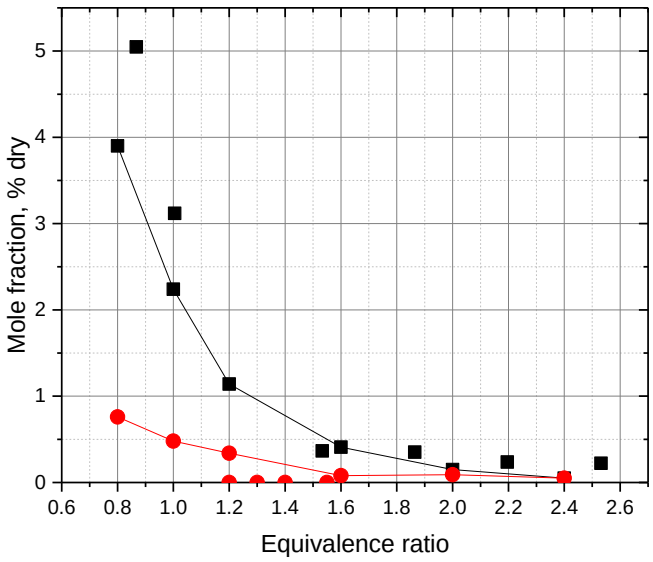

(b)

Figure 5.19: Concentrations of CO_2, CO, O_2, and NO in flames of H_2, CO, CO_2 in the air at different equivalence ratios. (a) simulated CO, ●; simulated CO_2, ◀; simulated H_2O, ▶; measured CO, ●; measured CO_2, ◀; (b) simulated O_2, ■; simulated NO, ●; measured O_2,■; measured NO,●.

Table 5.12. Simulated concentrations of CO, O_2, CO_2, and NO in flames of H_2, CO, CO_2in air.

Combustion	Reactant					Products							
Equivalence Ratio	H_2%	CO%	CO_2%	O_2%	N_2%	T(K)	O_2%	CO%	NO%	H_2%	N_2%	CO_2%	H_2O%
0.80	0.02	0.18	0.20	0.13	0.47	2329	3.90	3.05	0.76	0.03	51.23	38.82	2.20
1.00	0.02	0.20	0.23	0.11	0.43	2340	2.24	4.94	0.48	0.05	46.90	42.87	2.50
1.20	0.03	0.23	0.25	0.10	0.39	2336	1.14	7.12	0.34	0.10	43.08	45.52	2.70
1.60	0.03	0.26	0.29	0.09	0.34	2325	0.41	12.52	0.08	0.11	36.70	47.12	3.06
2.00	0.03	0.28	0.32	0.08	0.29	2317	0.15	17.22	0.09	0.10	31.77	47.32	3.33
2.40	0.03	0.30	0.34	0.07	0.26	2301	0.05	20.69	0.05	0.34	28.01	47.57	3.29

The simulation results are basically consistent with the experiment results. Note however that the % of NO is not correct. Measured concentrations of NO are a few ppms so the concentration of this product is 10^{-6} mole/m^3. But from **Table 5.12**, it is clear that the calculated mole fraction is about 0.1% (1000 ppm) or, equivalently, 10^{-3} mole/m^3. This is a consequence

of the accuracy of the MGCE method which depends on the chosen number of composition vectors.

5.2.3 Safety: gaseous explosions

In industries, explosions represent a significant risk and there is a need to be able to foresee the energetics of the underlying reactions. One parameter is the maximum explosion overpressure which can be observed when a flammable cloud confined into a closed vessel explodes. A flame front usually is triggered into the cloud and propagates transforming the reactants into burnt products into such short laps of time (milliseconds) that the reactions can be considered isochoric and adiabatic. In SAFEKINEX project[77], the maximum explosion pressures for various gases under various initial T and P conditions and various vessels were measured.

These situations were simulated using CIRCE and the "adiabatic and isochoric reaction module". Traditional combustion gases were retained: H_2, CO, CO_2, O_2, N_2, H_2O.

Results obtained with the methane-air mixture at various dilutions and ignited at ambient conditions are shown in **Figure 5.20** and compared with experimental data. The simulations results are larger than experimental data by 10% at the stoichiometry and more near the flammability limits (5% and 15% CH_4). The reason for this is well known and comes from the fact that the flame ball touches the upper wall (due to the action of the buoyancy forces acting on the light hot products) well before the end of the combustion so that heat is lost and the combustion is not perfectly adiabatic.

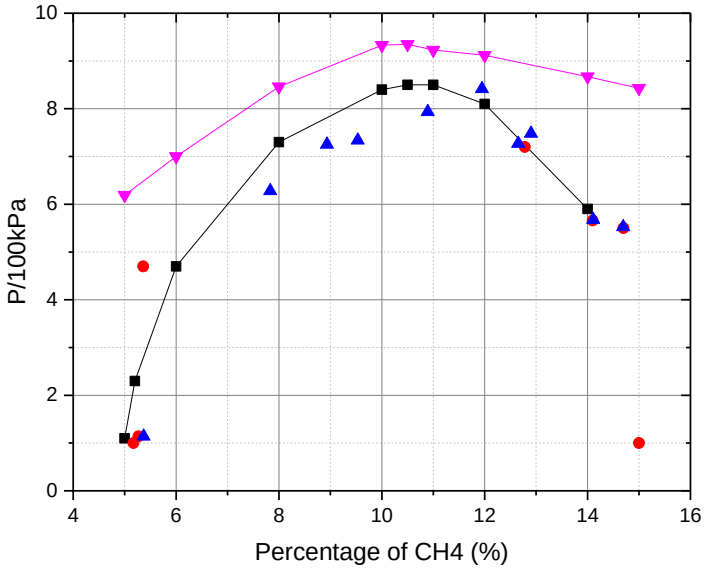

Figure 5.20. p_{ex}/p_i for methane/air mixtures at 1 bar and 20°C. Simulation 20°C 1bar, ◀; INERIS 20-dm^3 (exp wire),■; INERIS 2000-dm^3 (hot spot),●; INERIS 2000-dm^3 (elect. Spark),▲.

When the temperature increases, the flame velocity increases and this effect is less pronounced and the trends are correctly predicted **(Figure 5.21**).

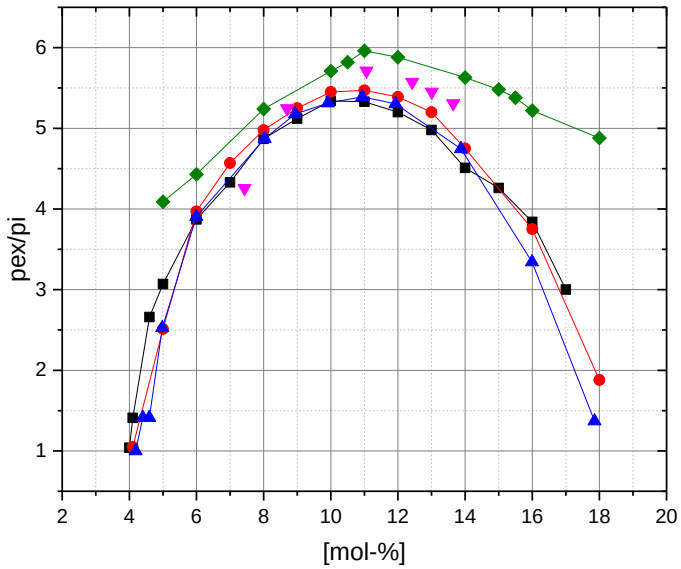

Figure 5.21. p_{ex}/p_i for methane/air mixtures at 1 bar and 200 °C. BAM 2.8-dm^3, ■; BAM 6.0-dm^3, ●;TU Delft 20-dm^3, ▲; INERIS-2000-dm^3-elect.spark ,▼;simulation.

When the initial pressure is increased, the explosion overpressure should increase in proportions. The comparison between the experimental results and the simulations is shown on

Figure 5.23 and again the agreement is correct if the specificity of the flame propagation is accounted for. Similar conclusions for both elevated initial pressure and temperature (**Figure 5.22**).

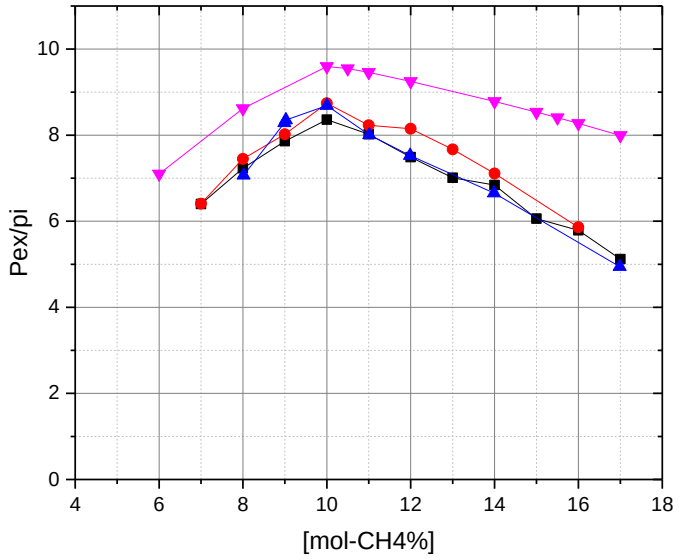

Figure 5.23. p_{ex}/p_i for methane/air mixtures at 10 bar and 20 °C. BAM 2.8-dm^3, ■; BAM 6.0-dm^3, ●; TU Delft 20-dm^3 , ▲; Simulation, ▼;

The above figure showed the simulation result is consistent with the experimental results.

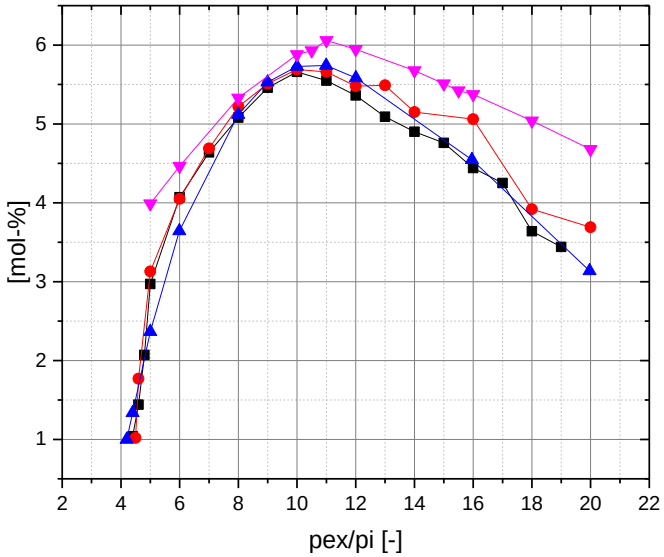

Figure 5.24. p_{ex}/p_i for methane/air mixtures at 10 bar and 200 °C. BAM 2.8-dm^3, ■; BAM 6.0-dm^3, ●; TU Delft 20-dm^3, ▲; simulation, ▼.

Experiments were also performed with hydrogen-air mixtures at different initial pressures and temperatures. The simulations were performed using the same procedure. The results are presented in **Figure 5.25**. Clearly, the simulations are closer to the experiments. The reason is hydrogen-air flames propagate 10 times faster than methane-air flames so that the thermal losses are smaller.

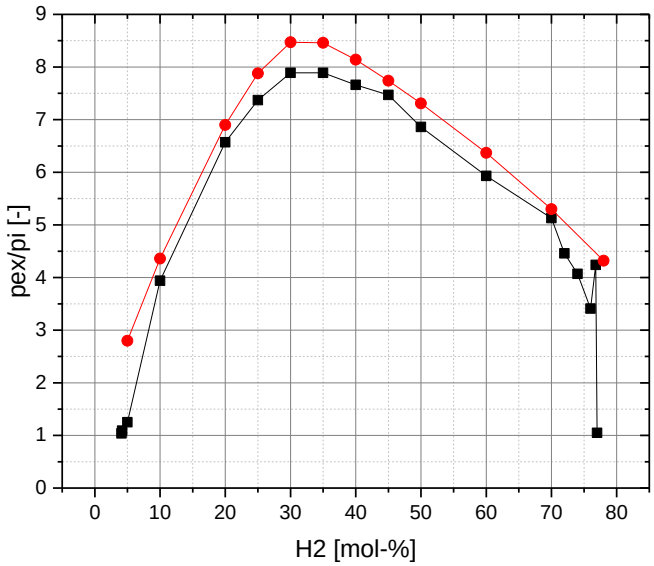
pex/pi [-]
H2 [mol-%]
0
1
2
3
4
5
6
7
8
9
0
10
20
30
40
50
60
70
80

(a)

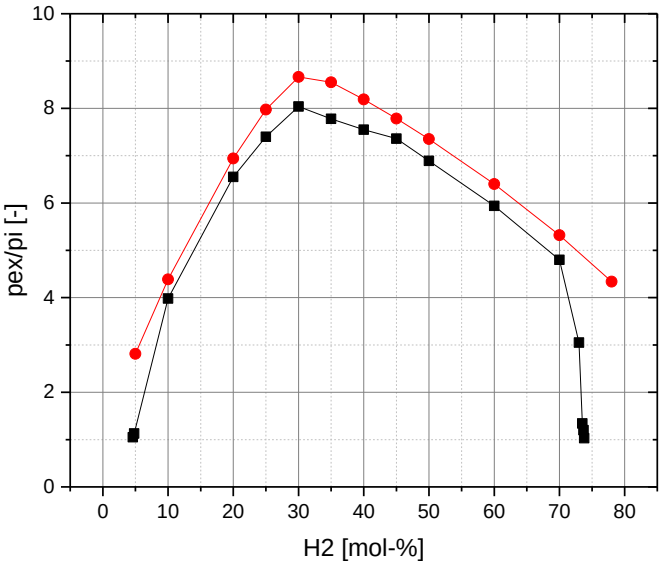
pex/pi [-]
H2 [mol-%]
0
2
4
6
8
10
0
10
20
30
40
50
60
70
80

(b)

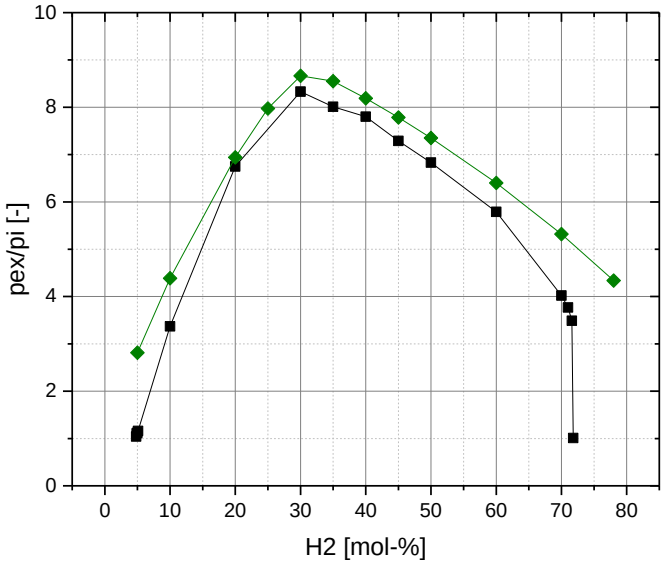

(c)

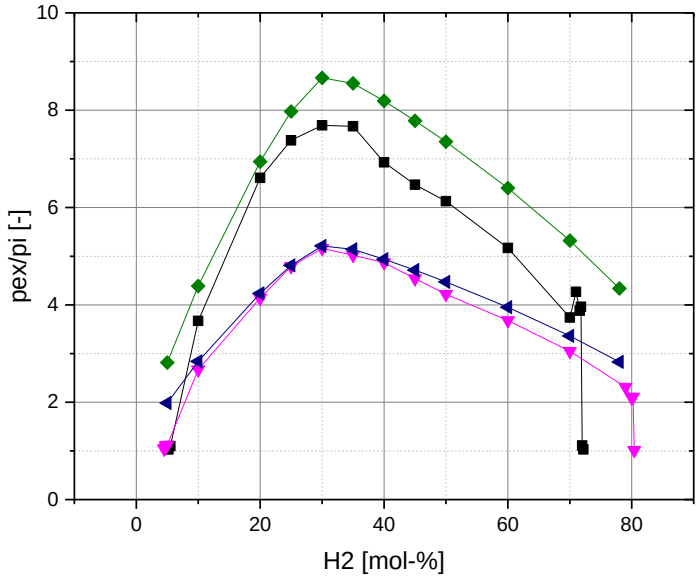

(d)

Figure 5.25. Comparison of experimental results and simulation for the explosion of H_2 and air mixture at various initial pressures and temperatures in a closed adiabatic volume. (a) simulation 20°C 1bar, ●; BAM 2.8-dm^3 20°C 1bar,■; (b) simulation 20°C 5bar, ●; BAM 2.8-dm^3 20°C 5bar,■; (c) simulation 20°C 10bar, ●; BAM 2.8-dm^3 20°C 10bar,■; (d) simulation 20°C 1bar, ◆; BAM 2.8-dm^3 20°C 1bar,■; simulation 250°C 30bar, ◀; BAM 2.8-dm^3 250°C 30bar, ◀.

5.2.4 “Green solvent” extraction

Extraction is a key operation in chemical engineering. Solvents are often expensive because of their high physical-chemical properties and may be environmentally unfriendly. Alternative green solvents are looked for, and supercritical fluids like CO_2 in certain conditions may be of interest. The solubility is the property of gases for instance (CO_2 here) to be dissolved in liquids (methanol here). The specific difficulty is linked to the possibility of the mixture to cross the supercritical domain. The general character of the LCVM EoS offers in principle the possibility to deal with the supercritical state since no reference pressure is used to couple the EoS with G^E. A typical example concerning the solubility of methanol in CO_2 is described (**Figure 5.26**). In this example, CO_2 is supercritical above 7 MPa whereas methanol is not. The resulting mixture produces nevertheless a gaseous and a liquid phase even above 7 bar with a partition between the two compounds[78]. The simulation strategy enables to mimic this behavior although with a reduced accuracy as compared to the preceding examples. A possible reason for this may lie in the facts that the parameters of the EoS are only approximate using the Constantinou approach and that the deviations become more influencing when P and T are not far from the critical points.

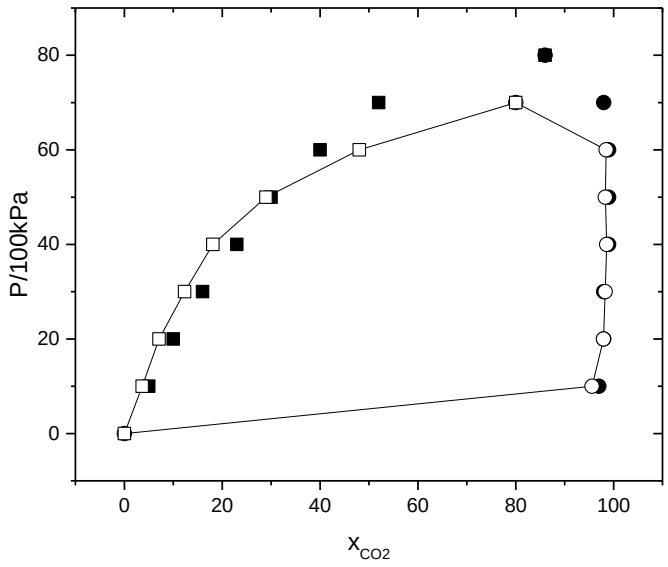

Figure 5.26. Prediction of the solubility of methanol in CO_2 at 313.15K using the LCVM/departure function/MGCE methods (CIRCE code). Experimental data by Suzuki et al.[78] at 313K. Simulations: vapor, ○; experiments: vapor, ●; simulations: liquid, □; experiments: liquid, ■.

6 Conclusions and perspectives

If the industrial aspect of processes in which chemical reactions occur is considered, there is a need to be able to foresee the evolution of the chemical reaction (yield, heat releases…) as a function of the process conditions (temperature, pressure…). When the variability of the components and reaction conditions are to be considered, the reality of the reaction may be complex including not only reactions with multiple components but also phase changes, energy considerations, and the modeling may prove difficult.

In this domain, significant efforts were deployed since at least one century based on the resources of modern thermodynamics and a number of codes were developed over the last decades (since the seventies), some being public but many others are in-house made to better fit with some specific applications.

Most of them are based on the principle that the Gibbs free energy should be minimum at equilibrium at least for a reaction occurring at constant temperature and constant pressure. To do this, a list of the potential products has first to be defined from the database of the code and usually a step by step minimizing technique is used to find the composition producing the smallest value of the Gibbs free energy.

In the most renown codes, the Lagrange multipliers method (LM) is employed, a robust mathematical approach and particularly efficient computationally speaking. More exotic techniques were nevertheless tested like the global optimization (SIMPLEX), genetic algorithm, but which do not solve the difficulties associated with the use of the Lagrange multiplier technique. Firstly, in the LM methods, a step-by-step approach is implemented (as

for instance a Newton-Raphson method). At best, the closest minimum to the initial “guess” is found. But for multiphase reactive mixtures, and non-ideal mixtures, the Gibbs function may be strongly nonconvex with a multitude of local minima and there is no guarantee that the absolute minimum will be found. Secondly, it is necessary to linearize the Gibbs function which induces mathematical issues (convergence difficulties).

To solve these difficulties, a Monte Carlo technique was developed during this Ph.D. work associated with a Gaussian elimination method (MGCE method) to ensure the atom balance is entirely satisfied. By performing several runs of the same simulation with the same number of composition vectors, it is possible to estimate the accuracy of the final result. Although computationally much more demanding than the traditional Lagrange multiplier methods, it seems to be far more reliable. This method (MCGE) can calculate a reactive multiphase equilibrium where LM based methods just fail.

It is also shown that the availability and accuracy of the thermodynamic data is a significant limitation in the predictability of the software. The energies and entropies of formation of the product need to be self-consistent and, for this, using data (experimental or theoretical) from different sources should be avoided. Data scattering/mismatch larger than a few kJ/mole may significantly impair the predictions as shown in the present work. Similarly, the models used to estimate the non-ideality of the fluids influence the accuracy of the simulation. In this Ph.D. work, the “group contribution theory”, as implemented in UNIFAC, is used to describe the molecules and all their thermodynamic properties: the activity coefficients, the equation of state coefficients, the energy of formation, the entropy of formation, and heat capacity… To

do this, correlations from the literature were compiled and adapted whenever required (for instance, to adapt the Joback's approach to the UNIFAC groups). Several applications to well-documented test cases seem to validate the robustness of this choice. Note that the LCVM equation of state was implemented to estimate the influence of the intermolecular forces since the latter is fully consistent with the UNIFAC coefficient of activities.

The last limitation (of chemical thermodynamic equilibrium codes) in the predictability is the choice of the product list. In this work, the influence of this aspect is shown: the absence of some critical products could strongly bias the final result but also incorporating products which are unlikely within the reaction conditions can also produce wrong results. In this work, a method is first proposed to identify an "exhaustive" list of final products based on the molecular composition of the reactants (based on the Brignole's idea of constituting "realizable" molecules using the group contribution theory). Secondly, a way to sort the products as a function of the reaction conditions is proposed. The idea is to guess a step by step decomposition balancing the reaction based on the established list of "realizable" molecules. Then the Gibbs energy of each reaction helps to select those reactions that are the most likely to occur.

These various methods were integrated into a new software CIRCE. CIRCE code was developed from scratch during this Ph.D. work. CIRCE contains two main blocks. One is devoted to the creation and evolution of the product database. On the basis of a simple description of each molecule (from their constitutive groups), the various models (Joback, Constantinou, Gani,..) are run to calculate the required thermodynamic data. In this block, the

Brignole's methodology can also be implemented to produce automatically a list of "possible products" starting from the atom balance of reactants. The second block offers the possibility to simulate three categories of chemical transformations: at constant pressure and temperature, adiabatic at constant pressure and adiabatic at constant volume. The user defines first the reactants (atom balance and initial enthalpy), the reaction conditions and obtains the final list of products, concentration and final energy, temperature and pressure.

Various practical applications are given in this memory.

The code is working satisfactorily and meets the initial objectives. Nevertheless, some issues remain:

1. As it stands, the MGCE algorithm is robust but computationally tedious and thus needs improvements. For instance, a distillation with three elements, four products, 2 phases requires 253 seconds on a laptop when the accuracy of 1% is looked for. The first cost of the computations is the constitution of an acceptable set of composition vectors (i.e. satisfying the atom balance). The larger the number of products (for a fixed number of atoms), the larger the probability for a composition vector to rejected. A refined mathematical approach is certainly achievable. The second source of cost is the calculation of the activity coefficients for each composition vector. And the last source of cost is the desired accuracy of the simulation. For these two last sources of cost, potential solutions could be parallelizing the code or coupling the MCGE and LM methods;
2. The "group contribution theory" proved efficient but seems presently limited to organic chemistry. Minerals may also be considered and an extension of the group contribution theory

may be envisioned to address this;

3. The selection method to sort out the “relevant” products list is not complete enough since, for instance, it does not include reactions between two reactants. Furthermore, kinetics although being an important aspect, is not accounted for and it is believed that existing tools (NIST, CHEMKIN,…) may not be flexible enough (comprehensive, consistent,…). Some ideas were suggested like the Bell-Evans-Polanyi method;

4. On the practical applications, the introduction of catalysts or other reaction promoters (microwaves, electrical fields, ultrasounds) needs to be investigated. It seems that many of them may be modeled as a Gibbs energy “source” but the mathematical formulation needs to be worked out.

Appendices

Appendix A: analytical derivation of equation ((3.2)

The starting equation is the same s the eqn. (2.61), but considers 3 components where component 1 is the only liquid (hence γ_1=1), 2 and 3 are gases where 3 is an inert (n_3=constant):

$$G = n_1\mu_1 + n_2\mu_2 + n_3\mu_3 + n_1RT\ln\left(\frac{n_1}{n_1}\right) + n_2RT\ln\left(\frac{n_2}{n_2+n_3}\right) + n_3RT\ln\left(\frac{n_3}{n_2+n_3}\right) + n_1RT\ln\gamma_1 + n_2RT\ln\gamma_2 + n_3RT\ln\gamma_3 \quad \text{(A1)}$$

When a derivation against n_1 is applied:

$$\frac{dG}{dn_1} = \mu_1 + \frac{dn_2}{dn_1}\mu_2 + \frac{dn_2}{dn_1}RT\ln\left(\frac{n_2}{n_2+n_3}\right) + n_2RT\frac{\frac{dn_2}{dn_1}\frac{n_3}{(n_2+n_3)^2}}{\frac{n_2}{n_2+n_3}} + n_3RT\frac{-\frac{dn_2}{dn_1}\frac{n_3}{(n_2+n_3)^2}}{\frac{n_3}{n_2+n_3}} + \frac{dn_2}{dn_1}RT\ln(\gamma_2) + n_2RT\frac{d\gamma_2}{dn_1\gamma_2} + n_3RT\frac{d\gamma_3}{dn_1\gamma_3} \quad \text{(A2)}$$

Since:

$$x_2 = \frac{n_2}{n_2+n_3} \quad \text{(A3)} \qquad 1 - x_2 = \frac{n_3}{n_2+n_3} \quad \text{(A4)}$$

$$\frac{dn_2}{dn_1} = -A \quad \text{(A5)} \qquad \frac{n_3}{n_2} = \frac{1-x_2}{x_2} \quad \text{(A6)}$$

$$dn_2 = dx_2\frac{(n_2-n_3)^2}{n_3} \quad \text{(A7)}$$

(A2) simplifies to:

$$\frac{dG}{dn_1} = \mu_1 - A\mu_2 - ART\ln x_2 - ARTx_3 + ARTx_3 - ART\ln\gamma_2 + RT\left[-A\cdot n_2\frac{d\gamma_2}{\gamma_2 dn_2} - A\frac{n_3 d\gamma_3}{\gamma_3}\right] \quad \text{(A8)}$$

And is minimized using:

$$\frac{dG}{dn_1} = 0$$

$$0 = \mu_{10} - A \cdot \mu_{20} - A \cdot R \cdot T \cdot ln(x_2) - A \cdot R \cdot T$$

$$\cdot \left[ln\gamma_2 + \frac{d\gamma_2}{dx_2} \cdot \frac{(1 - x_2) \cdot x_2}{\gamma_2} + \frac{d\gamma_3}{dx_2} \cdot \frac{(1 - x_2)^2}{\gamma_3} \right]$$

Which is eqn.(3.2).

Appendix B: Equation of states and molecular interactions

From the mid-17th century, people began to study the low-pressure gas PVT relationship. They found three types of the empirical law of gas were established: Boyle's law, Gay Lussac's law and Avogadro's law. The following composite equation can be obtained:

$$Pv=nRT \quad \text{(B1)}$$

which is the 'ideal gas equation of state' based on the assumption that gaseous molecules act as perfectly rigid spheres without any attractive or repulsive forces between them and the environment.

In practice, molecules in real gases are submitted to attractive and repulsive forces which relative influence depends on the proximity of the molecules and thus on the specific volume, temperature,… The deviation from the ideal gas law is measured using the compressibility factor expressed as:

$$Z = \frac{Pv}{RT} \quad \text{(B2)}$$

The ideal gas equation of state is a particular case of the equation of state when Z = 1. The difference between Z and 1 quantifies the difference between the real gas and the ideal gas state. A physically interesting limit is that between the liquid and the gaseous state. This limit disappears when the fluid is above the critical point (Tc and Pc). It was shown that the behavior of all real gases could be collapsed into a single graph using $Tr=T/Tc$ and $Pr=P/Pc$ as adimensional parameters of the T and P (Figure B1).

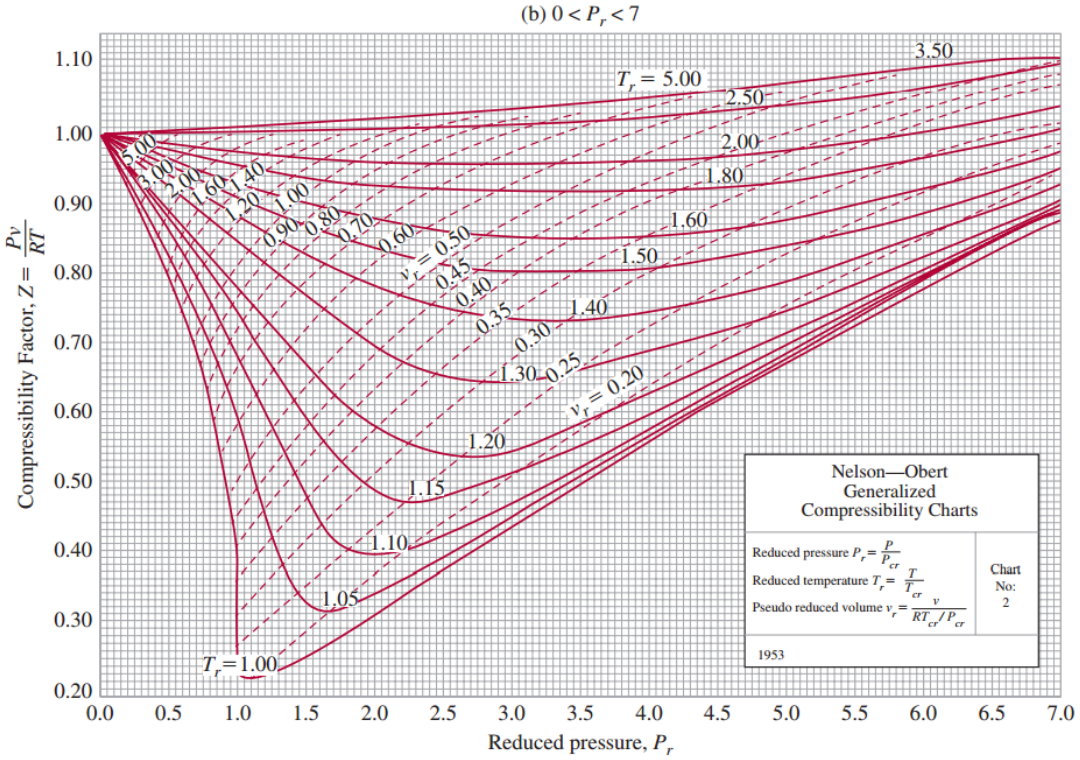

Figure B1. the generalized compression factor diagram.

Fig. B1 shows that the ideal gas equation of state can fit very accurately when T and P are far from Tc and Pc.

In 1893, Van der Waals concluded that for real gases:

(i) The volume occupied by the molecules is not zero and should be subtracted from the total volume to retrieve the real free volume.

(ii) Molecules interact with various forces which change their velocities, and thus the pressure and a correction term should be added. Such forces should be proportional to the number volumetric density of the molecules (=1/molar volume) and inversely proportional to the distance between two molecules. And this distance is inversely proportional to the number volumetric density of the molecule.

The final formulation is:

$$\left(P + \frac{a}{v_m^2}\right)(v_m - b) = RT \qquad \text{(B3)}$$

Where a and b are constants (v_m is the molar volume). The constant 'b' is related to the volume occupied by the gas molecule ("co-volume" $m^3 \cdot mol^{-1}$) while 'a' is related to the influence of the molecular interaction (energy term in $Pa \cdot m^6 \cdot mol^{-2}$). Equation (B3) is a "cubic" equation since it normally has three characteristic roots when the temperature and pressure are suitable. It can be demonstrated that a and b are related to the critical parameters P_c, T_c, and v_c. (Since at the critical point the first and second derivative of P as function of v_m is zero). Qualitatively at least, the Van der Waals equation can predict the gas and liquid behavior including phase changes.

The ideal gas can be considered as a limiting case of the van der Waals equation of state when P tends to zero since in such conditions v_m tends to infinity in such a way that the correction terms are negligible. This remark is used to calculate the "departure function".

It was recognized that although being significant progress, the Van der Waals equations is deficient on many aspects and alternative EoS, based on a very similar formulation, were proposed later like the RK equation,[21] the SRK[22] EoS and the well-known Peng-Robinson EoS.[23]

	Avantages	Drawbacks
VdW	A feasible methodology is given.	Poor for liquid phase properties.
RK	Generally good for gas phase properties. Satisfactory for gas phase fugacity calculation Pr < Tr/3. Satisfactory for enthalpy departure and entropy departure calculations.	Poor for liquids (needs additional correlations)
SRK	Serves similar functions as the Redlich Kwong EOS (RK) but requires more parameters. Satisfactory for polar systems, but not used in the petroleum engineering.	Relatively poor for liquids.

PR	PR obtains better liquid densities than SRK. Serves similar functions as the Redlich Kwong EOS but requires more parameters. PR does a better job (slightly) for gas and condensate systems than SRK.	More limited than SRK for strongly polar systems

Table B1. the advantage and inconvenient for the different cubic equations.

The latter, detailed below, is particularly efficient in predicting liquid densities and vapor pressures even on the saturation line.

$$\mathrm{P} = \frac{RT}{v-b} - \frac{\alpha(T)}{v(v+b)+b(v-b)} \tag{B4}$$

Where for a pure component:

$$\alpha(T) = \alpha(T_C) \cdot \alpha(T_r, \omega) \tag{B5}$$

Where $\alpha(T)$ is the energy parameter of equation B5, $\alpha(T_r, \omega)$ is dimensionless, which dependent on the critical temperature and acentric factor, $\alpha(T_c)$ is defined as below:

$$\alpha^{1/2}(T_r, \omega) = 1 + \kappa\left(1 - T_r^{1/2}\right) \tag{B6}$$

With $\kappa = 0.37464 + 1.54226\omega - 0.26992\omega^2$

$$\alpha(Tc) = 0.45724\,\frac{R^2 T_c^2}{P_c} \tag{B7}$$

And the co-volume parameter b is a constant given by:

$$b(Tc) = 0.07780\,\frac{RTc}{P_c} \tag{B8}$$

Appendix C: UNIFAC and Joback's correlations

C1-The group contribution theory and UNIFAC

The UNIFAC model combines the UNIQUAC (Universal Quasi-Chemical) model and the functional group's concept considering that a physical property of a fluid can be linearly correlated to the contributions of some typical molecules' functional groups. In the UNIFAC model, the activity coefficients of molecules in mixtures are determined by summing up the contributions of UNIFAC groups.

The UNIFAC model distinguishes two categories of groups: subgroups and Main groups (table C1). Each main group corresponds to one or more subgroups that share the same interaction parameters with other groups a_{mn} (see after). Each subgroup is characterized by a volume R_k and surface area Q_k. The latter parameters are important to calculate the molecular surface or volume related parameters such as solvation, viscosity…

Table C1: UNIFAC subgroups and Main groups extracted from the DDBST database.

No.	Sub group name	Maingroup	No.	Sub group name	Maingroup	No.	Sub group name	Maingroup	No.	Sub group name	Maingroup
1	CH3	[1]CH2	31	CH3NH	[15]CNH	61	FURFURAL	[30]FURFURAL	91	HCCLF2	[45]CCLF
2	CH2	[1]CH2	32	CH2NH	[15]CNH	62	DOH	[31]DOH	92	CCLF3	[45]CCLF
3	CH	[1]CH2	33	CHNH	[15]CNH	63	I	[32]I	93	CCL2F2	[45]CCLF
4	C	[1]CH2	34	CH3N	[16](C)3N	64	BR	[33]BR	94	AMH2	[46]CON(AM)
5	CH2=CH	[2]C=C	35	CH2N	[16](C)3N	65	CH=-C	[34]C=-C	95	AMHCH3	[46]CON(AM)
6	CH=CH	[2]C=C	36	ACNH2	[17]ACNH2	66	C=-C	[34]C=-C	96	AMHCH2	[46]CON(AM)
7	CH2=C	[2]C=C	37	C5H5N	[18]PYRIDINE	67	DMSO	[35]DMSO	97	AM(CH3)2	[46]CON(AM)
8	CH=C	[2]C=C	38	C5H4N	[18]PYRIDINE	68	ACRY	[36]ACRY	98	AMCH3CH2	[46]CON(AM)
9	ACH	[3]ACH	39	C5H3N	[18]PYRIDINE	69	CL-(C=C)	[37]CLCC	99	AM(CH2)2	[46]CON(AM)
10	AC	[3]ACH	40	CH3CN	[19]CCN	70	C=C	[2]C=C	100	C2H5O2	[47]OCCOH

11	ACCH3	[4]ACCH2	41	CH2CN	[19]CCN	71	ACF	[38]ACF	101	C2H4O2	[47]OCCOH
12	ACCH2	[4]ACCH2	42	COOH	[20]COOH	72	DMF	[39]DMF	102	CH3S	[48]CH2S
13	ACCH	[4]ACCH2	43	HCOOH	[20]COOH	73	HCON(..	[39]DMF	103	CH2S	[48]CH2S
14	CH2=C	[2]C=C	44	CH2CL	[21]CCL	74	CF3	[40]CF2	104	CHS	[48]CH2S
15	CH3OH	[6]CH3OH	45	CHCL	[21]CCL	75	CF2	[40]CF2	105	MORPH	[49]MORPH
16	H2O	[7]H2O	46	CCL	[21]CCL	76	CF	[40]CF2	106	C4H4S	[50]THIOPHEN
17	ACOH	[8]ACOH	47	CH2CL2	[22]CCL2	77	COO	[41]COO	107	C4H3S	[50]THIOPHEN
18	CH3CO	[9]CH2CO	48	CHCL2	[22]CCL2	78	SIH3	[42]SIH2	108	C4H2S	[50]THIOPHEN
19	CH2CO	[9]CH2CO	49	CCL2	[22]CCL2	79	SIH2	[42]SIH2	109	NCO	[51]NCO
20	CHO	[10]CHO	50	CHCL3	[23]CCL3	80	SIH	[42]SIH2	118	(CH2)2SU	[55]SULFONES
21	CH3COO	[11]CCOO	51	CCL3	[23]CCL3	81	SI	[42]SIH2			
22	CH2COO	[11]CCOO	52	CCL4	[24]CCL4	82	SIH2O	[43]SIO			
23	HCOO	[12]HCOO	53	ACCL	[25]ACCL	83	SIHO	[43]SIO			
24	CH3O	[13]CH2O	54	CH3NO2	[26]CNO2	84	SIO	[43]SIO			
25	CH2O	[13]CH2O	55	CH2NO2	[26]CNO2	85	NMP	[44]NMP			
26	CHO	[13]CH2O	56	CHNO2	[26]CNO2	86	CCL3F	[45]CCLF			
27	THF	[13]CH2O	57	ACNO2	[27]ACNO2	87	CCL2F	[45]CCLF			
28	CH3NH2	[14]CNH2	58	CS2	[28]CS2	88	HCCL2F	[45]CCLF			
29	CH2NH2	[14]CNH2	59	CH3SH	[29]CH3SH	89	HCCLF	[45]CCLF			
30	CHNH2	[14]CNH2	60	CH2SH	[29]CH3SH	90	CCLF2	[45]CCLF			

Where AC is the aromatic carbon, THF is the tetrahydrofuran group, AM is the C-O-N group, NMP is the N-methyl-pyrrolidone group, and the MORPH is the morpholine.

An example of molecules breakdown in subgroups is given in Figure C1.

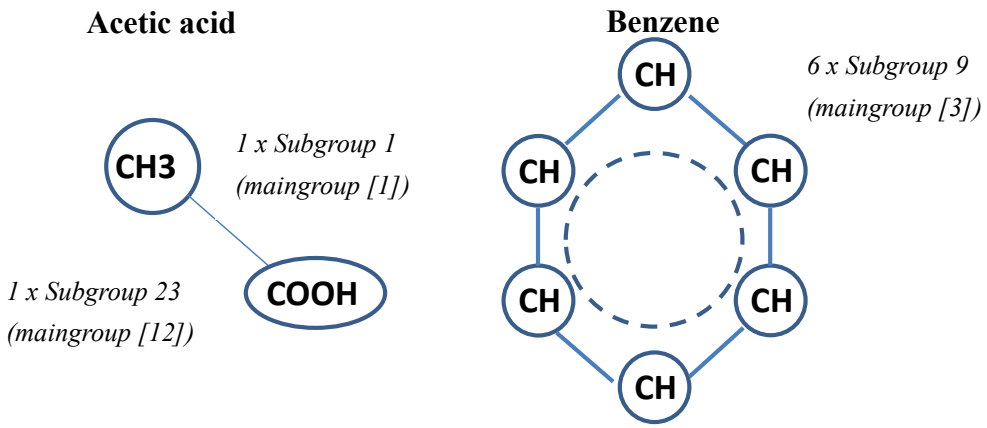

Figures C1. Two examples of molecules broken into their UNIFAC functional groups.

The UNIFAC model includes two contributions: a combinatorial part and a residual part

(the combinatorial activity coefficient γ_i^c and the residual activity coefficient γ_i^r of molecule i in the mixture while j is the groups in n types of groups):

$$\ln \gamma_i = \ln \gamma_i^c + \ln \gamma_i^r \quad \text{(C1)}$$

The combinatorial part of the activity coefficient is:

$$\ln \gamma_i^c = \ln \frac{\phi_i}{x_i} + \frac{z}{2} q_i \ln \frac{\theta_i}{\phi_i} + L_i - \frac{\phi_i}{x_i} \sum_{j=1}^{n} x_j L_j \quad \text{(C2)}$$

Where:

$$\theta_i = \frac{x_i q_i}{\sum_{j=1}^{n} x_j q_j} \quad \text{(C3)}$$

$$\phi_i = \frac{x_i r_i}{\sum_{j=1}^{n} x_j r_j} \quad \text{(C4)}$$

$$\text{And } L_i = \frac{z}{2}(r_i - q_i) - (r_i - 1) \quad \text{(C5)}$$

In these equations, θ_i and ϕ_i are the relative surface and volume of the molecule i in one mole of mixture, respectively, z is the coordination number of the system (i.e. the number of group neighbors for a given functional group, usually taken as 10), q_i is the molar surface area and r_i is the molar volume of molecule i (x_i is the molar fraction of molecule i in the mixture)

Parameters q_i and r_i are calculated from UNIFAC subgroup contributions as follows:

$$r_i = \sum_k v_k^{(i)} R_k \; ; \quad q_i = \sum_k v_k^{(i)} Q_k \quad \text{(C6)}$$

Where Q_k is the surface area of subgroup k, R_k is the volume of subgroup k, and $v_k(i)$ is the k_{th} functional group count in the molecule i. Table C2 shows the Q_k and R_k values for all the typical subgroups from UNIFAC.

Table C2. Examples of surface areas and volumes for UNIFAC subgroups.

No.	Subgroup	Main group	R	Q
1	CH3	[1]CH2	0.9011	0.848
2	CH2	[1]CH2	0.6744	0.54
3	CH	[1]CH2	0.4469	0.228

4	C	[1]CH2	0.2195	0
5	CH2=CH	[2]C=C	1.3454	1.176
6	CH=CH	[2]C=C	1.1167	0.867
7	CH2=C	[2]C=C	1.1173	0.988
8	CH=C	[2]C=C	0.8886	0.676
9	ACH	[3]ACH	0.5313	0.4
10	AC	[3]ACH	0.3652	0.12
11	ACCH3	[4]ACCH2	1.2663	0.968
12	ACCH2	[4]ACCH2	1.0396	0.66
13	ACCH	[4]ACCH2	0.8121	0.348
14	OH	[5]OH	1	1.2
15	CH3OH	[6]CH3OH	1.4311	1.432
16	H2O	[7]H2O	0.92	1.4
17	ACOH	[8]ACOH	0.8952	0.68
18	CH3CO	[9]CH2CO	1.6724	1.488
19	CH2CO	[9]CH2CO	1.4457	1.18
20	CHO	[10]CHO	0.998	0.948
21	CH3COO	[11]CCOO	1.9031	1.728
22	CH2COO	[11]CCOO	1.6764	1.42
23	HCOO	[12]HCOO	1.242	1.188
24	CH3O	[13]CH2O	1.145	1.088
25	CH2O	[13]CH2O	0.9183	0.78
26	CHO	[13]CH2O	0.6908	0.468
27	THF	[13]CH2O	0.9183	1.1
28	CH3NH2	[14]CNH2	1.5959	1.544
29	CH2NH2	[14]CNH2	1.3692	1.236
30	CHNH2	[14]CNH2	1.1417	0.924
31	CH3NH	[15]CNH	1.4337	1.244
32	CH2NH	[15]CNH	1.207	0.936
33	CHNH	[15]CNH	0.9795	0.624
34	CH3N	[16](C)3N	1.1865	0.94
35	CH2N	[16](C)3N	0.9597	0.632
36	ACNH2	[17]ACNH2	1.06	0.816
37	C5H5N	[18]PYRIDINE	2.9993	2.113
38	C5H4N	[18]PYRIDINE	2.8332	1.833
39	C5H3N	[18]PYRIDINE	2.667	1.553
40	CH3CN	[19]CCN	1.8701	1.724
41	CH2CN	[19]CCN	1.6434	1.416
42	COOH	[20]COOH	1.3013	1.224
43	HCOOH	[20]COOH	1.528	1.532
44	CH2CL	[21]CCL	1.4654	1.264
45	CHCL	[21]CCL	1.238	0.952
46	CCL	[21]CCL	1.0106	0.724
47	CH2CL2	[22]CCL2	2.2564	1.988
48	CHCL2	[22]CCL2	2.0606	1.684
49	CCL2	[22]CCL2	1.8016	1.448
50	CHCL3	[23]CCL3	2.87	2.41

The residual contribution to the activity coefficient γ^r, which expresses the impact of intermolecular interactions is given as:

$$\ln \gamma_i^r = \sum_{k \epsilon groups} v_k^{(i)} \left(\ln \Gamma_k - \ln \Gamma_k^{(i)} \right) \quad \text{(C7)}$$

In this equation, $\Gamma_k$represents the residual activity coefficient of subgroup k in the mixture and $\Gamma_k^{(i)}$ the residual activity coefficient of subgroup k in the pure molecule i. BothΓ_k and $\Gamma_k^{(i)}$ share the same functional form:

$$\ln \Gamma_k = Q_k \left[1 - \ln(\sum_m \theta_m \Psi_{mk}) - \sum_m \frac{\theta_m \Psi_{mk}}{\sum_n \theta_n \Psi_{nm}}\right] \quad \text{(C8)}$$

Where the surface fraction of group m in the mixture θ_m is expressed as:

$$\theta_m = \sum_m \frac{Q_m X_m}{\sum_n Q_n X_n} \quad \text{(C9)}$$

And the mole fraction of group m in the mixture X_m is expressed as:

$$X_m = \frac{\sum_i v_m^{(i)} x_i}{\sum_i \sum_k v_k^{(i)} x_i} \quad \text{(C10)}$$

And Ψ_{mn} is:

$$\Psi_{mn} = exp\left(-\frac{a_{mn}}{T}\right) \quad \text{(C11)}$$

a_{mn} represents the interaction energy between the groups m and n (expressed in temperature units). Some examples of interaction parameters are presented in Table C3.

Table C3. Examples of group interaction parameters.

a_{mn}	CH_2	C=C	Char	CH_{ar}
CH_2	0	86.02	61.13	76.5
C=C	-35.36	0	38.81	74.15
CH_{ar}	-11.12	3.446	0	167.0
$C_{ar}CH_3$	-69.7	-113.6	-146.8	0

C2-Adaptation of Joback's method to the UNIFAC group contribution theory

The Joback's method uses the group contribution theory as an extension of the pioneering work of Parks and Huffmann[58]. The groups of atoms considered by Joback are given in table C4. By comparison with table C2, it can be seen that those groups may differ from UNIFAC group topology.

Table C4. JOBACK's groups and corresponding weighting parameters.

Group	T_c[a]	P_c[b]	V_c[c]	T_b[d]	T_m[e]	H_{form}[f]	G_{form}[g]	A[h]	b	C	d	H_{fusion}[i]	H_{vap}[j]	A[k]	B
	Critical State Data			Temperatures of Phase Transitions		Chemical Caloric Properties		Ideal Gas Heat Capacities				Enthalpies of Phase Transitions		Dynamic Viscosity	

Non-ring groups															
-CH_3	0.0141	−0.0012	65	23.58	−5.10	−76.45	−43.96	1.95E+1	−8.08E−3	1.53E−4	−9.67E−8	0.908	2.373	548.29	−1.719
-CH_2-	0.0189	0.0000	56	22.88	11.27	−20.64	8.42	−9.09E−1	9.50E−2	−5.44E−5	1.19E−8	2.590	2.226	94.16	−0.199
>CH-	0.0164	0.0020	41	21.74	12.64	29.89	58.36	−2.30E+1	2.04E−1	−2.65E−4	1.20E−7	0.749	1.691	-322.15	1.187
>C<	0.0067	0.0043	27	18.25	46.43	82.23	116.02	−6.62E+1	4.27E−1	−6.41E−4	3.01E−7	−1.460	0.636	−573.56	2.307
=CH_2	0.0113	−0.0028	56	18.18	−4.32	−9.630	3.77	2.36E+1	−3.81E−2	1.72E−4	−1.03E−7	−0.473	1.724	495.01	−1.539
=CH-	0.0129	−0.0006	46	24.96	8.73	37.97	48.53	−8.00	1.05E−1	−9.63E−5	3.56E−8	2.691	2.205	82.28	−0.242
=C<	0.0117	0.0011	38	24.14	11.14	83.99	92.36	−2.81E+1	2.08E−1	−3.06E−4	1.46E−7	3.063	2.138	n. a.	n. a.
=C=	0.0026	0.0028	36	26.15	17.78	142.14	136.70	2.74E+1	−5.57E−2	1.01E−4	−5.02E−8	4.720	2.661	n. a.	n. a.
≡CH	0.0027	−0.0008	46	9.20	−11.18	79.30	77.71	2.45E+1	−2.71E−2	1.11E−4	−6.78E−8	2.322	1.155	n. a.	n. a.
≡C-	0.0020	0.0016	37	27.38	64.32	115.51	109.82	7.87	2.01E−2	−8.33E−6	1.39E-9	4.151	3.302	n. a.	n. a.
Ring groups															
-CH_2-	0.0100	0.0025	48	27.15	7.75	−26.80	−3.68	−6.03	8.54E−2	−8.00E−6	−1.80E−8	0.490	2.398	307.53	−0.798
>CH-	0.0122	0.0004	38	21.78	19.88	8.67	40.99	−2.05E+1	1.62E−1	−1.60E−4	6.24E−8	3.243	1.942	−394.29	1.251
>C<	0.0042	0.0061	27	21.32	60.15	79.72	87.88	−9.09E+1	5.57E−1	−9.00E−4	4.69E−7	−1.373	0.644	n. a.	n. a.
=CH-	0.0082	0.0011	41	26.73	8.13	2.09	11.30	−2.14	5.74E−2	−1.64E−6	−1.59E−8	1.101	2.544	259.65	−0.702
=C<	0.0143	0.0008	32	31.01	37.02	46.43	54.05	−8.25	1.01E−1	−1.42E−4	6.78E−8	2.394	3.059	-245.74	0.912
Halogen groups															
-F	0.0111	−0.0057	27	−0.03	−15.78	−251.92	−247.19	2.65E+1	−9.13E−2	1.91E−4	−1.03E−7	1.398	−0.670	n. a.	n. a.
-Cl	0.0105	−0.0049	58	38.13	13.55	−71.55	−64.31	3.33E+1	−9.63E−2	1.87E−4	−9.96E−8	2.515	4.532	625.45	−1.814
-Br	0.0133	0.0057	71	66.86	43.43	−29.48	−38.06	2.86E+1	−6.49E−2	1.36E−4	−7.45E−8	3.603	6.582	738.91	−2.038
-I	0.0068	−0.0034	97	93.84	41.69	21.06	5.74	3.21E+1	−6.41E−2	1.26E−4	−6.87E−8	2.724	9.520	809.55	−2.224
Oxygen groups															
-OH (alcohol)	0.0741	0.0112	28	92.88	44.45	−208.04	−189.20	2.57E+1	−6.91E−2	1.77E−4	−9.88E−8	2.406	16.826	2173.72	−5.057
-OH (phenol)	0.0240	0.0184	−25	76.34	82.83	−221.65	−197.37	−2.81	1.11E−1	−1.16E−4	4.94E−8	4.490	12.499	3018.17	−7.314
-O- (nonring)	0.0168	0.0015	18	22.42	22.23	−132.22	−105.00	2.55E+1	−6.32E−2	1.11E−4	−5.48E−8	1.188	2.410	122.09	−0.386
-O- (ring)	0.0098	0.0048	13	31.22	23.05	−138.16	−98.22	1.22E+1	−1.26E−2	6.03E−5	−3.86E−8	5.879	4.682	440.24	−0.953
>C=O (nonring)	0.0380	0.0031	62	76.75	61.20	−133.22	−120.50	6.45	6.70E−2	−3.57E−5	2.86E−9	4.189	8.972	340.35	−0.350
>C=O (ring)	0.0284	0.0028	55	94.97	75.97	−164.50	−126.27	3.04E+1	−8.29E−2	2.36E−4	−1.31E−7	0.	6.645	n. a.	n. a.
O=CH- (aldehyde)	0.0379	0.0030	82	72.24	36.90	−162.03	−143.48	3.09E+1	−3.36E−2	1.60E−4	−9.88E−8	3.197	9.093	740.92	−1.713
-COOH (acid)	0.0791	0.0077	89	169.09	155.50	−426.72	−387.87	2.41E+1	4.27E−2	8.04E−5	−6.87E−8	11.051	19.537	1317.23	−2.578
-COO- (ester)	0.0481	0.0005	82	81.10	53.60	−337.92	−301.95	2.45E+1	4.02E−2	4.02E−5	−4.52E−8	6.959	9.633	483.88	−0.966
=O (other than above)	0.0143	0.0101	36	−10.50	2.08	−247.61	−250.83	6.82	1.96E−2	1.27E−5	−1.78E−8	3.624	5.909	675.24	−1.340
Nitrogen groups															
-NH_2	0.0243	0.0109	38	73.23	66.89	−22.02	14.07	2.69E+1	−4.12E−2	1.64E−4	−9.76E−8	3.515	10.788	n. a.	n. a.
>NH (non-ring)	0.0295	0.0077	35	50.17	52.66	53.47	89.39	−1.21	7.62E−2	−4.86E−5	1.05E−8	5.099	6.436	n. a.	n. a.
>NH (ring)	0.0130	0.0114	29	52.82	101.51	31.65	75.61	1.18E+1	−2.30E−2	1.07E−4	−6.28E−8	7.490	6.930	n. a.	n. a.
>N- (nonring)	0.0169	0.0074	9	11.74	48.84	123.34	163.16	−3.11E+1	2.27E−1	−3.20E−4	1.46E−7	4.703	1.896	n. a.	n. a.

-N= (nonring)	0.0255	-0.0099	n. a.	74.60	n. a.	23.61	n. a.	n. a.	n. a.	n. a.	n. a.	n. a.	3.335	n. a.	n. a.
-N= (ring)	0.0085	0.0076	34	57.55	68.40	55.52	79.93	8.83	−3.84E-3	4.35E−5	−2.60E−8	3.649	6.528	n. a.	n. a.
=NH	n. a.	n. a.	n. a.	83.08	68.91	93.70	119.66	5.69	−4.12E−3	1.28E−4	−8.88E−8	n. a.	12.169	n. a.	n. a.
-CN	0.0496	−0.0101	91	125.66	59.89	88.43	89.22	3.65E+1	−7.33E−2	1.84E−4	−1.03E−7	2.414	12.851	n. a.	n. a.
$-NO_2$	0.0437	0.0064	91	152.54	127.24	−66.57	−16.83	2.59E+1	−3.74E−3	1.29E−4	−8.88E−8	9.679	16.738	n. a.	n. a.
Sulfur groups															
-SH	0.0031	0.0084	63	63.56	20.09	−17.33	−22.99	3.53E+1	−7.58E−2	1.85E−4	−1.03E−7	2.360	6.884	n. a.	n. a.
-S- (nonring)	0.0119	0.0049	54	68.78	34.40	41.87	33.12	1.96E+1	−5.61E−3	4.02E−5	−2.76E−8	4.130	6.817	n. a.	n. a.
-S- (ring)	0.0019	0.0051	38	52.10	79.93	39.10	27.76	1.67E+1	4.81E−3	2.77E−5	−2.11E−8	1.557	5.984	n. a.	n. a.

[a]T_c is critical temperature; [b]P_c is critical pressure; [c]V_c is critical volume; [d]T_b is the boiling temperature; [e]Tm is the melting temperature; [f]H_{form} is enthalpy of formation; [g]G_{form} is Gibbs of formation; [h]a is the parameter of heat capacity; [i]H_{fusion} is enthalpy of formation; [j]H_{vap} is enthalpy of vaporization A and B are dynamic viscosity.

An example of the use of the Joback's method is proposed first. Propane is described using three groups in the Joback's method: two methyl groups (-CH_3) and one methylene group (-CH_2). Since the methyl group is present twice, its contribution has to be added twice. The calculated properties are calculated by simple summation of the weighing parameters extracted from table C4. The results for propane are given in table C5.

Table C5. Application of JOBACK's method to propane.

	-CH_3		-CH_2-				
Property	No. of groups	Group value	No. of groups	Group value	Sum of Goup value	Estimated Value	Unit
T_c[a]	2	0.0141	1	0.0189	0.0471	427.34	K
P_c[b]	2	-0.0012	1	0	-0.0024	44.09	bar
V_c[c]	2	65	1	56	186	203.5	cm3/mol
T_b[d]	2	23.58	1	22.88	70.04	268.04	K
T_m[e]	2	-5.1	1	1127	1116.8	123.57	K
$H_{formation}$[f]	2	-76.45	1	-20.64	-173.54	-105.25	kJ/mol
$G_{formation}$[g]	2	-43.96	1	8.42	-79.5	-2562	kJ/mol
C_{pa}[h]	2	1.95E+01	1	-9.09E-01	38.091		

C_{pb}	2	-8.08E-03	1	9.50E-02	0.07884		
C_{pc}	2	1.53E-04	1	-5.44E-05	0.0002516		
C_{pd}	2	-9.67E-08	1	1.19E-08	-1.815E-07		
C_p	at T=300 K					75.3264	J/(mol*K)
H_{fusion}[i]	2	0.908	1	2.59	4.406	3.53	kJ/mol
H_{vap}[j]	2	2.373	1	2.226	6.972	20.47	kJ/mol

[a] T_f is the temperature of freezing; [b] pc is critical pressure; [c] vc is critical volume; [d] T_b is boiling temperature; [e] T_m is the temperature of melting; [f] H_f is enthalpy of formation; [g] G_f is Gibbs free energy of formation; [h] Cp is heat capacity; [i] h_{fusion} is enthalpy of fusion; [j] h_{vapo} is enthalpy of vaporization.

To adapt the Joback's method to the chosen equation of state (LCVM) and the formulation of the coefficient of activity, the Joback's groups of atoms have to be modified to correspond to those of UNIFAC. This was done by assembling the Joback's group to generate UNIFAC groups. For instance, the AC-OH UNIFAC (sub)group is considered. This UNIFAC-subgroup consists of two JOBACK subgroups: one '=C<' group (ring group) and one '-OH' group. If the parameter "boiling point" is to be calculated, the contribution of the Joback's '=C<' group (31.01) is added to that of '-OH' (92.88) to give a (sub)group contribution of 123.89 for UNIFAC AC-OH(sub)group. All other thermodynamic parameters can be calculated this way. The result of this work is given in table C6 for those UNIFAC subgroups which not appear in the original Joback's method (the results are registered into the "Joback.csv" file).

Table C6. JOBACK's method adapted to the UNIFAC subgroup topology.

(Unifac)subgroup	(Unifac)Main group	mw[a]	Cp(A)[b]	Cp(B)	Cp(C)	Cp(D)	Hf[c]	Gf[d]	na[e]	vc[f]	tb[g]	tf[h]	tc[i]	pc[j]	h_{vapo}[k]	omega[l]
1	1	15.034	19.5	-0.00808	0.000153	-9.67E-08	-76.45	-43.96	4	65	23.58	-5.1	0.0141	-0.0012	2.373	-10.75
2	1	14.026	-0.909	0.095	-5.4E-05	1.19E-08	-20.64	8.42	3	56	22.88	11.27	0.0189	0	2.226	16.19
3	1	13.018	-23	0.204	-0.00027	1.2E-07	29.89	58.36	2	41	21.74	12.64	0.0164	0.002	1.691	50.97
4	1	12.01	-66.2	0.427	-0.00064	3.01E-07	82.23	116.02	1	27	18.25	46.43	0.0067	0.0043	3.302	53.24
5	2	27.044	15.6	0.0669	7.57E-05	-6.74E-08	28.34	52.3	5	102	43.14	4.409999	0.0242	-0.0034	1.724	-14.86
6	2	26.036	-16	0.21	-0.00019	7.12E-08	75.94	97.06	4	92	49.92	17.46	0.0258	-0.0012	4.41	18.12
7	2	26.036	-4.5	0.1699	-0.00013	4.3E-08	74.36	96.13	4	94	42.32	6.82	0.023	-0.0017	2.138	-13.26
8	2	25.028	-36.1	0.313	-0.0004	1.82E-07	121.96	140.89	3	84	49.1	19.87	0.0246	0.0005	2.661	-0.58
9	3	13.018	-2.14	0.0574	-1.6E-06	-1.59E-08	2.09	11.3	2	41	26.73	8.13	0.0082	0.0011	2.544	-1.28
10	3	12.01	-8.25	0.101	-0.00014	6.78E-08	46.43	54.05	1	32	31.01	37.02	0.0143	0.0008	3.059	539.17

[a] mw is the molecular weight; [b] Cp is heat capacity; [c] H_f is enthalpy of formation; [d] G_f is Gibbs free energy of formation; [e] na is the number of atom of this group; [f] vc is critical volume; [g] t_b is boiling temperature; [h] t_f

is the temperature of freezing; [i] tc is critical temperature; [j] pc is critical pressure; [k] h_{vapo} is enthalpy of vaporization; [l] omega is the acentric factor.

Appendix D: Ganis's and Brignole's method

In CIRCE, the possibility is offered the user to define from the atomic composition of the reactant(s)to look for all the potential but viable products that could appear in the reactive process.

The principle of the method was developed by R.Gani and E.A.Brignole[79] in 1983 for the selection of solvents in separation processes. R.Gani achieved the complete development in 2002. The group contribution technique is used to construct the potential molecules. First, intermediate molecules (more appropriately: radicals) are built by bridging groups with several free valences. Terminal groups (with a single free valence) would complete these intermediate molecules.

The UNIFAC (sub) groups with free attachments (or bonds) have one or more attachments for combination among themselves. Groups with only one free attachment are defined as "terminal" groups. All other groups with more than one free attachment are defined as "intermediate" groups. According to their "bonding likelihood" three types of intermediate groups were defined: radial, linear and mixed. The "free" attachments of a group are characterized according to:

i) the attachment status, which accounts for the combinatory properties (according to which a specific atom does not combine equally with all other atoms or groups of atoms);

ii) the valence i.e. the number of attachments.

About the attachment status, eight types of attachments were defined as shown in table D1 on the basis of the electronegativity of the groups.

Table D1. the different types of attachments.

M:	severely restricted attachment, e.g.,"-OH", "CH_3O-".
J:	partially restricted attachment, e.g.,"-CH_2Cl".
L:	Unrestricted carbon attachment in single valence or linear dual valence groups.
K:	unrestricted carbon attachment of paraffinic groups, e.g."-CH_2-","-CH<".
I	aromatic carbon ring attachment such as ACH
H	substituted aromatic carbon ring attachment such as ACCL
M	unrestricted attachment in a carbon linked to an aromatic carbon such as ACCH2-
J	unrestricted attachments in a "radial" carbon linked to an aromatic carbon, such as ACCH<

To define an intermediate molecule (IMS), L and K groups are associated and M and J groups are added to complete it (final molecule or FMS). But doing this, constraints i) and ii) need to be fulfilled. On this basis, the authors proposed more accurate rules as summarized in table D2.

Table D2. Construction rules of a stable molecule (where K is the number of occurrence of group K for instance)

Type of Compound	IMSs	FMSs
Aliphatic	$K \leq M + J/2 + 2$	$K \leq M + J/2$
Aromatic	$I + H = 6$	$I + H = 6$
Aliphatic-aromatic	$K \leq M + J/2$ $I + H = 6$	$K \leq M + J/2$ $I + H = 6$
Cyclic		$K \leq M + J/2$

The labeling of some major UNIFAC groups is given in table D3, and examples of IMSs and FMSs are given.

Table D3. UNIFAC group attachment characterization and examples of molecules construction.

Group Characterization	IMSs	FMSs
Paraffinic/ *(CH_2)(J,2)* *(CHCl):(L,2)* *(CH=CH):()* *():()* *(CH_3):()*	*(CHCl)(CH=CH)(CH_2)* *M=0;J=2;* *L=2 K=2* *M+J/2+2=3 thus:* $K \leq M + J/2 + 2$ *(feasible IMS)*	*(CH_3)$_2$(CH=CH)(CHCl)(CH_2)* *M=2; J=2; L=2; K=2* *M+J/2=3, thus :* $K \leq M + J/2$*Feasible FMS* *(CH_3)(CH=CH)(CHCl)(CH_2)(OH)* *M=1; J=2; L=2; K=3* *M+J/2=2 thus:* $K > M + J/2$

		Unfeasible FMS
Aromatic *($ACCH_3$):(H,1)* *(ACH):(I,1)* *(ACOH):(H,1)*		*(ACH_3)(ACCH3)(ACOH)* *I=3; H=3;* $I + H = 6$ *feasible Molecule*
Aliphatic-aromatic *(ACCH2):(H,1)(M,1)* *(AC) (H,1) (M,1)*	*(AC)($ACH)_3$($ACCH_2)_2$* *M=3; J=0; I=3;* *H=3; K=0* *M+J/2+2=3* *I+H =6* *(feasible IMS)*	*($OH)_2$(AC)($ACH)_3$($ACCH_2)_2$(CH_3O)* *M=3;J=0;I=3;H=3;K=3* *M+J/2 =3* *I+H =6* *(feasible FMS)*

In CIRCE, this method is implemented as follows:

1) selection of the intermediate and terminal groups by the atoms availability in the reactants;
2) Construction of IMSs by systematically associating L, M and J groups up to a maximum of 12 and in the limit of the atom balance (number of atoms of the reactants). The IMSs not satisfying the feasibility rules are eliminated;
3) Completion of the possible molecules (FMSs) by adding the available terminal groups systematically. The FMSs not satisfying the feasibility rules are eliminated.

For instance, if ethane C_2H_6 is the initial reactant, So all the generated molecule which the element number less than the C_2H_6 and C_2H_6 will be considered as these possible final molecules. The considered groups will be the organic groups which can compose the molecule of C_2H_6 and the molecule which has fewer elements than C_2H_6. Here the method of Monte Carlo has been used to propose a combination each time. So at this moment, there are these groups of groups autonomous: $=CH_2$, $\equiv CH$,$-CH_3$, CH_4, -H which satisfied the rule and Conservation of Mass. So the program can give the only product is 'CH_4, C, H_2, C_2H_2, C_2H_4 and C_2H_6'.

Appendix E: EoS and departure functions

The departure function is defined for any thermodynamic property as the difference between the property for ideal gas and the property of the real fluid (liquid or gas). This function was used to calculate the real fluid properties.

Let U be a function of T, v, so U=U(T, *v*). According to the Maxwell relationship, the full set differential of U is:

$$dU = (\frac{\partial U}{\partial T})_v dT + (\frac{\partial U}{\partial v})_T dv \tag{E1}$$

According to the definition of heat capacity at constant volume:$\left(\frac{\partial U}{\partial T}\right)_v = Cv$, and the basic equations of thermodynamics $dU = TdS - pdv$, the equation $(\frac{\partial U}{\partial v})_T = T\left(\frac{\partial S}{\partial v}\right)_T - P$ and the Maxwell relationship, $(\frac{\partial S}{\partial v})_T = \left(\frac{\partial P}{\partial T}\right)_v$.

We can derive the definition of departure equation:

$$dU = C_v dT + \left\{T\left(\frac{\partial p}{\partial T}\right)_v - P\right\} dv \tag{E2}$$

Similarly, the enthalpy can be derived as below:

$$(\mathrm{h} - h^0)_{T,P} = \int_{P=0}^{P} \left[v - T\left(\frac{\partial v}{\partial T}\right)_P\right]_T dP \tag{E3}$$

$$= \int_{P=0}^{P} d(Pv) + \int_{v=\infty}^{v} \left[T\left(\frac{\partial P}{\partial T}\right)_v - P\right]_T dv \qquad (since\ v = \infty\ as\ P = 0) \tag{E4}$$

$$= Pv - (Pv)_{P=0} + \int_{v=\infty}^{v} \left[T\left(\frac{\partial P}{\partial T}\right)_v - P\right]_T dv \tag{E5}$$

$$= Pv - RT + \int_{v=\infty}^{v} \left[T\left(\frac{\partial P}{\partial T}\right)_v - P\right]_T dv \tag{E6}$$

$$\text{Or } (h - h^0)_{T,P} = RT(Z-1) + \int_{v=\infty}^{v} \left[T\left(\frac{\partial P}{\partial T}\right) - P\right]_T dv \tag{E7}$$

The same rule applied to the entropy:

$$(s - s_0)_{T,P} = -\int_{P=0}^{P} \left[\left(\frac{\partial v}{\partial T}\right)_P - \frac{R}{P}\right]_T dP \tag{E8}$$

$$= \int_{v=\infty}^{v} \left[\left(\frac{\partial P}{\partial T}\right)_v\right]_T dv + \int_{P=0}^{P} P\frac{dP}{P} \tag{E9}$$

$$= \int_{v=\infty}^{v} \left(\frac{\partial P}{\partial T}\right)_v dv + \int \left[R\frac{d(Pv)}{Pv} - R\frac{dv}{v}\right] \tag{E10}$$

$$= \int_{v=\infty}^{v} \left(\frac{\partial P}{\partial T}\right)_v dv + R\int_{Pv=RT}^{Pv} d\ln(Pv) - \int_{v=\infty}^{v} R\frac{dv}{v} \tag{E11}$$

$$= R\ln\left(\frac{Pv}{RT}\right) + \int_{v=\infty}^{v} \left[\left(\frac{\partial P}{\partial T}\right)_v - \frac{R}{v}\right] dv \tag{E12}$$

Or $$(s - s^0)_{T,P} = R\ln Z + \int_{v=\infty}^{v} \left[\left(\frac{\partial P}{\partial T}\right)_v - \frac{R}{v}\right]_T dv \tag{E13}$$

Substituting equation of state of PENG Robinson into the equation (E7) and (E13), which yields:

$$h - h^0 = RT(Z-1) + \frac{T\left(\frac{\partial a}{\partial T}\right) - a}{2\sqrt{2}b}\ln\left\{\frac{Z + b\left(1+\sqrt{2}\right)}{Z + b\left(1-\sqrt{2}\right)}\right\} \tag{E14}$$

$$s - s^0 = R\ln(Z-1) + \frac{1}{2\sqrt{2}b}\frac{\partial a}{\partial T}\ln\left\{\frac{Z + b\left(1+\sqrt{2}\right)}{Z + b\left(1-\sqrt{2}\right)}\right\} \tag{E15}$$

Where $$\frac{\partial a}{\partial T} = -\frac{0.45724R^2T_c^2\kappa}{P_c}\sqrt{\frac{a}{TT_c}} = -\frac{a\kappa}{\sqrt{\alpha TT_c}} \tag{E16}$$

Appendix F: EoS, fugacities and activities

The definition of the fugacity coefficient φ for a real fluid is:

$$G(T,P)_{real} - G(T,P)_{ideal} = R.T.ln\left(\frac{f}{P}\right) = R.T.ln\,\varphi \qquad \text{(F1)}$$

Where the fugacity is f (by definition the fugacity of an ideal gas is P). The fugacity can be calculated bearing in mind that during an isothermal expansion the real gas behaves as an ideal gas when P tends to zero, and thus the molar volume tends to infinity (v^{∞} when P→0). This asymptotic point is common to the calculation of the fugacity for the real gas (to obtain f) and for the ideal gas (to get P). The common asymptotic point disappears and gives (F1) by a difference. This equation should be taken into account: dG=-S.dT+v.dP. In this case, dT=0 so that:

$$\ln\left(\frac{f}{P}\right) = \int_{ideal}^{real}\frac{v}{RT}dP = \int_{ideal}^{real}\frac{d(Pv)}{RT} - \int_{v=\infty}^{v}\frac{P}{RT}dv = \frac{1}{RT}*(Pv-RT) - \frac{1}{RT}\int_{v=\infty}^{v}Pdv \qquad \text{(F2)}$$

Equation (E18) reduces to:

$$\ln\varphi = \ln\left(\frac{f}{P}\right) = Z - 1 - \frac{1}{RT}\int_{v=\infty}^{v}Pdv \qquad \text{(F3)}$$

Where $Z=Pv/RT$ is the compressibility coefficient (=1 for an ideal gas). This equation is used to calculate φ_i for every pure compound.

By definition, the partial fugacity varies:

$$RTd\ln\hat{f}_i = \hat{v}_i dP = \left(\frac{\partial v}{\partial n_i}\right)dP \qquad \text{(F4)}$$

The partial volume can be eliminated using the rules for partial differentiation:

The Euler's chain is used as:

$$\left(\frac{\partial v}{\partial n_i}\right)\left(\frac{\partial n_i}{\partial P}\right)\left(\frac{\partial P}{\partial v}\right) = -1 \tag{F5}$$

Substituting the equation (F5) into the (F4):

$$RTd\ln\hat{f}_i = \left(\frac{\partial v}{\partial n_i}\right)dP = \hat{v}_i dP = -\left(\frac{\partial P}{\partial n_i}\right)dv \tag{F6}$$

Adding RT dln(v/RT) to each side,

$$RTd\ln\frac{\hat{f}_i v}{RT} = -\left(\frac{\partial P}{\partial n_i}\right)d(v) + RTd\ln\frac{v}{RT} = \left[-\left(\frac{\partial P}{\partial n_i}\right) + \frac{RT}{v}\right]dv \tag{F7}$$

This equation (F7) can be integrated between v and at infinity, where the mixture tends toward ideality ($\hat{f}_i \to y_i \cdot P$ and $\frac{R\cdot T}{v} \to P$) so that after some manipulations:

$$RT\ln\hat{\varphi}_i = RT\ln\frac{\hat{f}_i}{y_i P} = \int_v^\infty \left(\frac{\partial P}{\partial n_i} - \frac{RT}{v}\right)dv - RT\ln Z \tag{F8}$$

And:

$$\ln(\hat{\varphi}_i) = \ln\left(\frac{\hat{f}_i}{y_i P}\right) = -\frac{1}{RT}\int_{v=\infty}^{v}\left[\left(\frac{\partial P}{\partial n_i}\right)_{T,v,n_j} - \frac{1}{v}\right]dv - \ln Z \tag{F9}$$

Then, the fugacity coefficients are linked to the equation of state of the pure components and the mixture (equations F3 and F9). And the link with the activity coefficients is:

$$\ln\gamma_i = \ln\frac{\hat{\varphi}_i}{\varphi_i} \tag{F10}$$

Appendix G: Organization of CIRCE

Overall organization

CIRCE software structure is designed around a core file of 'main.c' and many other function files. The functional structure of software is recalled below (figure G1).

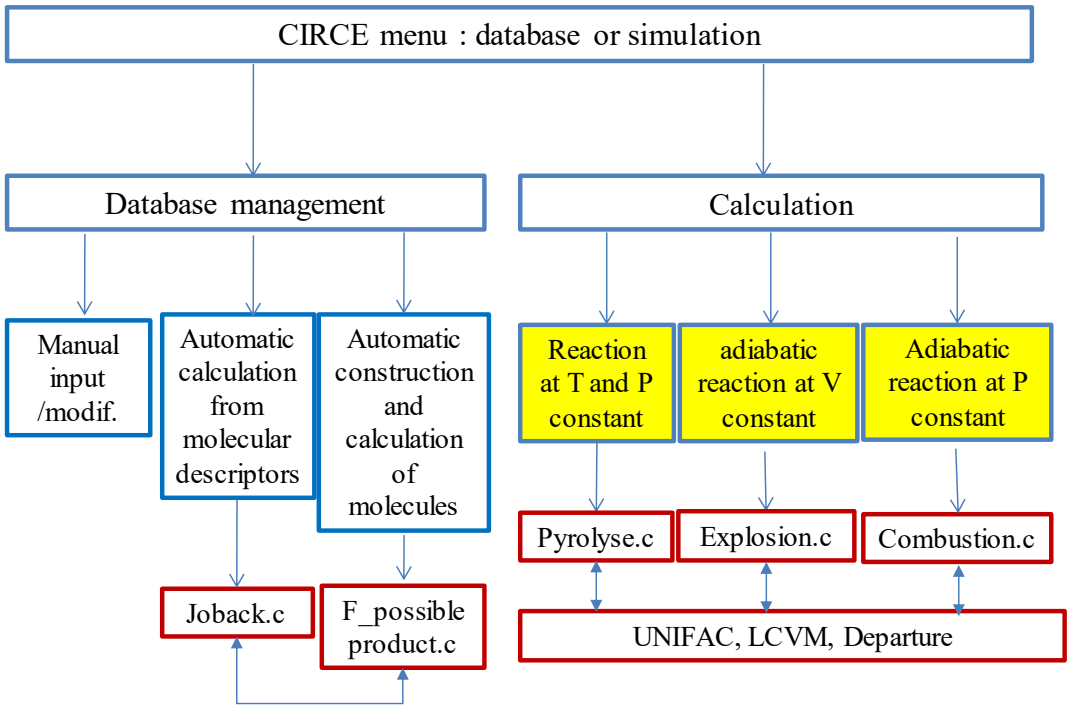

Figure G.1. Functional structure of the software CIRCE (in red squares: main routines)

Again, CIRCE consists of two separate blocks.

- The database implementation block which offers the user the possibility to introduce, create new components and modify as desired the thermodynamic properties calculated by the code which implements UNIFAC for molecular descriptors, a modified Joback's method and the Constantinou's methods for the ideal gas thermodynamic properties. A "product list generator" is programmed which offers the user the possibility to create new products from the reactants composition.

- The simulation block incorporates three separate routines to simulate the various reaction modes: at constant P and T (“pyrolysis”), adiabatic and constant pressure (“combustion”) and adiabatic and at constant volume (“explosion”). The common functions are UNIFAC for the activity coefficients, the LCVM EoS for the departure functions. The user is asked to select a list of products from the database

The organization of the subroutines and functions is presented in figure G2 and the roles of them are provided in table G1:

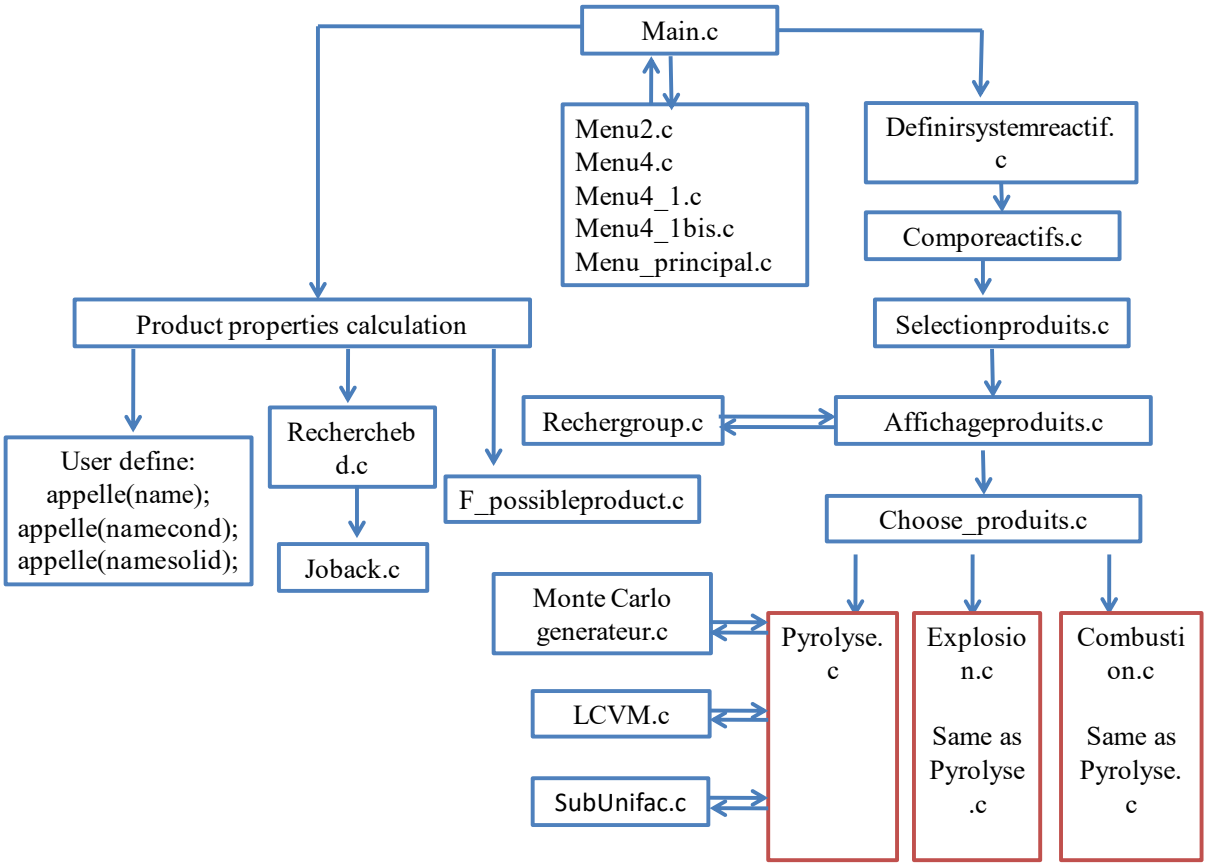

Figure G.2. CIRCE coding structure.

Table G.1. Description of the subroutines of CIRCE.

CIRCE.h	Header program: contains the declaration of the functions (sub routines) for CIRCE.

Unifac.h	Header program: contains the declaration of the functions (sub routines) for UNIFAC.
EOSPengRobinson.c	Calculates the departure function.
F_possibleproduct.c	Generates the possible products (Brignole's method).
LCVM.c	Calculates the activity coefficients through LCVM EoS.
MT.c	Generates a random number using the MT technique.
Monte Carlo generateur.c	Generates a given number of composition vectors.
SubUnifac.c	Calculates the activity coefficients of a mixture (a composition vector) at a given temperature.
Accueil.c	Displays the welcome address (figure G.4).
Affichage.c	Displays the content of the total database(only the formulae).
Affichagecompo.c	Displays the atomic (molecular) composition of the reactants.
Affichageproduits.c	Displays the list of the products to be selected to run a simulation
Ajoutbasededonnee.c	Opens the file groups.csv for the user to introduce a new molecule (name and subgroups) and stores in groups.csv.
Appellefichier.c	Call and open a file.
Combustion.c	Calculates the final composition, enthalpy, volume and temperature of an adiabatic reaction at constant pressure.
Comporeactifs.c	From the formula of the reactants given by the user (CnHmOp…), this function extracts the atomic composition of the reactants and stores it in the file elementaire.csv.
Creactiontableau.c	Creates a double dimensional array.
Creactiontableaufloat.c	Creates a double dimensional array (float type).
Definirsystemereactif.c	Offers the user the possibility to define the reactants either through the formula or as a mixture of products from the database. The enthalpy of formation of the reactants and the specific heat has to be provided too.
Explosion.c	Calculates the final composition, enthalpy, pressure and temperature of an adiabatic reaction at constant volume.
Extrairenom.c	Locates the name of a molecule in the product database and extracts its ranking number (from files donne.csv, donnecond.csv, donnesolid.csv).
Extrairenombre.c	Extracts the thermodynamic properties from the product database on the basis the ranking number of the molecule (from files donne.csv, donnecond.csv, donnesolid.csv).
Extrairenombregroupe.c	Extracts the number and index of UNIFAC group from the file groups.csv.
Fugacitysolid.c	Calculates the fugacity of a solid.
Initialisertab.c	Sets to zero a table (array).
Joback.c	Calculates the thermochemical properties of each product using the JOBACK's methodology (enthalpy and entropy of formation, heat capacity at 5 temperatures, critical parameters.
Main.c	Loads the database from the hard memory and organizes the other subroutines as function of the location in the code and choices operated by the user
Menu2.c	Displays the menu of figure G.9
Menu_principal.c	Displays the menu of figure G.5
Pyrolyse.c	Calculates the final composition, enthalpy and volume of an isothermal and isobaric reaction.
Recherche	Checks if the product exists into the files group.csv, and gives its tracking number if the product exists.
Recherchedeproduits.c	Checks if the product exists into the database (files donne.csv, donnecond.csv, and donnesolid.csv) and gives its tracking number if the product exists. If not the sub routine addresses Ajoutbasededonnee.c.
Rechergroup.c	Extracts the UNIFAC subgroups information for a product from the database (in files donne.csv, donnecond.csv, donnesolid.csv).
Selectionproduits.c	On the basis of the atomic composition of the reactants, sorts the products which may appear in the equilibrium.

Choose_produits.c	Select the products from the list of product proposed by the function Selectionproduits.c.
Suppressiontableau.c	Deletes a two-dimensional array created using the function Creactiontableau.c.
Suppressiontableaufloat.c	Deletes a two-dimensional array created using the function Creactiontableaufloat.c.

Workflow of the software

CIRCE version 1.0 is developed in C language (NetBeans IDE) and is compiled for execution on Windows. The routines are compiled together in a single executable (CIRCE_xxxx_lcvm_eos.exe) which call/fill data files (xxxx.cvs) as shown in figure G3.

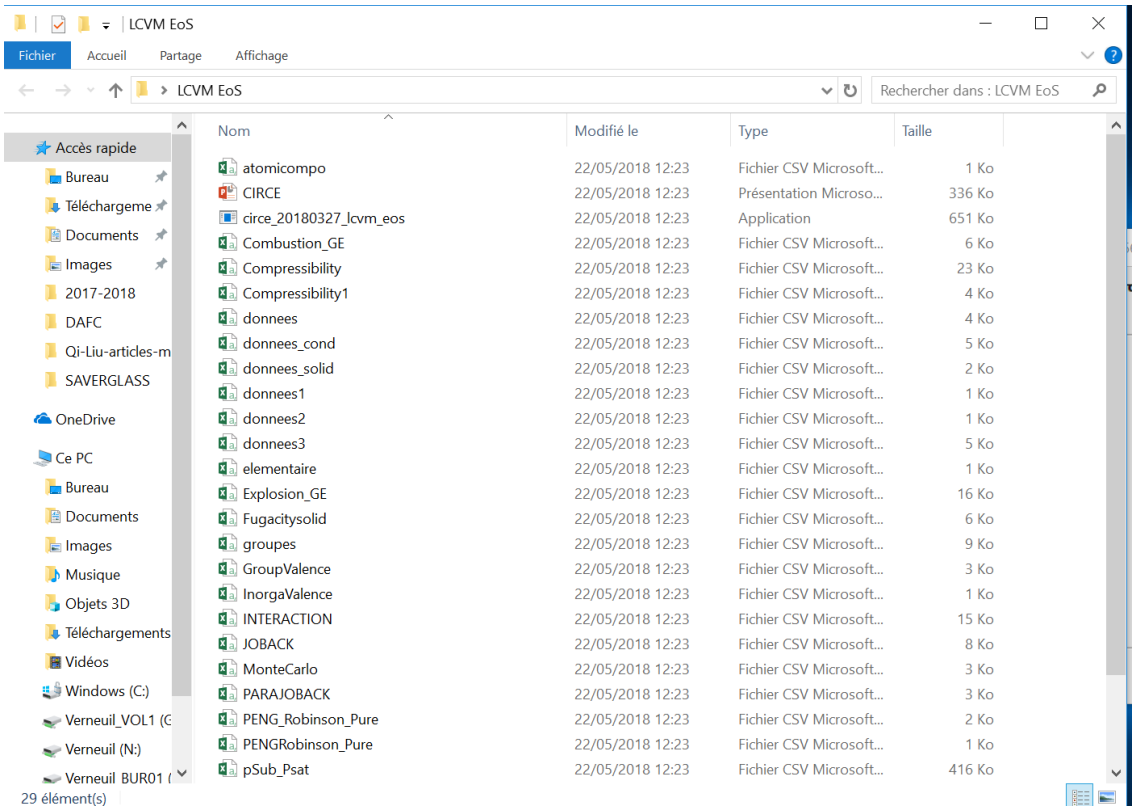

Figure G.3. CIRCE folder.

When CIRCE executable is launched, the following screen appears (figure G.4)

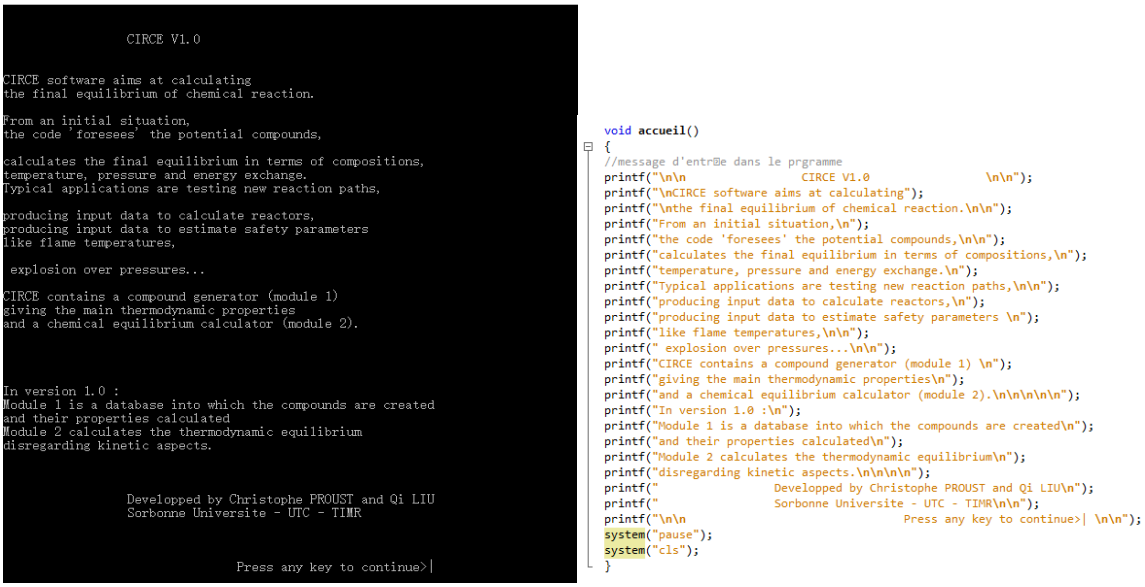

Figure G.4. CIRCE first screen and coding.

The second screen enters the interactive menu (figure G.5). The first choice is to start the simulations. The second choice can open the file of the tutorial in PPT (Figure G.6).

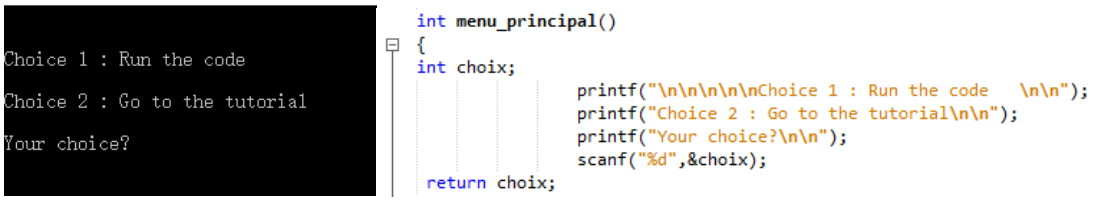

Figure G.5. Start of the interactive menu.

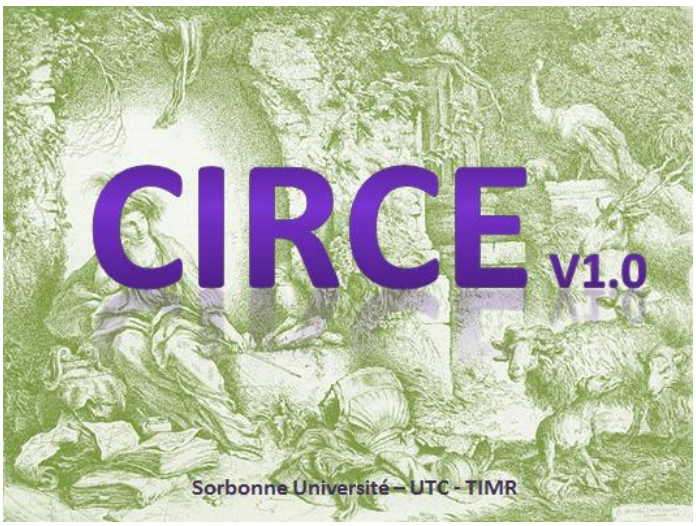

Figure G.6. first page of the tutorial.

When the first choice in figure G.5 is selected, the following screen appears (figure G.7):

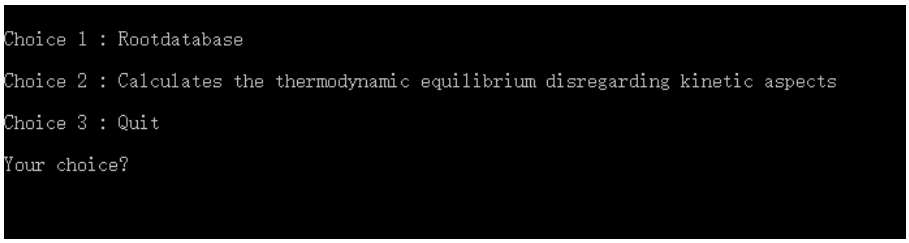


```
int menu_principal1()
{
int choix;
                printf("\n\n\n\n\nChoice 1 : Rootdatabase      \n\n");
                printf("Choice 2 : Calculates the thermodynamic equilibrium disregarding kinet
ic aspects\n\n");
                printf("Choice 3 : Quit\n\n");
                printf("Your choice?\n\n");
                scanf("%d",&choix);
 return choix;
```

Figure G.7. entering the simulation part of CIRCE.

Management of the database

As soon as “Choice 1” is selected the informative message from figure G.8 appears followed by a selection of additional choices (figure G.9).

```
void avertissement()
{
//Consigne pour une bonne utilisation des fichiers associ@s au programme

printf("    CONDITIONS D UTILISATION DES FICHIERS DE SYSTEMES REACTIFS\n\n\n");
printf("    Pour que le traitement des fichiers se deroule correctement il faut
:\n\n");
printf("    Que le fichiers 'resultats.csv' soit ferme\n\n");
printf("    Le fichier 'resultats.csv' est recree a chaque calcul, il peut donc
 etre modifie sans consequence\n\n\n");
printf("    Conserver la mise en forme des fichiers de systemes reactifs, a sav
oir::\n\n");
printf("    La premiere ligne est reservee a l intitule des colones\n\n");
printf("    Conserver l'ordre des colonnes\n\n");
printf("    Conserver le format.csv\n\n");
printf("    En cas de bug, ouvrir le fichier de systeme reactif avec bloc note
et verifier qu'il se termine par un et un seul passage a la ligne\n\n\n\n\n");
printf("    Par convention, en cas de non convergence d'un calcul, le programme
 ecrira une pression ou une temperature nulle dans le fichier 'resultat.csv'\n\
n\n\n\n");

system("pause");
}//fin du calcul de l'enthalpie;
```

Figure G.8. initial message displayed when starting the menu ‘rootdatabase”

```
Choice 1 :Consult/Modify the database;
Choice 2 :Add manually a new product;
Choice 3 :Generate automatically a lot of products;
Choice 4 :Exit
Your choice?
```

Figure G.9. First menu of the database part of CIRCE

If the first option is chosen, three excel files are opened(NetBeans IDE function “appelle” opening and displaying files "donnee.csv", "donnee_cond.csv", "donnee_solid.csv"), displaying the thermodynamic data of the vapors, liquids, and solids. The data can be seen (figure G.10). The user can directly modify the data in the tables and register them.

```
//the choice 1;
if (choix1==1)//Choix 4.1
{
    appelle(name);
    appelle(namecond);
    appelle(namesolid);
}
```

	A	B	C	D	E	F	G	H	I	J	K	L	M	N	O
1	Produit	DHf	DS	Cp1	Cp2	Cp3	Cp4	Cp5	Tc	Pc	omega	polar	number	record	sub
2	H20	-241826	188.824	33.6	41	53	57	59	647.29	220	0.344	1	1	1	16
3	0H2	-241826	188.824	33.6	41	53	57	59	647.29	220	0.344	1	1	1	16
4	C2H60	-235100	282.7	65.440002	141.54	302.44	409.44	516.44	513.85	61.4	0.644	1	3	1	1
5	H60C2	-235100	282.7	65.440002	141.54	302.44	409.44	516.44	513.85	61.4	0.644	1	3	1	1
6	0C2H6	-235100	282.7	65.440002	141.54	302.44	409.44	516.44	513.85	61.4	0.644	1	3	1	1
7	C2H402	-472090	162.63	98.239998	138.38	162.48	200.94	237.84	587.55	54.62663	0.52666	1	2	1	1
8	C3H80	-296431	193.34	44.490002	71.760002	137.95	273.45999	462.37	522.56	57.56641	0.56982	1	3	2	1
9	CH20	-118133	143.65	72.010002	76.419998	61.23	56.84	47.330002	436.8	51.90642	0.23004	1	1	1	20
10	02	0	204.82	29.3	34.8	37.135	37.7	38.209	154.59	50.4	0.0222	1	1	1	200

Figure G.10. first option of menu figure G.9

The second option enables the user to define a new molecule (Figure G.11). The user is asked to write the name of the new molecule (under the form: H_2O) and to give the phase (gas, liquid or solid). The program verifies whether this molecule is available or not in the phase in the database using Recherchedeproduits.c.

```
Define the atomic composition of the product (atoms in proper format, ex : (C
) or (Zn))

Attention to respect the majuscules and minuscules

H2O

First define the molecular structure
(UNIFAC format) in the groups.csv file,save and close.
Then a second file called donnees.csv will generate the required thermodynami
c property.
You can modify directly in this file if needed.


Press any key to continue


if H2O is a gas, choose 1, a condensed, choose 2

2

Number of elements in the database: 33

 element research: H2O


the item was in position 1
```

```
printf("\nif %s is a gas, choose 1, a condensed, choose 2\n\n",nomreac[0]);
scanf("%d",&i);
moderecherche=0;//Indique que la fonction recherche  peut proposer  d'ajouter un élément.

if (i==1)
{
    //comporeactifs(nomreac,elem,comporeac,1,nbrelem);
    rang=recherchebd(nbrproduitsbase,nomreac,base,name,moderecherche,1);
    nbrproduitsbase=fichier(base,name);
    //printf("nbrelem=%d\n",nbrelem);
};

if (i==2)
{
    rang=recherchebd(nbrproduitsbasecond,nomreac,basecond,namecond,moderecherche,1);
    nbrproduitsbasecond=fichier(basecond,namecond);
};

if (i==3)
{
    rang=recherchebd(nbrproduitsbasesolid,nomreac,basesolid,namesolid,moderecherche,1);
    nbrproduitsbasesolid=fichier(basesolid,namesolid);
};
```

Figure G.11. second option of the menu in figure G.9.

If the third option is chosen, the program generates all possible products automatically as a function of the elementary composition of the reactants (using the function 'F_possibleproduct.c'). The principles are described in appendix D. $C_2H_6O_2$ is chosen as the examples shown in figure G.12.

```
define the mixture CxHyOxNz.
C2H6O2
```

```
if (choix1==3)
{
    F_compositionanalysis(enregistremolecular,elem,nbrelem);
    getchar();
};//Fin du choix n°3;
```

Figure G.12. Third option from the menu of figure G.9

Table G.2. The result of the Third option from the menu of the database.

CH_3OH	CH_3COOH	$OH\text{-}CH_2\text{-}CH_2\text{-}OH$	$CH_3\text{-}CH_3$	C_2H_5OH	HCOOH	CH_4	$OH\text{-}CH_2\text{-}OH$	$CH3\text{-}CH\text{-}(OH)_2$	H_2
CO_2	CO	O_2	H_2O_2						

Simulating chemical transformations

If the second option of the menu of figure G.7 is selected the simulation part of the CIRCE will be operated. At first, the initial temperature and pressure of the system should be defined (Figure G.13).

```
Initial temperature (in K)
298.15

Initial pressure (in bar absolute)
1
```

Figure G13. First information needed to run a simulation.

Then the reactants need to be defined either via the atomic composition of the reactants (a sort of mixture of atoms) or as a mixture of molecules extracted from the database (figure G.14).

```
Definition of the reactants:

     Choice 1: By a Mixture of products from the database

     Choice 2: From the atomic composition

     Your choice?
```

Figure G.14. The two options to define the reactants.

In the second case, the atomic composition of the reactants (under the form: CnHmOp…), enthalpy of formation and average specific capacity have to be provided. In the first case, the user defines how many reactants, extracted from the database, would form the reactive mixture

(figure G.15). Then for each reactant, the user writes the chemical formula and its proportions in the reactive mixture. The program verifies each reactant is available in the database and extracts the specific heat (average value between the standard temperature and the initial temperature given at the beginning 300 K) and the enthalpy of formation. For the mixture, the program calculates the enthalpy of formation and specific heat. The user is invited to confirm the two latter parameters or modify them, for instance to simulate an additional source/sink of free energy in the system. When a reactant is not in the database the user is invited to create with the functions used to generate the database. All these small operations are implemented in the function definirsystemreactif.c.

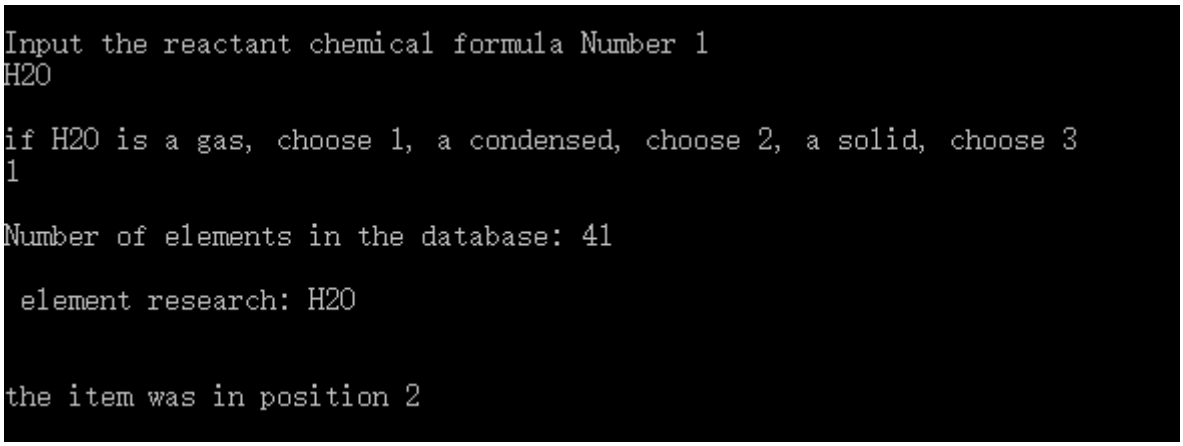

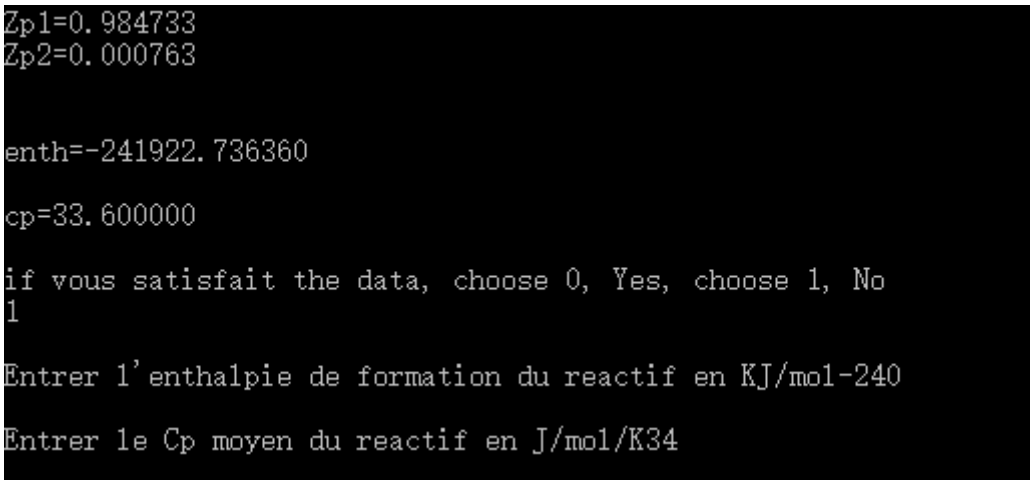

Figure G.15. after choosing 1 of figure G.14.

The list of the potential final products is extracted from the database on the basis of the atomic composition of the initial mixture using function ‘Selectionproduits.c’ (Figure G.16). Then a sub-selection can be made using the function ‘suppression_produits.c’

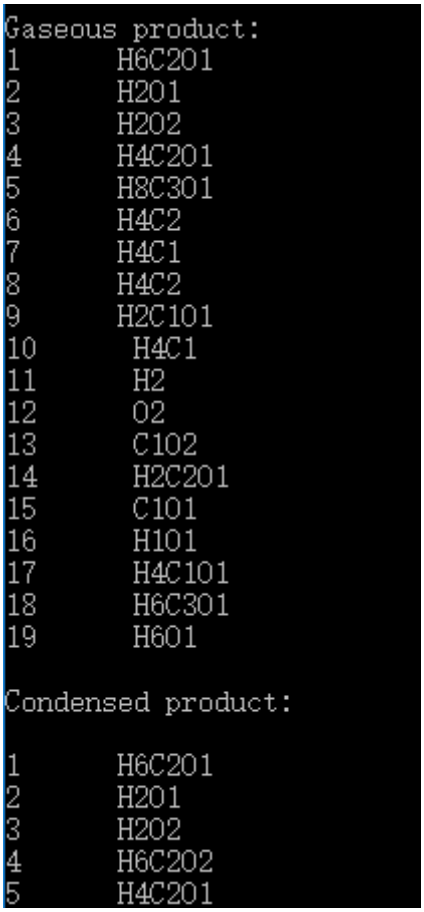

Figure G.16. List of the potential products.

The initializing set is completed and the simulation can be run. Three options are offered to the user as shown in figure G.17.

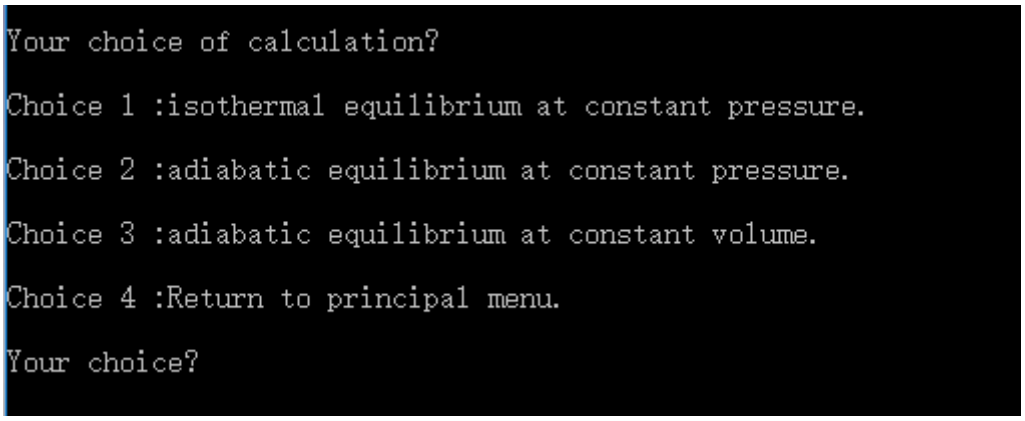

Figure G.17. Simulation options (in 'mainc.c').

The corresponding simulation modules are respectively the pyrolysis.c, combustion.c, and the explosion.c (Figure G.18).

```
                                if(choix4==1)//Pyrolyse
                                {
                                    printf(" Choice 1: pyrolysis_MonteCarlo_LCVM_UnifacModifie\n Choice 2: return to the last menu\n");
                                    scanf("%d",&choix5);


                                    if(choix5==1)
                                    {
                                        Pyrolyse_Monte_Carlo_LCVM_Unifac(nbrproduits,nbrproduitscond,nbrproduitsolid,nbrelem,proprietes_produits,proprietes_produitscond,proprietes_produitsolid,comporeac,compositionproduits,compositionproduitscond,compositionproduitsolid,T,P,elemreac,nbrelemreac,hglobalreac,indiceproduits,indiceproduitscond,indiceproduitsolid,nomproduits,nomproduitscond,nomproduitsolid,ni);
                                    };
                                }
```

a-pyrolyse.c

```
                            if(choix4==2)//Combustion;
                            {
                                u=0;
                                printf(" Choice 1: Distillation_Isobare_Monte_Carlo_LCVM_UnifacModifie\n Choice 2: retour au menu precedent\n");
                                scanf("%d",&choix5);


                                if(choix5==1)
                                    {
                                        Distillation_Isobare_Monte_Carlo_LCVM_Unifac (nbrproduits,nbrproduitscond,nbrproduitsolid,nbrelem,proprietes_produits,proprietes_produitscond,proprietes_produitsolid,comporeac,compositionproduits,compositionproduitscond,compositionproduitsolid,T,P,elemreac,nbrelemreac,hglobalreac,indiceproduits,indiceproduitscond,indiceproduitsolid,nomproduits,nomproduitscond,nomproduitsolid,ni);
                                    };

                            };
```

b-combustion.c

```
                        if(choix4==3)//dans le menu d'Explosion.
                        {
                            printf(" Choice 1: Distillation_Isochore_LCVM_UnifacModifie\n Choice 2: retour ←
au menu precedent\n");
                            scanf("%d",&choix5);


                            if(choix5==1)
                            {
                    Distillation_Isochore_Monte_Carlo_LCVM_Unifac (nbrproduits,nbrproduitscond,nbrproduitsolid,nbre←
lem,proprietes_produits,proprietes_produitscond,proprietes_produitsolid,comporeac,compositionproduits, compositionprodu←
itscond,compositionproduitsolid, T,P,V,elemreac,nbrelemreac,hglobalreac,indiceproduits,indiceproduitscond,indiceproduit←
solid,nomproduits,nomproduitscond,nomproduitsolid,ni);
                            };
                        };
```

c-explosion.c

Figure G.18. Some organizational details of the simulation block of CIRCE.

The organization of ‘pyrolyse.c’ is described as follow. First, the user is invited to define the number of composition vectors on which it is used to minimize the Gibbs free energy. Immediately after the Monte Carlo generator is operated to generate a sequence of random numbers on the part of the list of products for which a random search is allowed (the rest is deduced using the Gaussian elimination method). Function Montecarlogenerateur.c (Figure G.19) will both operate the Monte Carlo method and the Gaussian Elimination method to provide the required number of vectors. The progression of the selection can be followed (Figure G.19-bottom).

```
   MonteCarlogenerateur(nbrproduits, nbrproduitscond, nbrproduitsolid,nbrelem, prop←
rietes_produits, proprietes_produitscond, proprietes_produitsolid, comporeac, compos←
itionproduits, compositionproduitscond, compositionproduitsolid,elempresents, nbrele←
mpresents, indiceproduits, indiceproduitscond,indiceproduitsolid, nomproduits, nompr←
oduitscond, nomproduitsolid, ni,xi,compositionrecord);

for(essai=0;essai<10000;essai++)
    {
        fprintf(Pyrolyse_GE,"essai=%d\n",essai);

        for(i=0;i<nbrproduitstotal;i++)
    {
        xi[i]=compositionrecord[essai][i];
    }
```

Figure G.19. Monte Carlo generator.

Try for each composition vector and each product the departure function need to be calculated. At first, P and T and the critical parameters (*Tc*, *Pc*, omega) are provided to the function PENGRobinson.c which calculates Hdeparture, Sdeparture, Cpdeparture (Figure G.20)

```
    PENG_Robinson_for_HSCp (nbrproduits, nbrproduitscond, nbrproduitsolid, nomproduits, nomproduitscond, nomproduitsolid, proprietes_produits, proprietes_produitscond, proprietes_produitsolid, Tf, Pi, Hdeparture, Sdeparture, Cpdeparture);
    Solid_Heat_Capacity(nbrproduitsolid, nomproduitsolid, proprietes_produitsolid, Tf, Pi, compositionproduitsolid, Cpsolid);
```

Figure G.20. Calculating the departure function.

The departure function, the Gibbs energy of formation of the pure and ideal gas component and the specific heat capacity of each product enables to calculate chemical potentials at *T* and *P* of the pure components (figure G.21).

```
    sommehi=0;
    for (i=0;i<nbrproduits;i++)
    {
        cp[0]=proprietes_produits[i][2];
        cp[1]=proprietes_produits[i][3];
        cp[2]=proprietes_produits[i][4];
        cp[3]=proprietes_produits[i][5];
        cp[4]=proprietes_produits[i][6];
        //printf("Avant calculfonctiont Tf=%f\n",Tf);
        calculfonctiont(proprietes_produits[i][0],proprietes_produits[i][1],Tref,Tf,cp,ft);
        //printf("Apres calculfonctiont Tf=%f\n",Tf);
        dh[i]=ft[0]+Hdeparture[i];
        printf("h[%d] vaut %f\n",i,dh[i]);
        ds[i]=ft[1]-8.314*log(Pi)+Sdeparture[i];
        printf("s[%d] vaut %f\n",i,ds[i]);
        dG[i]=(dh[i]-Tf*ds[i]);
        printf("g[%d] vaut %f\n",i,dG[i]);
    };
```

Figure G.21. Chemical potentials of the pure components at T and P.

To estimate the influence of the intermolecular forces, the activity coefficients need to be calculated at *T* and *P*. This is the duty of the function 'f_LCVM_UNIFAC' (Figure G.22).

```
        f_LCVM_Unifac(nbrproduits,nbrproduitscond,nbrproduitsolid,nbrelem,proprietes_produits,proprietes_produitscond,proprietes_produitsolid,comporeac,compositionproduits,compositionproduitscond,Ti,Pi,elempresents,nbrelempresents,indiceproduits,indiceproduitscond,nomproduits,nomproduitscond,ni,Tf,Fp,Fg,Fl,activ,xi,&Hex,matrice_interactiongas,Recordgroup_intergas, Sub_rang_jobackgas, matrice_QRgas, nbrgroupegas,matrice_interactionliquid,Recordgroup_interliquid, Sub_rang_jobackliquid, matrice_QRliquid, nbrgroupeliquid, recordPsat, polar,Vliquide);
```

Figure G.22. The function to calculate the activity coefficients.

This function calls a set of sub-functions (figure G.23) to calculate the activity coefficients at

1 bar absolute and T according to UNIFAC theory.

```
        //printf("nbrproduitscond=%d\n",nbrproduitscond);
        Unifac_NameComp_NYU_NumGroup(nbrproduits,&NumGroupgas,proprietes_produits,NY←
Ugas, Recordgroup_intergas,Maingroup_intergas,Sub_rang_jobackgas,nbrgroupegas, SUBGR←
OUPgas);
```

A-the function to organize the parameter for the other function of UNIFAC.

```
        Unifac_nyu_Mw_Q_r_psi(NYUliquid, nyuliquid, Mwliquid, Qliquid, r1liquid, p←
siliquid, nbrproduitscond, NumGroupliquid, Rliquid, Tf, matrice_interactionliquid,←
Recordgroup_interliquid,Maingroup_interliquid, SUBGROUPliquid, nbrgroupeliquid, ma←
trice_QRliquid);
```

B-calculation of the number of subgroups in the mixture

```
        Unifac_lngamma_Com(nyugas,xigas,r1gas,lngamma_Comgas,thetagas,Lgas,nbrprod←
uits,NumGroupgas,Qgas,qgas,Rgas,matrice_QRgas, Sub_rang_jobackgas,nbrgroupegas);
        Unifac_lnGAMMA_ResP(nyugas,Qgas,psigas,lnGAMMA_ResPgas,nbrproduits,NumGrou←
pgas);
        Unifac_lnGAMMA_ResM(xigas,nyugas,Qgas,psigas,lnGAMMA_ResMgas,nbrproduits,N←
umGroupgas);
        Unifac_lngamma(xigas,nyugas,Qgas,r1gas,psigas,lngammagas,nbrproduits,NumGr←
oupgas,thetagas,Lgas,qgas,Rgas,lngamma_Comgas,lnGAMMA_ResPgas,lnGAMMA_ResMgas,lnGA←
MMA_Resgas,GAMMAGAS);
```

C-calculation of the activity coefficients.

Figure G.23. Sub-functions to calculate the activity coefficients at 1 bar absolute pressure according to UNIFAC.

Functions Unifac_Lngamma_Com, Unifac_Lngamma_ResP, Unifac_Lngamma_ResM, Unifac_Lngammarespectively calculate the $\ln \gamma_i^C$, $\ln \gamma_{imixture}^R$,$\ln \gamma_{isinglegroup}^R$, and $\ln \gamma_i$.

$$\ln \gamma_i = \ln \gamma_i^C + \left(\ln \gamma_{imixture}^R - \sum \ln \gamma_{isinglegroup}^R\right) \quad \text{G.1}$$

The variable GAMMAGAS can give the value of the activity coefficient for the gas. The variable GAMMALIQUID can calculate the activity coefficient for the liquid. These activity coefficients are introduced into the LCVM equation to calculate the activity coefficient at P via the fugacities as explained in appendix F and G^E[i]. The excess Gibbs energy G^E[i]is calculated as the logarithm of the activity coefficient time the number of mole of the compound i and is added to the part of G_{mix}[i] associated to each compound and to the chemical potential times the number of mole of the compound i, dG[i](figure G.24).

```
sommehi=0;
for(i=0;i<nbrproduits;i++)
    {
        hi[i]=dG[i]+Gmix[i]+GE[i];
    }


for(i=nbrproduits;i<nbrproduitsgazliquid;i++)
    {
        hi[i]=dG[i]+Gmix[i]+GE[i];
    };


for(i=nbrproduitsgazliquid;i<nbrproduitstotal;i++)
    {
        hi[i]=dG[i];
    }
//printf("\n");
```

Figure G.24. Calculation of the total Gibbs energy associated to each compound i.

Then the sum of h[i] is performed for each composition vector to provide the total Gibbs energy of the mixture and the minimum is found on the ground of direct comparison (figure G.25).

```
if(MinGibbs>sommehi)
{
MinGibbs=sommehi;
```

Figure G.25. looking for the minimum Gibbs free energy of the reaction.

The other calculation options are extensions of ‘Pyrolyse.c’. In ‘combustion.c’, the function Pyrolyse.c is iterated until the final enthalpy equal the initial one by changing T according to the secant method (Figure G.26).

```
usystemeproduit=0.0;
for(i=0;i<nbrproduits;i++)
    {
        usystemeproduit+=yi[i]*(dh[i]-8.314*Tf);
    }
for(i=nbrproduits;i<nbrproduitsgazliquid;i++)
    {
        usystemeproduit+=yi[i]*(dh[i]-8.314*Tf);
    }
for(i=nbrproduitsgazliquid;i<nbrproduitstotal;i++)
    {
        usystemeproduit+=yi[i]*dh[i];
    }
```

```
if((hsystemeproduit-hsystemereactif)*(hsystemelimite1-hsystemereactif)<0)
{
    T2=Tf;
    hsystemelimite2=hsystemeproduit;
}
else
{
    T1=Tf;
    hsystemelimite1=hsystemeproduit;
}
Tf=(T1+T2)/2;
DT=fabs((hsystemeproduit-hsystemereactif)/((hsystemeproduit-hsystemereactif)/(T2-T1)));
iterationgenerale++;
```

Figure G.26. Adjusting the temperature in “Combustion” between two Pyrolysis.c runs.

The maximum number of iterations is 100 and DT<1 as a stop criterion.

The program provides T, P, V, total enthalpy and composition in each phase at the end of the calculation (Figure G.27). The result can also be extracted from file pyrolyse_GE.csv.

```
Here is the composition of the system in equilibrium:

Here is the volume of the reactor=0.024942
hsystemeproduit= -260849.61 J
sommeyigaz=0.388828
T=355K=82C
P=1bar

Phase solid = 0.00 pour cent du systeme

Composition de la phase solid:

Phase liquid = 61.12 pour cent du systeme

Composition de la phase condensee:
le produit C2H6O vaut 41.18 pourcent
le produit H2O vaut 58.82 pourcent




Phase gazeuxe=38.88 pour cent du systeme

Composition de la phase gazeuse:

le produit C2H6O vaut 63.86 pourcent
le produit H2O vaut 36.14 pourcent
```

```
        //printf("PV/RT=%f\n",F);
        printf("\nPhase solid = %.2f pour cent du systeme\n",sommeyisolid*100/sommey←
i);
        printf("\nComposition de la phase solid:\n");
        for(i=nbrproduitsgazliquid;i<nbrproduitstotal;i++)
        {
                //printf("xi[%d]=%f\n",i,xi[i]);
                yi[i]=yi[i]*100/sommeyisolid;
                printf("le produit %s vaut %.2f pourcent\n",nomproduitsolid[indicepr←
oduitsolid[i-nbrproduitsgazliquid]-1],yi[i]);
        };
```

Figure G.27. display of the results.

The result of the simulation can be shown by the figure G27.

```
//fprintf(pExplosion_GE,"Voici les energie du potentiel\n");
for(i=0;i<nbrproduits;i++)
    {
        Fi[i]=(dG[i]-Pf*V*100000+Gmix[i]+8.314*Tf*log(Pf));//C'est les formules de Helmholtz ici, il faut faire attention.
    }

for(i=nbrproduits;i<nbrproduitsgazliquid;i++)
    {
        Fi[i]=(dG[i]-Pf*V*100000+Gmix[i]);//C'est les formule de Helmholtz ici, il faut faire attention.
    };

//fprintf(pExplosion_GE,"\n");
for(i=nbrproduitsgazliquid;i<nbrproduitstotal;i++)
    {
        Fi[i]=dG[i];//C'est les formule de Helmholtz ici, il faut faire attention.
        //fprintf(pExplosion_GE,"Fi[%d]=%lf\n",i,Fi[i]);
    };
    //getchar();
```

Figure G.28. The function can calculate the explosion.

The calculation for the Helmholtz can be shown as above, which has been used in the

function of the explosion.

Reference:

[1] National Research Council, Impact of Advances in Computing and Communications Technologies on Chemical Science and Technology: Report of a Workshop. National Academies Press. National Academies Press (1999).

[2] C. Gopi Mohan, T. Gandhi, D. Garg, R. Shinde, Computer-assisted methods in chemical toxicity prediction, Mini reviews in medicinal chemistry. 7 (2007) 499-507.

[3] P. Middha, O.R. Hansen, Predicting deflagration to detonation transition in hydrogen explosions, Process Saf. Prog. 27 (2008) 192-204.

[4] R.I. Masel, Chemical kinetics and catalysis, Wiley-Interscience New York, 2001.

[5] T.F. Edgar, Process Engineering in the 21st Century: The Impact of Information Technology, Phillips Lecture (1999).

[6] M. Fermeglia, S. Pricl, G. Longo, Molecular modeling and process simulation: Real possibilities and challenges, Chemical and biochemical engineering quarterly 17 (2003) 19-30.

[7] R. Gautam, W.D. Seider, Computation of phase and chemical equilibrium: Part I. Local and constrained minima in Gibbs free energy, AlChE J. 25 (1979) 991-999.

[8] W.B. White, S.M. Johnson, G.B. Dantzig, Chemical equilibrium in complex mixtures, The Journal of Chemical Physics. 28 (1958) 751-755.

[9] B. MCBRIDE, S. Gordon, Computer program for calculation of complex chemical equilibrium compositions and applications, (1996).

[10] C. Morley, Gaseq: a chemical equilibrium program for Windows, http:// www. gaseq. co. uk (2005).

[11] J.C. Westall, J.L. Zachary, F. Morel, MINEQL: A computer program for the calculation of chemical equilibrium composition of aqueous systems, Water Quality Laboratory, Ralph M. Parsons Laboratory for Water Resources and Environmental Engineering [sic], Department of Civil Engineering, Massachusetts Institute of Technology, 1976.

[12] L.E. Fried, Cheetah 1.0 users manual, Lawrence Livermore National Lab., CA (United States), 1994.

[13] M.V. Mironenko, S.A. Grant, G.M. Marion, R.E. Farren, FREZCHEM2 A Chemical Thermodynamic Model for Electrolyte Solutions at Subzero Temperatures, COLD REGIONS RESEARCH AND ENGINEERING LAB HANOVER NH, 1997.

[14] Z. Zainal, R. Ali, C. Lean, K. Seetharamu, Prediction of performance of a downdraft gasifier using equilibrium modeling for different biomass materials, Energy Convers. Manage. 42 (2001) 1499-1515.

[15] W. Reynolds, The element potential method for chemical equilibrium analysis: Implementation in the interactive program STANJAN, version 3, Technical Rept. (1986).

[16] U.R. Kattner, The thermodynamic modeling of multicomponent phase equilibria, JOM 49 (1997) 14-19.

[17] P. Atkins, L. Jones, Chemical principles, Macmillan, 2009.

[18] A.D. McNaught, A. Wilkinson, Compendium of chemical terminology. IUPAC recommendations, (1997).

[19] S. Martin, Code de prédiction des propriétés dangereuses de substances réactives. in: P.Christophe, (Ed.), UTC, INERIS, 2011, pp. 87.

[20] H.K. Onnes, Théorie générale de l'état fluide, Through Measurement to Knowledge, Springer, 1991, pp. 89-124.
[21] O. Redlich, J.N. Kwong, On the thermodynamics of solutions. V. An equation of state. Fugacities of gaseous solutions, Chem. Rev. 44 (1949) 233-244.
[22] G. Soave, Equilibrium constants from a modified Redlich-Kwong equation of state, Chem. Eng. Sci. 27 (1972) 1197-1203.
[23] D.Y. Peng, D.B. Robinson, A new two-constant equation of state, Ind. Eng. Chem. Fundam. 15 (1976) 59-64.
[24] B.E. Poling, E.A. Grens, J.M. Prausnitz, Thermodynamic properties from a cubic equation of state: avoiding trivial roots and spurious derivatives, Industrial & Engineering Chemistry Process Design and Development 20 (1981) 127-130.
[25] C. Boukouvalas, N. Spiliotis, P. Coutsikos, N. Tzouvaras, D. Tassios, Prediction of Vapor-Liquid Equilibrium with the LCVM Model: A Linear Combination of the Vidal and Michelsen Mixing Rules Coupled with the Original UNIFAC and the t-mPR Equation of State, Fluid Phase Equilibria 92 (1994) 75-106.
[26] C. Coquelet, A. Chapoy, D. Richon, Development of a new alpha function for the Peng–Robinson equation of state: comparative study of alpha function models for pure gases (natural gas components) and water-gas systems, Int. J. Thermophys. 25 (2004) 133-158.
[27] N. Spiliotis, C. Boukouvalas, N. Tzouvaras, D. Tassios, Application of the LCVM model to multicomponent systems: Extension of the UNIFAC interaction parameter table and prediction of the phase behavior of synthetic gas condensate and oil systems, Fluid Phase Equilibria 101 (1994) 187–210.
[28] E.C. Voutsas, C.J. Boukouvalas, N.S. Kalospiros, D.P. Tassios, The performance of EoS/G E models in the prediction of Vapor-Liquid Equilibria in asymmetric systems, Fluid Phase Equilib. 116 (1996) 480-487.
[29] B.J. McBride, S. Gordon, Computer program for calculation of complex chemical equilibrium compositions and applications: II. Users manual and program description, NASA reference publication 1311 (1996) 84-85.
[30] Aspen Physical Property System: Physical Property Methods, (2010).
[31] D.P. Bertsekas, Constrained optimization and Lagrange multiplier methods, Academic press, 2014.
[32] M. Cowperthwaite, W. Zwisler, Tiger computer program documentation, DTIC Document, 1974.
[33] J. Blecic, J. Harrington, M.O. Bowman, TEA: A Code Calculating Thermochemical Equilibrium Abundances, The Astrophysical Journal Supplement Series 225 (2016) 4.
[34] G. Dantzig, S. Johnson, W. White, A linear programming approach to the chemical equilibrium problem, Manag. Sci. 5 (1958) 38-43.
[35] R. Gautam, W.D. Seider, Computation of phase and chemical equilibrium: Part II. Phase-splitting, AlChE J. 25 (1979) 999-1006.
[36] C.A. Meyer, Calculation of chemical and phase equilibria, University of Cape Town, 1996.
[37] M.L. Michelsen, The isothermal flash problem. Part I. Stability, Fluid Phase Equilib. 9 (1982) 1-19.
[38] M.L. Michelsen, The isothermal flash problem. Part II. Phase-split calculation, Fluid Phase Equilib. 9 (1982) 21-40.
[39] A.V. Levy, S. Gómez, The tunneling method applied to global optimization, Numerical optimization 1981 (1985) 213-244.
[40] A. Bonilla-Petriciolet, G.P. Rangaiah, J.G. Segovia-Hernández, Constrained and unconstrained Gibbs free energy minimization in reactive systems using genetic algorithm and differential evolution with tabu list, Fluid Phase Equilib. 300 (2011) 120-134.

[41] F. Jalali, J. Seader, Homotopy continuation method in multi-phase multi-reaction equilibrium systems, Comput. Chem. Eng. 23 (1999) 1319-1331.
[42] G.I. Burgos-Solórzano, J.F. Brennecke, M.A. Stadtherr, Validated computing approach for high-pressure chemical and multiphase equilibrium, Fluid Phase Equilib. 219 (2004) 245-255.
[43] G.B. Dantzig, Origins of the simplex method, ACM, 1990.
[44] C. Rossi, L. Cardozo-Filho, R. Guirardello, Gibbs free energy minimization for the calculation of chemical and phase equilibrium using linear programming, Fluid Phase Equilib. 278 (2009) 117-128.
[45] A. Selamat, N.T. Nguyen, H. Haron, Intelligent Information and Database Systems: 5th Asian Conference, ACIIDS 2013, Kuala Lumpur, Malaysia, March 18-20, 2013, Proceedings, Springer, 2013.
[46] G.P. Rangaiah, Evaluation of genetic algorithms and simulated annealing for phase equilibrium and stability problems, Fluid Phase Equilib. 187 (2001) 83-109.
[47] J. Gmehling, J. Rarey, J. Menke, Dortmund Data Bank, Oldenburg (29/08/2013) http://www.ddbst.com (2008).
[48] T. Hino, Y. Song, J.M. Prausnitz, Liquid-liquid equilibria and theta temperatures in homopolymer-solvent solutions from a perturbed hard-sphere-chain equation of state, J. Polym. Sci., Part B: Polym. Phys. 34 (2015) 1961-1976.
[49] N. Metropolis, S. Ulam, The monte carlo method, Journal of the American statistical association 44 (1949) 335-341.
[50] N. Metropolis, The beginning of the Monte Carlo method, Los Alamos Science 15 (1987) 125-130.
[51] A. Fredenslund, R.L. Jones, J.M. Prausnitz, Group-contribution estimation of activity coefficients in nonideal liquid mixtures, AlChE J. 21 (1975) 1086-1099.
[52] A.L. Lydersen, M.E.E. Station, Estimation of critical properties of organic compounds by the method of group contributions, University of Wisconsin, 1955.
[53] L. Constantinou, R. Gani, New group contribution method for estimating properties of pure compounds, AlChE J. 40 (1994) 1697-1710.
[54] K.G. Joback, R.C. Reid, Estimation of pure-component properties from group-contributions, Chem. Eng. Commun. 57 (1987) 233-243.
[55] K. Klincewicz, R. Reid, Estimation of critical properties with group contribution methods, AlChE J. 30 (1984) 137-142.
[56] D. Ambrose, Correlation and estimation of vapour-liquid critical properties. Part 1: Critical temperatures of organic compounds, (1978).
[57] Z.k. Kolská, M. Zábranský, A. Randova, Group contribution methods for estimation of selected physico-chemical properties of organic compounds, Thermodynamics-Fundamentals and Its Application in Science, InTech, 2012.
[58] G.S. Parks, H.M. Huffman, Free energies of some organic compounds, (1932).
[59] D. Ambrose, Correlation and Estimation of Vapour-liquid Critical Properties, National Physical Library, 1978.
[60] D. Ambrose, Correlation and Estimation of Vapour-liquid Critical Properties: Critical pressures and critical volumes of organic compounds, National Physical Laboratory, 1979.
[61] B.E. Poling, J.M. Prausnitz, O.C. John Paul, R.C. Reid, The properties of gases and liquids, Mcgraw-hill New York, 2001.
[62] D.R. Stull, E.F. Westrum, G.C. Sinke, The chemical thermodynamics of organic compounds, (1969).
[63] E. Brignole, M. Cismondi, Molecular design-generation & test methods, (2003).

[64] S.C. Moldoveanu, Pyrolysis of organic molecules: applications to health and environmental issues, Elsevier, 2009.
[65] R. Kee, F. Rupley, J. Miller, M. Coltrin, J. Grcar, E. Meeks, H. Moffat, A. Lutz, G. Dixon-Lewis, M. Smooke, CHEMKIN Release 4.1, Reaction Design, San Diego, CA (2006).
[66] F. Jensen, Introduction to computational chemistry, John wiley & sons, 2017.
[67] J. Frank, Introduction to computational chemistry, (1999).
[68] W.G. Mallard, F. Westley, J. Herron, R.F. Hampson, D. Frizzell, NIST chemical kinetics database, Version 2Q98, National Institute of Standards and Technology, Gaithersburg, MD. USA (1998).
[69] N.M. Marinov, A detailed chemical kinetic model for high temperature ethanol oxidation, Int. J. Chem. Kinet. 31 (1999) 183-220.
[70] G. Corliss, Which root does the bisection algorithm find?, Siam Review 19 (1977) 325-327.
[71] H. Yoshida, F. Kiyono, H. Tajima, A. Yamasaki, K. Ogasawara, T. Masuyama, Two-stage equilibrium model for a coal gasifier to predict the accurate carbon conversion in hydrogen production, Fuel 87 (2008) 2186-2193.
[72] M. McHugh, M.E. Paulaitis, Solid solubilities of naphthalene and biphenyl in supercritical carbon dioxide, J. Chem. Eng. Data 25 (1980) 326-329.
[73] H. Knapp, " Vapor-Liguid Equilibria for Mixtures of Low Boiling Substances" Part1-4, DECHEMA Chemistry Data Series (1982).
[74] J. Griswold, S. Wong, Phase-equilibria of the acetone-methanol-water system from 100 degrees C into the critical region, Chemical Engineering Progress Symposium Series, 1952, pp. 18-34.
[75] J.M. Most, M.T. Giudici-Orticoni, M. Rousset, M. Bruschi, Biomass for Energy: Energetic and Environmental Challenges of Biofuels, Global Change, Energy Issues and Regulation Policies, Springer, 2013, pp. 179-203.
[76] A.A. Konnov, I.V. Dyakov, J. de Ruyck, Nitric oxide formation in premixed flames of H2+ CO+ CO2 and air, Proceedings of the Combustion Institute 29 (2002) 2171-2177.
[77] K. Holtappels, Project SAFEKINEX, Contract No. EVG1-CT-2002-00072, Deliverable (2002).
[78] K. Suzuki, H. Sue, M. Itou, R.L. Smith, H. Inomata, K. Arai, S. Saito, Isothermal vapor-liquid equilibrium data for binary systems at high pressures: carbon dioxide-methanol, carbon dioxide-ethanol, carbon dioxide-1-propanol, methane-ethanol, methane-1-propanol, ethane-ethanol, and ethane-1-propanol systems, J. Chem. Eng. Data 35 (1990) 63-66.
[79] R. Gani, E. Brignole, Molecular design of solvents for liquid extraction based on UNIFAC, Fluid Phase Equilib. 13 (1983) 331-340.